DEVELOPMENT OF POLYMERIC SORBENT BASED ANALYTICAL METHODS FOR ACTINIDES

By
SUMANA PAUL
CHEM01201004015
Bhabha Atomic Research Centre, Mumbai

A thesis submitted to the
Board of Studies in Chemical Sciences

In partial fulfillment of requirements
for the Degree of
DOCTOR OF PHILOSOPHY
of
HOMI BHABHA NATIONAL INSTITUTE

October, 2015

Homi Bhabha National Institute[1]

Recommendations of the Viva Voce Committee

As members of the Viva Voce Committee, we certify that we have read the dissertation prepared by Ms. Sumana Paul entitled "Development of polymeric sorbent based analytical methods for determination of actinides" and recommend that it may be accepted as fulfilling the thesis requirement for the award of Degree of Doctor of Philosophy.

Chairman - **Prof. K.L. Ramakumar** **Date:** 25 4, 2016

Guide / Convener - **Prof. A.K. Pandey** Pandey **Date:** 25.4.2016

Pmaiti 25.4.16

Examiner - **Prof. Pralay Maiti** **Date:**

25/4/2016

Member 1- **Prof. B.S. Tomar** **Date:**

Rmtripathi

Member 2- **Prof. R.M. Tripathi** **Date:**

Final approval and acceptance of this thesis is contingent upon the candidate's submission of the final copies of the thesis to HBNI.

I/We hereby certify that I/we have read this thesis prepared under my/our direction and recommend that it may be accepted as fulfilling the thesis requirement.

Date: 25.4.2016

Place: HBNI, Mumbai

Pandey

Guide

---

[1] This page is to be included only for final submission after successful completion of viva voce.

Version approved during the meeting of Standing Committee of Deans held during 29-30 Nov 2013

STATEMENT BY AUTHOR

This dissertation has been submitted in partial fulfillment of requirements for an advanced degree at Homi Bhabha National Institute (HBNI) and is deposited in the Library to be made available to borrowers under rules of the HBNI.

Brief quotations from this dissertation are allowable without special permission, provided that accurate acknowledgement of source is made. Requests for permission for extended quotation from or reproduction of this manuscript in whole or in part may be granted by the Competent Authority of HBNI when in his or her judgment the proposed use of the material is in the interests of scholarship. In all other instances, however, permission must be obtained from the author.

Sumana Paul

DECLARATION

I, hereby declare that the investigation presented in the thesis has been carried out by me. The work is original and has not been submitted earlier as a whole or in part for a degree/diploma at this or any other Institution / University.

Sumana Paul

DEDICATED TO

My Teachers, Friends & Family .....

List of Publications arising from the Thesis

Journal

1. Tailored bi-functional polymer for actinides monitoring;

Sumana Paul, Ashok K. Pandey, Pranaw Kumar, Santu Kaity and S.K. Aggarwal;

Analytical Chemistry, 86 (13), 2014, 6254–6261.

2. Chemically selective polymer substrate based direct isotope dilution alpha spectrometry of Pu;

Sumana Paul, Ashok K. Pandey, R.V. Shah and S.K. Aggarwal;

Analytica Chimica Acta, 878 (2015) 54–62.

3. Superparamagnetic bi-functional composite bead for thermal ionization mass spectrometry of plutonium(IV) ions;

Sumana Paul, Ashok K. Pandey, Raju V. Shah, D. Alamelu and Suresh K. Aggarwal;

RSC Advances, 6 (2016) 3326–3334.

4. Polymeric material based reservoirs for thermal ionization mass spectrometric determination of uranium(VI) and plutonium(IV) ions in environmental and process aqueous samples;

Sumana Paul, Ashok K. Pandey, Raju V. Shah, K. Sasi Bhusan and Suresh K. Aggarwal;

Journal of Analytical Atomic Spectrometry, 31 (2016) 985–993.

Symposium

1. Synthesis of a bi–functionalized polymer for Pu and Am sequestration;
   Sumana Paul, Pranaw Kumar, A.K. Pandey and S.K. Aggarwal; Proc. of DAE-BRNS ISMC-2012 Symposium, M-02, p. 498.
2. Development of phosphoric acid functionalised sorbents for selective preconcentration of Actinides;

Sumana Paul, Pranaw Kumar, A.K. Pandey and S.K. Aggarwal; Proc. of 11th DAE-BRNS NUCAR 2013 Symposium, B-17, p. 211.

3. Membrane based Isotope Dilution Alpha Spectrometry (MEM–IDAS) for Determination of Plutonium concentration;

   Sumana Paul, R.V. Shah, A.K. Pandey and S.K. Aggarwal; Proc. of NAC-V 2014 symposium, Paper No. D-40, Page 304.
4. Gel based loading for determination of Pu isotopic composition by Thermal Ionization Mass Spectrometry;

   Sumana Paul, R.V. Shah, A.K. Pandey and S.K. Aggarwal; Proc. of 28th ISMAS-WS-2014, Paper CP-32, Page 238.
5. Membrane based isotope dilution alpha spectrometry for determination of plutonium concentration;

   Sumana Paul, R.V. Shah, A.K. Pandey and S.K. Aggarwal; Proc. of ISMC-2014, Paper No. A–127, p. 110.
6. Selective extraction of plutonium from nitric acid medium by bifunctional polyethersulfone beads for quantification with thermal ionisation mass spectrometry;

   Sumana Paul, A.K. Pandey and S.K. Aggarwal; Proc. of NUCAR- 2015, Paper No. E-46, Page No. 393.
7. Resin bead-thermal ionization mass spectrometry for determination of plutonium concentration in irradiated fuel dissolver solution;

   Sumana Paul, R.V. Shah, A.K. Pandey and S.K. Aggarwal; Proc. of 29th ISMAS-WS-2015, Paper No. CP-30, Page No. 173.

Sumana Paul

ACKNOWLEDGEMENTS

At the outset, I wish to express my deepest and sincere gratitude to my guide, Prof. Ashok K. Pandey, Radiochemistry Division, B.A.R.C. for his valuable guidance, constant encouragement and persistent motivation. His wide knowledge and logical way of thinking and reasoning on scientific problems helped me immensely during the course of work. I am thankful to him for sharing his knowledge and scientific understanding during the fruitful discussions with me throughout the work.

I convey my heartfelt gratitude to Dr. Suresh K. Aggarwal, former Head, Fuel Chemistry Division for his tremendous support and encouragement. His advice and comments have been priceless and played a significant role in documenting my work.

I take this opportunity to express my sincere regards and deepest appreciation to my colleague Dr. Arnab Sarkar, with whom I started my first scientific endeavor after joining FCD, BARC, for sharing his work experience and scientific knowledge with me. His enthusiasm and constant encouragement helped me to initiate and continue my work regarding the study of actinides.

It gives me a great pleasure to acknowledge my senior colleague Shri Ankush R. Parab, for providing me the training necessary for handling radioactive materials. I would also like to thank my colleagues Dr. Radhika Rao, Shri Raju V. Shah, Shri K. Sasi Bhusan, and Shri S. Jagdish Kumar for sharing their experimental expertise and scientific knowledge with me. Without their help it would not have been possible to carry out the mass spectrometric studies of actinides.

I would take this opportunity to thank the respected members of my doctoral committee Prof. K.L. Ramakumar (Chairman), Prof. B.S. Tomar (member) and Prof. R.M. Tripathi (member) for their critical reviews and valuable suggestions during the annual progress reviews and pre-synopsis presentation.

I would also like to thank my colleagues Shri Santu Kaity, Radiometallurgy Division and Dr. C.B. Basak, Glass & Advanced Metallurgy Division for providing the SEM images, Shri T.V. Vittal Rao, Fuel Chemistry Division for carrying out the porosity measurements, Dr. Y.K. Bhardwaj for carrying out tensile strength measurements and Dr. Manjulata Sahu for providing DSC data.

My sincere thanks are due to all of my colleagues from Mass Spectrometry Section, FCD for their help, suggestion and encouragement.

I would like to express my sincere gratitude to Dr. K.L. Ramakumar once again for his constant support and encouragement as Director, Radiochemistry and Isotope Group (RC&IG).

I am thankful to all my friends for their encouragement and support. I greatly value their friendship and deeply appreciate their belief in me.

I cannot imagine my current position without the blessings of my teachers and will always be indebted to them.

Most importantly, I owe my heartfelt gratitude to my family for their constant encouragement, care and never fading love. Their blessings and good wishes have helped me to achieve what I am today. Finally, I would like to express my endless thanks and appreciations to my husband for his support and care.

October, 2015 Sumana Paul

FCD, BARC, Mumbai.

CONTENTS

Page No.

2.4. Characterization techniques

2.5. Detection and quantfication of actinides

3.3. Results & discussions

6.3. Results & discussion

Synopsis

Various activities involved in the utilization of nuclear energy can cause radiotoxic contamination of natural waters, soil and biological systems. Due to the high degree of radiological toxicity associated with actinides, they impose major concern even when present at ultratrace levels. Therefore monitoring of actinides in various environmental and biological systems is of utmost importance. Also, precise and accurate determination of actinides is required at different stages of the nuclear fuel cycle, e.g. input accountability at reprocessing plants, material accounting in the dissolver solution, burn-up determination, recovery of precious actinides from radioactive waste, and also for nuclear forensics. Various analytical methods have been developed and are applied for the determination of actinides in environmental and nuclear samples; the most widely used methods being either radiometric techniques like gross alpha counting by liquid scintillation, alpha spectrometry, gamma spectrometry or mass spectrometric techniques like thermal ionization mass spectrometry (TIMS) and inductively coupled plasma mass spectrometry (ICPMS) [1–4]. However, quantification of actinides by conventional instrumental techniques is limited by several interferences e.g. radiation selectivity in liquid scintillation counting, α energy overlap in α-spectrometry, isobaric and/or polyatomic interferences in TIMS and ICPMS, and abundance sensitivity problems. Therefore, sample pretreatment, removal of matrix and selective preconcentration of the analyte are necessary to obtain a good signal as well as to minimize the effect of various interferences. Despite the improvements in the instrumental analysis, the preconcentration step plays an important role in the monitoring of actinides not only by enhancing the analytical range but also by providing chemical selectivity in the actinide detection methods. Also during preconcentration, it is possible to introduce suitable internal standards for the quantification of actinides. The commonly used separation methods for α spectrometry or mass spectrometry are coprecipitation, solvent extraction, ion exchange, and extraction chromatography using TEVA, TRU or UTEVA resins [5–8]. However, these methods involve multiple steps and the preconcentration factors achieved are relatively small. Extraction chromatographic microflow system or cloud point extraction procedure has been developed that can be coupled to either ICPMS or α spectrometry for quantification of actinides [9,10].

Motivation of the present work

In recent years, sorption preconcentration of actinides has been employed to develop combined and hybrid methods for their determination in complex environmental and biological matrices. Synthesis and designing of new sorbents with specified properties for quantitative recovery of actinides from diverse samples remains a difficult task. Ligands anchored on silica supports, superparamagnetic Fe_3O_4 nanoparticles and graphene oxide have been employed for selective sequestration of actinides and fission products from complex aqueous media [11-13]. However, these materials are more suited for the removal of matrix and separation of target actinide, rather than for analytical applications. Therefore, it would be interesting to investigate the possibility of directly subjecting a solid-phase sorbent to conventional analytical techniques such as α spectrometry and TIMS for quantification of the analyte preconcentrated in its matrix. Direct analysis of actinides from a solid phase sorbent would minimize the sample manipulation steps required for removal of the undesirable sample matrix without sacrificing the preconcentration factor.

Chapter 1: Introduction

This chapter describes the significance of quantification of the major actinides, viz. U, Pu and Am which are produced in nuclear reactors and are available at various stages of nuclear fuel cycle. The monitoring of these actinides in different environmental and biological matrices is also important because of their associated radio-toxicity. The chapter includes a brief description of the basic chemical properties of Pu, U and Am. The chapter also gives a short account of the conventional separation techniques reported in literature for these actinides, which include coprecipitation, solvent extraction, ion-exchange and extraction chromatography. The advantages as well as limitations of these conventional separation techniques have also been discussed. Literature survey of the conventional as well as hyphenated instrumental techniques, employed for the quantification of actinides, is also included in this chapter. The scope and aim of the present work, along with the importance of phosphate functionalized extractants for the actinides, has also been discussed at the end of this chapter.

Chapter 2: Experimental methods

The details of the experimental methods for the synthesis, characterization and physico-chemical properties of various polymeric substrates have been given in this chapter. The chapter also includes the details of all the reagents and chemicals used in the present work. The (phosphate+sulfate) and (phosphate+quaternary ammonium) functionalized polymeric substrates were synthesized by photo-induced free radical grafting method. The bifunctional polymer, developed in the present work, was tailored in different ways e.g. self-supported disc, anchored on a porous poly(ethersulfone) membrane, bifunctional magnetic poly(ethersulfone) beads etc. Principles of various instrumental techniques, used in the present work for the characterization of these polymeric substrates, like scanning electron microscopy, secondary ion mass spectrometry, vibrating sample magnetometry, atomic force microscopy etc. are also described in this chapter. Various radiotracers e.g. ^{233}U, ^{241}Am and $^{238-242}$Pu etc. were extensively used in the present work to study the actinide extraction properties of the phosphate functionalized polymeric substrates and quantification by isotope dilution. Therefore nuclear reactions involved in the production of these radiotracers were mentioned in this chapter. The chapter also includes the details of the different aspects of radiotracer based measurements, associated safety factors and various radiation detectors used in the present work.

Chapter 3: Development of bi–functional polymeric sorbents for selective preconcentration of actinides

This chapter describes the synthesis and characterization of phosphate functionalized polymers for selective preconcentration of actinides from aqueous medium. Monitoring of actinides in complex aqueous matrices with sophisticated conventional methods is affected by matrix interferences, spectral interferences, isobaric and polyatomic interferences, abundance sensitivity problems etc. To circumvent these limitations, a bifunctional polymer, containing phosphate and sulphonic acid, was synthesized by photo-induced free radical copolymerization for acidity-dependent extraction of actinides. The selection of the neutral phosphate group was based on the coordinating ability of the P=O moiety with actinide ions, while the sulfonic acid groups provide ion-exchange sites for charge balance and improve complexation kinetics. Self-supported bifunctional polymer discs were synthesized by irradiating an equimolar mixture of two monomers, phosphoric acid 2-hydroxyethyl methacrylate ester (HEMP) and 2-acrylamido-2-methyl-1-propanesulfonic acid (AMPS), in a UV reactor in presence of an initiator α,α′-dimethoxy-α-phenylacetophenone (DMPA). The bifunctional polymer was found to be better than the polymer containing either a phosphate group or a sulfonic acid group in terms of higher Pu(IV) sorption efficiency at 3−4 M HNO_3, selective preconcentration of Pu(IV) in the presence of a trivalent actinide such as Am(III), and preferential sorption of Pu(IV) in presence of a large excess of U(VI).

HEMP–co–AMPS polymer was found to be efficient for the sorption of Pu(IV) from 3-4 M HNO_3, where Pu exists as cationic or neutral species such as $[Pu(NO_3)_2]^{2+}$, $[Pu(NO_3)_3]^{+}$ or $[Pu(NO_3)_4]$. However, Pu(IV) sorption efficiency of HEMP–co–AMPS substantially reduces in 6–8 M HNO_3 medium, which could be attributed to the formation of anionic complexes like $[Pu(NO_3)_5]^{-}$ and $[Pu(NO_3)_6]^{2-}$ at higher HNO_3 concentrations. Therefore, another bifunctional polymer was synthesized from equimolar mixture of HEMP and (3-acrylamidopropyl)trimethyl ammonium chloride (APTAC), where the sulfonic acid functional groups were replaced by quaternary ammonium chloride i.e. a strong anion exchange group. The Pu(IV)-sorption efficiency, as well as selectivity towards Pu(IV) in presence of excess U(VI), was found to be higher for HEMP-co-APTAC than with either HEMP or APTAC polymer.

Chapter 4: Anchoring of a thin layer of bi–functional polymer on membrane for alpha spectrometric determination of Pu(IV)

This chapter describes the development of a membrane based alpha spectrometric method for the determination of Pu(IV) in complex aqueous samples. The quantification of Pu(IV) in the complex matrices by alpha spectrometry involves multiple steps, like selective matrix elimination, preconcentration of target actinide and solid alpha source preparation generally by evaporation or electrodeposition. For obtaining good quality alpha spectrum (full width at half maximum of 30–50 keV at 5.5.MeV), it is essential to prepare a thin, flat, uniform alpha source. To minimize the sample manipulation steps, a membrane based alpha spectrometry method was developed for the determination of Pu(IV)in the complex aqueous solutions. The HEMP-AMPS grafted poly(ethersulfone) (PES) membrane was used for preconcentration and subsequent quantification of Pu(IV) by α spectrometry. The choice of PES membrane was based on the fact that PES is UV active and, therefore, suitable for surface grafting and also has a porous structure that would provide high accessibility of binding sites to the complexing ions.

The monomers, HEMP and AMPS in 1:1 mole proportion, were anchored as 1−2 μm thin layer on a microporous PES membrane by photo-induced surface grafting. The thickness of the bifunctional layer on one surface of the poly(ethersulfone) membrane was optimized. The optimized membrane was used for preconcentration of Pu(IV) from aqueous solutions having 3–4 M HNO_3, followed by direct quantification of Pu(IV) in the membrane by alpha spectrometry, either using the absolute efficiency at a fixed counting geometry or by isotope dilution using ^{238}Pu spike. The chemical recovery efficiency of Pu(IV) was found to be 86±3% below Pu(IV) loading capacity (1.08 µg in 2X1 cm^2 of the membrane sample). The experiments with single representative actinides indicated that Am(III) did not sorb to significant extent (7%) but U(VI) sorbed with 78±3% efficiency from the solutions having 3 M HNO_3 concentration. However, Pu(IV) chemical recovery in the membrane remained unaffected from the solution containing 1:1000 wt. proportion of Pu(IV) to U(VI). Pu(IV) concentrations in the (U, Pu)C samples, irradiated fuel dissolver solutions as well as in various environmental and biological matrices were determined by membrane based alpha spectrometry. Membrane based alpha spectrometry significantly reduces analysis time and secondary waste generated since separate purification and alpha source preparation steps are eliminated.

Chapter 5: Magnetically retrievable bi-functional bead for thermal ionization mass spectrometry of Pu(IV)

This chapter describes the synthesis of magnetically retrievable bifunctionalized beads and applications of these beads for analysis of Pu(IV) by single bead based thermal ionization mass spectrometry (SB–TIMS). SB–TIMS offers numerous advantages for the determination of

Pu(IV) in complex aqueous samples such as the matrix and interfering ions removal in a single step, high selective preconcentration of Pu(IV), and also the single resin bead acts as a point source in mass spectrometry. However, the SB–TIMS methods reported in literature are based on the anion-exchange resins that lack the sorption-selectivity towards Pu(IV) and are not easily retrievable form a large volume sample. In this chapter, the synthesis of Fe_3O_4 nanoparticles-embedded, porous PES beads phase inversion technique is described. SPIONs coated with tetraethoxysilane (TEOS), were dispersed through a saturated solution of PES in DMF and the solution was added dropwise to water with continuous stirring to produce magnetic PES beads, having 0.5–1 mm diameter. The PES beads were equilibrated with an equimolar mixture of the two monomers HEMP and APTAC in (1:1) water:ethanol, followed by irradiation in a UV reactor for 15 minutes. The sorption studies indicated that the bifunctionalized PES beads consisting of phosphate and quaternary ammonium groups not only have a higher distribution coefficient (D) for Pu(VI) but also higher selectivity towards Pu(IV) ions with respect to U(VI) ions (D_{Pu}/D_U=11.5). The phosphate functionalized PES bead had comparable selectivity (D_{Pu}/D_U=9.1) but lower D value for Pu(IV). The quaternary ammonium functionalized PES beads were found to have lower selectivity and D values for Pu(IV) ions. The chapter also describes Pu isotopic analysis by SB–TIMS, in which ~1 µg of Pu in 3M HNO_3 medium, was equilibrated with a single bifunctional magnetic PES bead for one hour with continuous stirring. After equilibration, the bead was washed with 3M HNO_3, dried and loaded on a high purity rhenium filament for TIMS analysis. The analytical performance of the SB–TIMS for determination of Pu(IV) was compared with the solution based method, validated using Pu isotopic standard reference material SRM-947, and applied to the real samples such as dissolved solutions and soil leach liquors.

Chapter 6: Development of better polymeric substrates for thermal ionization mass spectrometric determination of Pu(IV)

This chapter describes the development of membrane based thermal ionization mass spectrometric method (Mem–TIMS) for simultaneous preconcentration of Pu(IV) from aqueous matrices, followed by determination of Pu isotopic composition and concentration. The major limitation of single bead–thermal ionization mass spectrometry seemed to be the very high analysis temperature, required for the evaporation of Pu(IV) sorbed in the bifunctionalised PES bead, which is not favorable for the instrument electronics. To overcome this problem, a supported liquid membrane (SLM) was developed for preconcentration of Pu(IV) from aqueous matrices, followed by determination of isotopic composition and concentration by direct loading of the membrane on the filament in TIMS. A thin, porous polypropylene (PP) membrane was chosen as the substrate for SLM, which easily decomposes at the analysis temperature. The PP membrane was dipped in a solution of phosphate based extractants, either tri-ethylhexylphosphate (TEHP) or di- ethylhexylphosphate (DEHP) or a mixture of both in various mole proportions, in ethanol so that the liquid extractant fills the pores of PP membrane. The phosphate functionalized SLMs were found to extract Pu(IV) with ~90% efficiency from ≥3 M HNO_3 medium. However, the selectivity of the SLM towards Pu(IV), in presence of competing actinides like U(VI), was dependent on the composition of the liquid extractants. For TIMS analysis, the phosphate functionalized SLM was equilibrated with 5-100 mL of 3M HNO_3 solutions for 8 hours with continuous stirring, washed and placed on a Re filament. The membrane based TIMS method was employed for the determination of ppb levels of Pu(IV) in groundwater, seawater and soil leach liquor samples, and also in dissolver solution containing large excess of U.

Chapter 7: Conclusion & future scope

The last chapter of the thesis gives the major conclusions of the present work which are summarized as follows:

1. The bi-functional HEMP-co-AMPS and HEMP-co-APTAC polymers were found to be selective for a particular actinide depending on the HNO_3 concentration of the medium. Both HEMP-co-AMPS and HEMP-co-APTAC have better extraction and stripping properties compared to HEMP polymer and sorb Pu(IV) preferentially in the presence of large excess of U(VI) ions.
2. The bi-functional HEMP-co-AMPS polymer was anchored as a thin film on the surface of a poly(ethersulphone) membrane, which served as a good source for quantification of Pu(IV) in complex aqueous matrices by alpha spectrometry. The two surfaces of PES membrane have different morphologies and the glossy surface served as a better alpha source than the rough surface. Membrane based alpha spectrometry was employed for determination of trace amounts of Pu(IV) in various biological & environmental samples and also in irradiated dissolver solution, containing large excess of U.
3. SB–TIMS method was developed for simultaneous preconcentration of plutonium using bifunctional magnetic PES beads, followed by determination of Pu isotopic composition and concentration. SB–TIMS method was found to provide comparable accuracy & precision with respect to the conventional solution based loading technique for TIMS. The method significantly reduces the analysis time & the amount of solid/liquid waste generated is minimized.
4. Phosphate functionalized supported liquid membrane (SLM) was synthesized for selective extraction of actinides from HNO_3 medium. Membrane based TIMS method was developed

for the determination of isotopic composition and concentration of Pu(IV) preconcentrated on the SLM. Mem–TIMS method was employed for the determination of ppb level of Pu(IV) in various complex matrices and the results were found to be comparable with the conventional solution based TIMS method.

References

1. Determination of plutonium isotopes in standard IAEA reference materials by destructive analytical technique; M. H. Nassef, S. A. El Mongy, A. M. Diaband M.S. EL-Tahawy; J. Nucl. Rad. Phy. 3 (2008) 21-30.
2. Current status of alpha-particle spectrometry; E. García-Toraño; App. Rad Iso. 64 (2006) 1273–1280.
3. Isotope ratio analysis of actinides, fission products, and geolocators by high-efficiency multi-collector thermal ionization mass spectrometry; S. Bürger, L.R. Riciputi, D.A. Bostick, S. Turgeon, E.H. McBay, M. Lavelle; Int. J. Mass Spectrom 286 (2009) 70–82.
4. Critical comparison of radiometric and mass spectrometric methods for the determination of radionuclides in environmental, biological and nuclear waste samples; Xiaolin Hou and Per Roos; Anal. Chim. Acta 608 (2008) 105–139.
5. Rapid method for the determination of actinides in soil and sediment samples by alpha spectrometry; N. Vajda, A. Törvényi, G. Kis-Benedek, C.K. Kim, B. Bene and Z . Mácsik; Radiochim. Acta 97 (2009) 395−401.
6. Separation techniques for low-level determination of actinides in soil samples; J. Eikenberg, M. Jäggi, H. Beer, M. Rüthi and I. Zumsteg; Appl. Radiat. Isot. 67 (2009) 776−780.

7. Determination of Pu, Am, U and Cs in large soil samples in the vicinity of the USDOE Waste Isolation Pilot Plant; P. Thakur and G. P. J. Mulholland; Radioanal. Nucl. Chem. 288 (2011) 499−506.
8. Rapid and automated sequential determination of ultra-trace long-lived actinides in air filters by inductively coupled plasma mass spectrometry; D. Larivière, K. Benkhedda, S. Kiser, S. Johnson, and R. Cornett; Anal. Methods 2 (2010) 259−267.
9. Bead injection extraction chromatography using high-capacity lab-on-valve as a front end to inductively coupled plasma mass spectrometry for urine radiobioassay; J. Qiao, X. Hou, P. Roos and M. Miro; Anal. Chem. 85 (2013) 2853−2859.
10. Cloud point extraction of plutonium in environmental matrixes coupled to icpms and α spectrometry in highly acidic conditions; C. Labrecque, L. Whitty-Léveillé and D. Lariviré; Anal. Chem. 85 (2013) 10549−10555.
11. Actinide sequestration by self-assembled monolayers on mesoporous supports; G.E. Fryxell, Y. Lin, S. Fiskum, J.C. Birnbaum, H. Wu, K. Kemner and S. Kelly; Environ. Sci. Technol. 39 (2005) 1324−1331.
12. Extraction of lanthanides and actinides by a magnetically assisted chemical separation technique based on CMPO-calix[4]arenes; S.E. Matthews, P. Parzuchowski, A. Garcia-Carrera, C. Grüttner, J. Dozol and V. Böhmer; Chem. Commun. Issue 5 (2001) 417−418.
13. Graphene oxide for effective radionuclide removal; A.Y. Romanchuk, A.S. Slesarev, S.N. Kalmykov, D.V. Kosynkin and J.M. Tour; Phys. Chem. Chem. Phys. 15 (2013) 2321–2327.

LIST OF FIGURES

LIST OF TABLES

Chapter 1

Introduction

1.1. Occurrence of Actinides

The actinide series comprises of 15 elements, from actinium to lawrencium, with atomic numbers ranging from 89 to 103. Among the actinides, thorium and uranium occur naturally in the earth's crust in substantial quantities. Uranium occurs in the earth's crust as a mixture of its oxides in the minerals uraninite, which is also called pitchblende because of its black color; whereas the most abundant thorium mineral is monazite. However most thorium minerals contain uranium and vice versa. The radioactive decay of uranium produces transient amounts of actinium and protactinium, whereas neptunium, americium, curium, berkelium and californium are occasionally produced from transmutation reactions in uranium ores. All other actinides are purely synthetic elements. Apart from naturally occurring uranium and thorium, synthetically produced plutonium is another actinide present on earth. All actinides are radioactive and release energy upon radioactive decay; uranium, plutonium and thorium are used in nuclear reactors and for nuclear weapons, and americium is used in the ionization chambers of most modern smoke detectors. All the actinides are radioactive and therefore require special care in their handling.

Transuranium isotopes are present in the environment on a global scale from nuclear weapons testing and satellite failure and on a local scale from nuclear operations and accidents. The high level waste (HLW) generated during spent nuclear fuel reprocessing contains unextracted U, Pu, various minor actinides such as Am, Np, Cm, and a host of fission product such as lanthanides, Tc, Pd, Zr, I, Cs, and Sr, along with activation products (Ni, Sb, Zr), structural elements (Fe, Ni,Co, Zr), and process chemicals (salts of Fe, Al, and Na). Since the present levels of contamination are typically low from the points of determination and radiological safety, sensitive analytical techniques are needed for the exact measurement. Plutonium has four long-lived α-emitting isotopes viz. ^{238}Pu ($t_{1/2}$ = 87.74 years), ^{239}Pu ($t_{1/2}$ =

24110 years), ^{240}Pu ($t_{1/2}$ = 6564 years) and ^{242}Pu ($t_{1/2}$ = 3.7x10^{5} years) and one β-emitting isotope in the environment, viz. ^{241}Pu ($t_{1/2}$ = 14.4 years), which are produced in nuclear reaction and decay processes according to the following equations:

$$^{238}U(n,\gamma)^{239}U \xrightarrow{\beta} {}^{239}Np(n,\gamma)^{239}Pu$$

$$^{239}Pu(n,\gamma)^{240}Pu(n,\gamma)^{241}Pu \xrightarrow{\beta} {}^{241}Am$$

$$^{235}U(n,\gamma)^{236}U \xrightarrow{\beta} {}^{236}Np(n,\gamma)^{237}Np(n,\gamma)^{238}Np \xrightarrow{\beta} {}^{238}Pu$$

^{241}Am ($t_{1/2}$ = 432 years) is a long-lived nuclide, which is the daughter product of ^{241}Pu ($t_{1/2}$ = 14.4 years). Due to the short half life of ^{241}Pu, there would be an increase in the level of ^{241}Am in the environment contaminated by Pu from nuclear explosions, authorized or accidental releases. Neptunium has one long-lived, α-emitting isotope ^{237}Np ($t_{1/2}$ = 2.14 x10^{6} years) that is present in the environment. ^{237}Np is produced by α -decay of ^{241}Am. ^{237}Np is also produced both from ^{238}U by fast neutron reaction and from ^{235}U by successive neutron capture and β-decay:

$$^{238}U \xrightarrow{(n,2n)} {}^{237}U \xrightarrow{\beta} {}^{237}Np$$

$$^{235}U \xrightarrow{(n,\gamma)} {}^{236}U \xrightarrow{(n,\gamma)} {}^{237}U \xrightarrow{\beta} {}^{237}Np$$

Accurate and rapid determination of actinides in the environment is becoming exceedingly important with the rising possibilities of contamination and public concern over the potential hazards, owing to the increased energy production by nuclear reactors all over the world, nuclear fuel reprocessing and waste disposal. A large number of analytical methods have been developed and applied for the determination of uranium, plutonium, neptunium and americium isotopes in environmental and nuclear samples using radiometric techniques like alpha, beta and gamma spectrometry, mass spectrometric techniques, X-ray spectrometry and neutron activation analysis. However separation and preconcentration of the target actinide is often necessary prior to its quantitative analysis, in order to eliminate all possible radioactive and non-radioactive interferences. The most important actinides that are used in large quantities are U and Pu and, therefore, their monitoring in the nuclear fuel cycles, geological, environmental and biological samples are of utmost importance. Monitoring of Am is also important as it is invariably associated with Pu as its decay product as discussed above.

1.2. Solution Chemistry of U, Pu and Am

Pu is the sixth member of the actinide group. In aqueous solutions Pu exists in the +3, +4, +5, and +6 oxidation states, the most stable form being Pu(IV). Because of the small difference (0.9 – 1.1 V) in the standard electrode potentials of various oxidation states of Pu in acidic solutions, they can coexist in solutions or can be turned to a given state by slightly modifying the redox conditions. The possibility of changing the oxidation state is of supreme importance in Pu radiochemistry, since the separation processes can be controlled by selectively maintaining a single oxidation state. The formation of complex ions in aqueous solutions with inorganic or organic ligands is another important feature of Pu chemistry. The ability of the various species to form complexes is dependent on the ionic potential. The relative complex forming tendency of Pu species is as follows:

$$\mathrm{Pu(IV)} > \mathrm{Pu(III)} \approx \mathrm{Pu(VI)}\ (\mathrm{PuO_2}^{2+}) > \mathrm{Pu(V)}\ (\mathrm{PuO_2}^{+})$$

The stability series of the inorganic complexes of tri-, tetra and hexavalent actinides are the same: OH^- > carbonate > oxalate > F^-, acetate$^-$ > SO_4^{2-} > NO_3^- > Cl^- > ClO_4^-.

There are small differences among the stability constants of the different actinides in same oxidation states. However, formation of a species is influenced by many parameters e.g. sample composition, presence of redox reagents, amount and stability of the reagents, kinetics of the process, etc. Grate et al. [1] determined the conditions for on-column oxidation of Pu(III) to Pu(IV) using $NaNO_2$, and studies on several reducing agents revealed rapid, quantitative on-column reduction of Pu by Ti(III). Lee et al. [2] investigated the oxidation states of Pu in hydrochloric acid medium by UV-visible-NIR absorption spectroscopy and found that oxidized Pu(VI) was reduced on-column by the anion exchange resin; similar conclusions were drawn on the interaction of Pu(VI) and UTEVA-extraction chromatographic resin [3]. Since tetravalent actinides have the highest complexing power, the adjustment of this valence state plays a crucial role in many separation procedures. Strong reducing agents e.g., hydrazine, hydroxylamine etc are adequate for the adjustment of the Pu(III) oxidation state. Trivalent Pu can be oxidized back to tetravalent species by various oxidizing agents. To stabilize the Pu(IV) state without further oxidizing it to Pu(V) or Pu(VI), only a few moderately strong oxidizing agents can be used, e.g., $NaNO_2$ can be added to nitric acid solutions and/or H_2O_2 can be added to hydrochloric acid solutions [4].

U is the fourth member of the actinide group. In aqueous solutions U exists in the +3, +4, +5, and +6 oxidation states, the most stable form being U(VI). Aqueous solutions containing U^{3+} ions rapidly oxidize with the evolution of hydrogen. U^{4+} ions are stable in aqueous solutions in absence of any oxidation agents like dissolved oxygen. Aqueous solutions of UO_2^{+} are prone to disproportionation and the range of stability of U(V) is therefore small. The relative stability of the various oxidation states of uranium strongly depends on the pH of the solution and the presence of complexing ligands. The rate of the redox transformations between the different oxidation states of uranium is rapid when there is no change in chemical composition between the oxidized and reduced forms, otherwise it is very slow. For example the reactions ($UO_2^{2+}+e^- =$

UO_2^+) and ($U^{4+}+e^- = U^{3+}$) are fast, while ($UO_2^{2+}+4H^++2e^- = U^{4+}+2H_2O$) is slow. The relative complex forming tendency of various U species is as follows:

$$U(IV) > U(VI) (UO_2^{2+}) >> U(III) > U(V) (UO_2^+)$$

The relative stability of the inorganic complexes of tri-, tetra and hexavalent actinides are the same: $F^- >> Cl^- > Br^- > F^- \approx I^-$; O >> S, Se > N >> P.

Am is the seventh member of the actinide group, the chemical “analogue” of the lanthanide Eu with similar electronic configurations (Am, $5f^27s^2$) and ionic radii (Am^{3+}, 98 nm). In aqueous solutions Am can exist in +3, +4, +5 and +6 oxidation states. Although Am(III) can be oxidized theoretically to Am(IV), the standard electrode potential of the Am^{4+}/Am^{3+} couple in acidic solution is very high (2.44 V), and in basic solution is significantly lower (0.4-0.5 V). Hence, the formation of Am(IV) is possible in basic solutions, in the presence of strong complexing agents, e.g., phosphates, but the species is unstable and will be reduced back to the trivalent state easily [5]. In aqueous solutions, Am can be oxidized to penta- and hexavalent states, forming the oxocations AmO_2^{2+} and AmO_2^+ respectively. In acidic solutions, the standard electrode potentials of the Am(V)/Am(III) and the Am(VI)/Am(III) couples are 1.74 and 1.69 V, respectively, that allows the formation of both species, but Am(V) disproportionate in acidic solutions as follows:

$$3AmO_2^+ + 4H^+ = 2AmO_2^{2+} + Am^{3+} + 2H_2O$$

Thus, the most stable form of Am is the trivalent state. In acidic solutions, Am(III) and Am(VI) can coexist while oxidized Am(V) and Am(VI) species are more stable in basic solutions. To oxidize Am to Am(VI), very strong oxidizing agent, e.g., Ag catalyzed $K_2S_2O_8$, is needed [6]. The formation of complex ions in aqueous solutions with inorganic or organic ligands is an important property of Am. The relative complex forming tendency of Am species depending on the ionic potential is as follows:

$$\mathrm{Am(VI)\ (AmO_2^{2+}) \approx Am(III) > Am(V)\ (AmO_2^{+})}$$

The absence of the tetravalent Am species and the chemical similarity of Am with lanthanides influence the separation possibilities of Am in spent nuclear fuel. The stability constants of various complexes of Am(III) with inorganic and organic complexing agents are reported by Myasoedov et al. [7]. The stability series of the inorganic complexes of Am(III) is the same as that of other actinides:

$$\mathrm{OH^-, CO_3^{2-} > F^-, HPO_4^{2-}, SO_4^{2-} > Cl^-, NO_3^- > ClO_4^-}$$

Thiocianate (SCN) complexes of Am do not have high stability but, because of the relatively high separation factors toward lanthanides, play an important role in Am chemistry.

1.3. Monitoring of actinides in aqueous streams

The most common methods for the determination of natural and anthropogenic radionuclides, in nuclear as well as environmental samples, are radiometric techniques like gross alpha and beta counting using either scintillation or proportional counters, alpha spectrometry and gamma spectrometry etc. Inorganic mass spectrometric techniques like thermal ionization mass spectrometry (TIMS) or inductively coupled plasma mass spectrometry (ICP-MS) are also widely used for the monitoring of actinides. For the determination of many specific actinides, both radiometric and mass spectrometric methods can be used. However the selection of method depends on several factors including detection limit, analytical accuracy and precision, and accessibility of the method. In addition, the sample preparation procedure, analysis time, plausible interferences, labour and cost effectiveness are also considered in the choice of analytical method. The principles and applicability of various radiometric and mass spectrometric methods for the determination actinides are discussed below.

1.3.1. Liquid Scintillation Counting

Liquid scintillation counting (LSC) is the technique of measurement of alpha and/or beta activity of a radioactive material, where the analyte is mixed with a liquid scintillator in order to allow efficient counting due to the intimate contact of the alpha/beta particles with the scintillator molecules and the resultant photon emissions are measured by a photomultiplier tube (PMT). The samples are either dissolved or suspended in a "scintillation cocktail" containing a solvent, typically benzene or toluene, and small amounts of “fluors or scintillators” and “wavelength shifter” [8]. The alpha/beta particle transfers kinetic energy to a solvent molecule and that energized solvent molecule then transfers the captured energy to other solvent molecules until the energy is finally transferred to a scintillator. The scintillator, following absorption of the transferred energy, will emit photons generally of wavelength lower than the working range of the PMT i.e. visible range. Therefore, scintillation cocktail contains a secondary phosphor, generally known as “wavelength shifter”, that absorbs the fluorescence energy of the scintillator and re-emit at a higher wavelength.

Figure 1.1. shows a schematic diagram of a typical liquid scintillation counter. The radioactive sample is mixed with the scintillation cocktail in a transparent, generally glass or plastic, vial that is placed inside the liquid scintillation counter (LSC). Most of the counters have two PMTs connected in a coincidence circuit. The coincidence circuit assures that genuine light pulses, which reach both the PMTs, are counted while spurious pulses, which would only affect one of the tubes, are ignored. Counting efficiency for the alpha particles is generally 100%, owing to its very short range; whereas counting efficiencies for beta particles vary depending on

its energy and can range from about 30% for ^{32}P ($E_{\beta,Max}$=1.709 MeV) to nearly 100% for ^{3}H ($E_{\beta,Max}$=18.6 keV) [8]. High-energy beta emitters, e.g. ^{32}P, can also be counted in a scintillation counter using an aqueous solution instead of a scintillation cocktail. This technique is known as Cherenkov counting, where the Cherenkov radiation associated with the high energy beta particles is detected directly by the PMTs, however the sample geometry can create variations in the output.

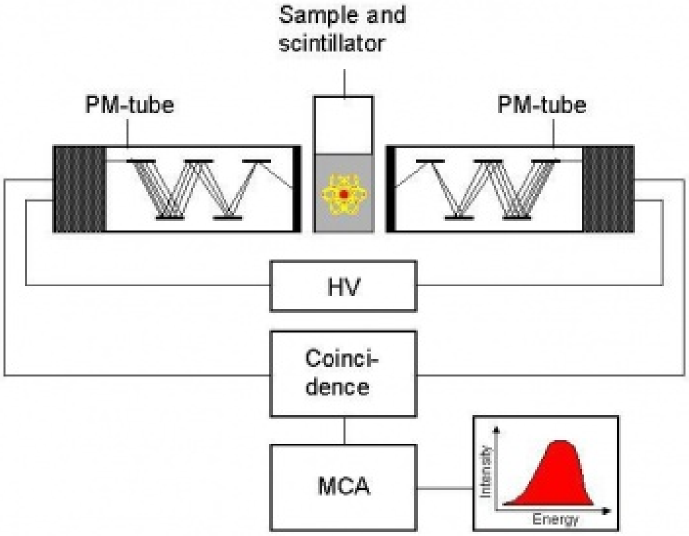

Figure 1.1. Liquid scintillation counting system for alpha and beta counting

Liquid scintillation counters have major advantages such as (i) high counting efficiency, (ii) minimum attenuation and self-absorption due to the mixing of the radioactive sample and the liquid scintillator which offers the unique possibility to detect low-energy β particles. Although, there exists some drawbacks e.g. high background, low energy resolution and quench effect. Commercial liquid scintillation counters, with favorably low or ultralow background, are used for the measurement of ^{241}Pu that emits weak β radiation ($E_{\beta,Max}$=20.8 keV). Liquid scintillation counting system has been developed for on-line detection of actinides in flowing organic solutions emerging from continuous rapid chemical separations by liquid-liquid extraction [9]. Detection limits of about 20 and 30 mBq were reported by Moreno et al. [10] and Hou et al. [11], respectively.

1.3.2. Alpha Spectrometry

In alpha spectrometry, the kinetic energy of an alpha particle is converted to an electronic signal, generally termed as a pulse, via semiconductor detector such that the height of pulse produced is proportional to the alpha energy and the number of pulses per unit time is proportional to the quantity of the parent radioisotope. For high resolution alpha spectrometry, semiconductor detectors, either silicon surface barrier (SSB) or passivated ion-implanted planar silicon (PIPS), coupled with high vacuum system and stable electronics are used [8]. As shown in Figure 1.2, the detector and alpha source are placed inside a vacuum chamber and the spectrum is recorded at a typical pressure of about 10^{-6} bar. The detector is connected to a preamplifier, an amplifier and a multi-channel analyser (MCA) for pulse height analysis.

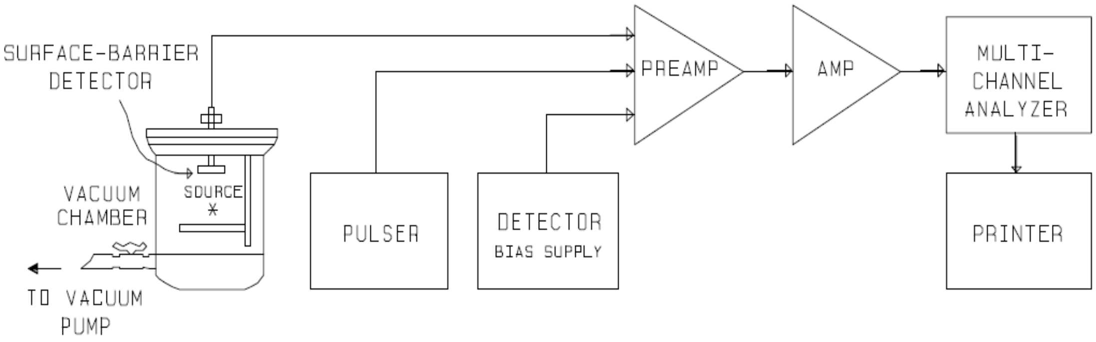

Figure 1.2. Block diagram of a typical alpha spectrometry system

Alpha spectrometry is one of the oldest, most widely used, and most sensitive nuclear analytical technique for the determination of alpha-emitting actinides e.g. ^{238}Pu, ^{239}Pu, ^{240}Pu, ^{242}Pu and ^{241}Am. The major advantages of alpha spectrometry are high sensitivity due to low background, high selectivity for alpha particles against other types of radiation and relatively low price of the equipment. Detection limits as low as 1 mBq/sample can be achieved using Si detectors, provided the sample chamber is free of contamination and counting time is around a couple of days [12]. However, because of similar energies of the alpha particles emitted by ^{239}Pu (5.16 MeV, 71%) and ^{240}Pu (5.17 MeV, 73%), these isotopes cannot be distinguished by standard Si detectors. Also significant overlapping between the alpha peaks of ^{238}Pu (5.46 MeV, 29.0% and 5.50 MeV, 71.0%) and ^{241}Am (5.44 MeV, 12.8% yield and 5.49 MeV, 85.2%) cannot be spectrometrically resolved [13-15]. Another major disadvantage of alpha spectrometry originates from the necessity of very thin, preferably monolayer source, which requires complete separation of the analytes from the matrix. Because of very short range of alpha particles in matter, the source thickness should not exceed a few micrometers otherwise alpha spectrum becomes degraded causing left-side tailing of peak and spectral resolution worsens [8]. Radiochemical separations and good quality alpha source together can ensure the quality of alpha spectrometric analysis. Separation techniques, often fairly sophisticated ones, have to be applied to remove major and minor components from the samples. The major spectral interferences in alpha spectrometric analysis of Pu can be ^{241}Am, ^{210}Po and ^{228}Th, partially overlapping with the ^{238}Pu alpha peak. Occasionally other radionuclides e.g., ^{224}Ra, ^{229}Th, ^{231}Pa, ^{232}U and ^{243}Am can also interfere in the Pu alpha spectrum. Traces of U, Th, and Np can contaminate the Pu source if chemical separations are not effective. For ^{241}Am, major interferences could be ^{228}Th, ^{210}Po etc. other than ^{238}Pu. ^{232}U (E_α=5.32 MeV, 61.8%) may also partially interfere at ^{241}Am alpha peak.

1.3.3. Gamma Spectrometry

Most of the radioactive sources produce gamma rays of various energies that are characteristic of the radionuclide present in the source, and intensities of gamma rays can be correlated with the amount of radionuclide. Gamma spectroscopy involves detection of these gamma emissions, followed by subsequent quantification of the radionuclides in the source. Gamma spectroscopy is extensively used for radiometric assay at the various stages of nuclear industry, geochemical investigation and astrophysics. The most commonly used gamma detectors are thallium doped sodium iodide (NaI/Tl) scintillation counters and high-purity germanium (HPGe) semiconductor detectors [8]. Gamma photons do not have any intrinsic charge and, therefore, cannot cause direct ionization or excitation of the medium through which it is passing; rather the measurement of gamma photons is dependent on their interaction with the electrons present in the neighboring medium.

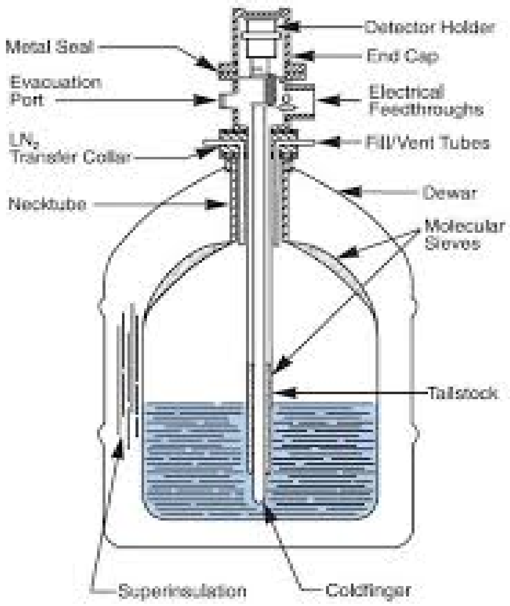

Figure 1.3. Block diagram of a typical high purity Ge (HPGe) detector

The schematic of a typical HPGe detector is shown in Figure 1.3. Similar to alpha spectrometer, the gamma detector is also connected to preamplifier, amplifier and multi-channel analyser (MCA) for pulse height analysis. The voltage pulse produced by the gamma photon in a detector is shaped by a multichannel analyzer (MCA). The multichannel analyzer receives the very small voltage signal produced by the detector, reshapes it into a Gaussian or trapezoidal shape, and converts that signal into a digital signal.

The n-type Ge detectors having thin Be windows and well-type geometry provides high counting efficiency, which in turn provides high sensitivity. Several reports were published for the determination of 0.05–1 Bq/g or higher levels of ^{241}Am in various matrices, like environmental, biological, geological, waste materials, river water, nuclear fallout etc. by gamma ray spectrometry using a high-resolution HPGe detector [16–20]. However, because of the relatively low energy of ^{241}Am gamma ray, self-absorption correction should be performed to obtain accurate analytical results [21–23]. ^{238}Pu, ^{239}Pu, ^{240}Pu and ^{241}Pu emit low energy gamma rays. Direct measurement of the gamma photons of Pu isotopes requires low energy photon detectors and can be employed only if the source has very high activity, e.g. spent fuel, due to very low abundance of Pu gamma rays [24, 25].

1.3.4. Mass Spectrometry

Mass spectrometry (MS) is an analytical technique, for the identification as well as quantification of the components present in a sample, on the basis of mass-to-charge (m/z) ratio and abundance of gas-phase ions [26]. These ions form sample, which may be in the form of either solid, liquid or gas, are separated according to their m/z ratio, typically by accelerating them under an electric or a magnetic field where all the ions having same m/z ratio will undergo the same amount of deflection. The beam of ions having same m/z ratio is then detected by a mechanism capable of detecting charged particles, such as a secondary electron multiplier, channeltron or Faraday cup. The mass spectrum is a plot of the relative abundance of detected ions as a function of the m/z ratio, which can be used for obtaining the information about elemental/isotopic composition of a sample, the masses of molecules, and to elucidate the chemical structures of large molecules such as peptides and other chemical compounds.

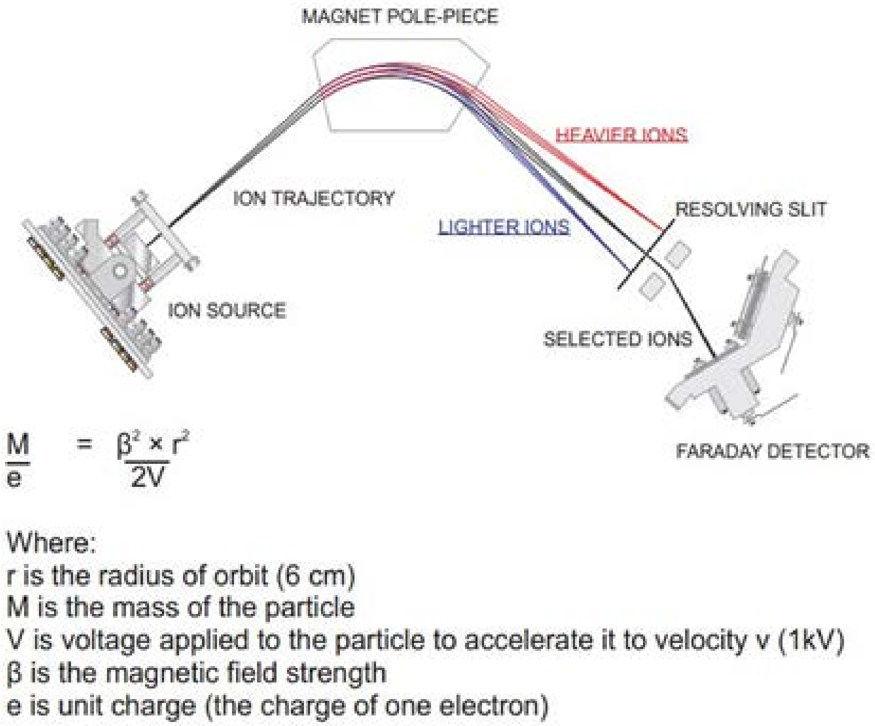

$$\frac{M}{e} = \frac{\beta^2 \times r^2}{2V}$$

Where:
r is the radius of orbit (6 cm)
M is the mass of the particle
V is voltage applied to the particle to accelerate it to velocity v (1kV)
β is the magnetic field strength
e is unit charge (the charge of one electron)

Figure 1.4. Block diagram of a thermal ionization mass spectrometer (TIMS)

As shown in Figure 1.4, a mass spectrometer consists of three components viz. an ion source, a mass analyzer and a detector. The ionizer converts a portion or whole of the sample into ions. There are many types of ionization methods used in mass spectrometry. The classic methods that most chemists are familiar with are Electron Impact (EI) and Fast Atom Bombardment (FAB). However these techniques are not popular in modern mass spectrometry, except EI employed for analyses of environmental samples by GC-MS. The techniques like atmospheric pressure chemical ionization (APCI), electrospray ionization (ESI), matrix assisted laser desorption ionization (MALDI) and other derivative methods have taken their place in the modern mass spectrometry laboratory. Others ionization methods include photoionization, glow discharge, desorption/ionization on silicon (DIOS), direct analysis in real time (DART), atmospheric pressure chemical ionization (APCI), secondary ion mass spectrometry (SIMS), spark ionization and thermal ionization (TIMS). Thermal ionization, also known as surface ionization or contact ionization, is a physical process whereby the atoms are desorbed from a hot surface, and in the process are spontaneously ionized. Spark ionization, also known as spark source ionization, is a method used to produce gas phase ions from a solid sample. The solid sample is vaporized and partially ionized by an intermittent discharge or spark. The differences in masses of the ions allow the mass analyzer to sort the ions by their m/z ratio. The detector measures the ion current and provides data for calculating the abundances of each ion present.

Thermal ionization mass spectrometry (TIMS) and inductively coupled plasma mass spectrometry (ICP-MS) are widely used for the determination for actinides [27–37]. In TIMS, the sample solution is loaded on a filament, commonly Re or Ta, followed by evaporation and ionization of the sample by heating the filament at an appropriate temperature. Generally the mass analyser in TIMS is a magnetic sector which is essential for providing "flat-topped" peaks for the masses, required for high-precision isotope ratios. In ICP-MS, sample is introduced through a nebulizer to produce a very fine aerosol, followed by introduction into an Argon plasma (~ 8000ºC) for ionization. For high precision analyses, simultaneous collection of all the isotopes of interest is very important, since intensities of the ion beams are susceptible to any small variation in the instrumental parameters during analysis.

1.3.5. Comparison of radiometric and mass spectrometric techniques for determination of actinides

Extensive studies have been carried out for critical comparison of the advantages and drawbacks of determination of actinides by various radiometric and mass spectrometric techniques [38–40], however good agreement of the results was achieved if the sample preparation method and sensitivity range of the given facility were suited to the analytical demands. In general, the radiometric methods are generally more sensitive for radionuclides having shorter half lives, while mass spectrometric methods are more appropriate for radionuclides having longer half lives. Due to the high sensitivity, accuracy and the easy access and cost-effectiveness of the radiation detectors, determination of short-lived radionuclides ($t_{1/2} <$ 10 years) and especially of those with gamma emissions is carried out only by radiometric methods.

Alpha spectrometry is the most frequently used technique for the routine determination of alpha emitting transuranium isotopes due to the relatively high sensitivity, selectivity, low detection limits and the relatively low cost instrumentation. Alpha spectrometry is especially useful for the measurement of Pu nuclides having high specific activities, e.g. it is the most sensitive technique for measurement of ^{238}Pu. All alpha emitting Pu isotopes, ^{238}Pu, ^{239}Pu, ^{240}Pu, and radioactive Pu tracers e.g., ^{236}Pu, ^{242}Pu, can be measured by alpha spectrometry. However by alpha spectrometry, the overlapping peaks of ^{239}Pu and ^{240}Pu cannot be resolved. Also determination of the long-lived uranium isotopes, viz. ^{234}U, ^{235}U and ^{238}U by alpha spectrometry is not amenable due to very long counting time and high activity requirements, though relatively short-lived ^{233}U can be easily determined [41]. Alpha spectrometry is also the method of choice for sensitive determination of ^{241}Am due to its high specific activity. Gamma spectrometry is another simple method for the determination of ^{241}Am (E_γ = 59.6 keV), but absorption and self–absorption of the low energy gamma radiation has to be taken into account, and sensitivity of gamma spectrometry for ^{241}Am is relatively low because of the high background of the gamma spectrometers. Gamma spectrometry is not suitable for the determination of low energy and low abundant gamma rays emitted by Pu isotopes.

When better resolution or higher sensitivity is required, mass spectrometric techniques sometimes offer better possibilities. ICP-MS has become an alternative technique for the determination of Pu isotopes. The detection limit of a typical quadrupole ICP-MS (Q-ICP-MS) is 10-100 fg/mL [42], which is comparable to the sensitivity of alpha spectrometry for ^{240}Pu ($t_{1/2}$ = 6564 years). Sensitivity of Q-ICP-MS for ^{239}Pu and ^{240}Pu is also similar to that of alpha spectrometry, but the advantage is ^{239}Pu/^{240}Pu ratio can be measured by ICP-MS, which is not possible by alpha spectrometry. On the other hand, in a mixture of ^{238}U and Pu, ^{238}Pu cannot be determined by ICP-MS due to isobaric interference, but can be determined by alpha spectrometry. Therefore these two techniques are complementing and not replacing each other. The detection limit of the high-performance sector field (SF) and multicollector (MC) ICP-MS facilities is about 1 to 2 orders of magnitude lower than that of Q-ICP-MS [43], which makes SF-ICP-MS superior to alpha spectrometry provided there is no isobaric interference. The major interference in ^{239}Pu determination is ^{238}U due to tailing and formation of UH^+, and the overall sensitivity of the method depends on the chemical purity of Pu. Although mass spectrometric techniques have generally low sensitivity for the ^{241}Am. The detection limit of SF-ICP-MS is ~1 fg/mL [11], i.e. 0.1 mBq/mL of ^{241}Am, which is again comparable to the sensitivity of alpha spectrometry for ^{241}Am. However the main difficulty in ICP-MS originates from isobaric and polyatomic interferences such as $^{241}Pu^+$, $^{240}Pu^1H^+$, $^{206}Pb^{35}Cl^+$, $^{204}Pb^{37}Cl^+$, and $^{205}Ti^{36}Ar^+$ etc. The major isobaric interference for ^{241}Am is due to ^{241}Pu and hence accurate determination of ^{241}Am by ICP-MS is possible only if high chemical purity of Pu is assured by proper separation technique.

TIMS has higher sensitivity for determination of ^{239}Pu and ^{240}Pu than ICPMS [44], and interferences due to U traces are less significant, but it requires a tedious sample preparation to produce the source in the form of a thin filament. Also, sample has to be in highly pure form in order to have good sensitivity, which requires rigorous sample pretreatment and separation steps prior to sample analysis. However, application of these MS techniques is limited by the limited number and availability of very sophisticated facilities. Chartier et al. [44] determined Am and Cm in spent nuclear fuel and compared ICPMS with TIMS. He demonstrated that TIMS is the most accurate method for isotope ratio measurement, but ICPMS results agreed with those of TIMS within 2.55% depending on the concentration ratios.

Table 1.1. Major interferences in determination of actinides by alpha spectrometry and mass spectrometry

Detection method	Radioisotopes (Energy in MeV)	Interferences (Energy in MeV)
Alpha spectrometry		
Spectral interferences	^{239}Pu (5.244)	^{240}Pu (5.255)
	^{228}Th (5.520)	^{241}Am (5.464), ^{243}Am (5.438)
	^{229}Th (5.168)	$^{239-240}$Pu (5.244-5.255)
	^{234}U (4.856)	^{237}Np (4.957)
	^{235}U (4.679)	^{244}Pu (4.665)
	^{237}Np (4.957)	^{242}Pu (4.983), ^{234}U(4.856)
	^{228}Th (5.520)	^{241}Am (5.464)
Matrix interferences (HF co-precipitation)	LnF_3, MgF_2, CaF_2, SrF_2, BaF_2, PbF_2	
ICP–MS		
Isobaric interferences	^{238}U	^{238}Pu
	^{241}Pu	^{241}Am
	^{243}Am	^{243}Cm
Polyatomic interferences	^{239}Pu	$^{238}U^{1}H$
	^{233}U	$^{232}Th^{1}H$
Abundance sensitivity interferences	^{237}Np, ^{239}Pu	^{238}U
	^{231}Pa, ^{233}U	^{232}Th

Traditional methods of quantification of actinides, including radiometry and mass spectrometry, requires sophisticated separation procedures to remove major and minor interfering components from the sample. Potentially, ^{239}Pu, ^{240}Pu, ^{242}Pu, ^{238}Pu, ^{233}U, and ^{241}Am are all amenable to determination by either alpha spectrometry or mass spectrometry, however the major interferences are different. For ^{239}Pu and ^{237}Np, ^{238}U is the most important interference due to the formation of the polyatomic UH^+ species and the spectral interference, respectively. The determination of ^{238}Pu is encumbered by serious isobaric interference from ^{238}U. The determination of ^{241}Am requires also very efficient separation from parent ^{241}Pu and treatment of larger sample masses to compensate for the typically low atom concentration. The requirements for purity are generally lower for many elements in case of ICP-MS compared to alpha spectrometry, but extremely high decontamination factors are required against the interferences like U, Pb, Hg, Tl, rare earth elements, or other actinides, in order to avoid isobaric or polyatomic interferences and to improve abundance sensitivity. A summary of the possible interferences encountered during the quantification of actinides by alpha spectrometric and mass spectrometric methods are listed in Table 1.1. To meet the demands of such high chemical purity, extensive matrix separation and sample purification methods are required, before unequivocal identification of specific actinide isotopes and their relative abundances.

1.4. Chemical Separation of Actinides

Actinides are amenable to a variety of chemical separation procedures including precipitation/coprecipitation, liquid-liquid extraction, ion-exchange chromatography, extraction chromatography, and a combination of two or more of these methods. Prior to chemical separation, sample pretreatment is important in order to obtain a homogeneous sample solution without any significant loss of the analyte, to ensure absence of any organic material that could form complexes with the analyte or the reagents and to remove any insoluble residues that would interfere during the subsequent chemical processing. For soil or sediment samples, pretreatment usually involves drying in an oven, homogenizing, sieving and removal of organic material by ashing followed by wet chemical destruction. In case of actinides, samples are usually ashed at 450-600 ºC for a couple of hours or days. Elevated temperatures are not desirable as that may lead to the formation of refractory particles.

For dissolution, several methods have been used including acid leaching with mineral acids, most frequently with 8 M HNO_3 [45–47] or aqua regia [34, 48, 49], or a mixture of mineral acids typically including nitric, hydrochloric, and hydrofluoric acids and hydrogen peroxide [50–52]. The most appropriate destruction technique for rapid and complete sample decomposition for the determination of actinides is fusion [53]. Significantly higher temperatures compared to the boiling points of the aqueous systems can be achieved by fusion with a variety of salts, like NaOH, $LiBO_2$, carbonate-borate an KF/pyrosulfate, thus speeding up the destruction process [54–56]. However, large amount of salts, often together with impurities, are transferred to the sample solution that may create problem during the subsequent chemical separation and quantification. Also relatively small amount of sample can be treated. In case of biological samples, complete destruction is usually carried out by combination of dry and wet chemical ashing. For efficient decomposition of organic materials, either Fenton's reaction using hydrogen peroxide and Fe^{2+} catalyst, or microwave digestion is employed [57–59]. A typical procedure used for the quantification of actinides in the environmental samples is shown in Scheme 1.1.

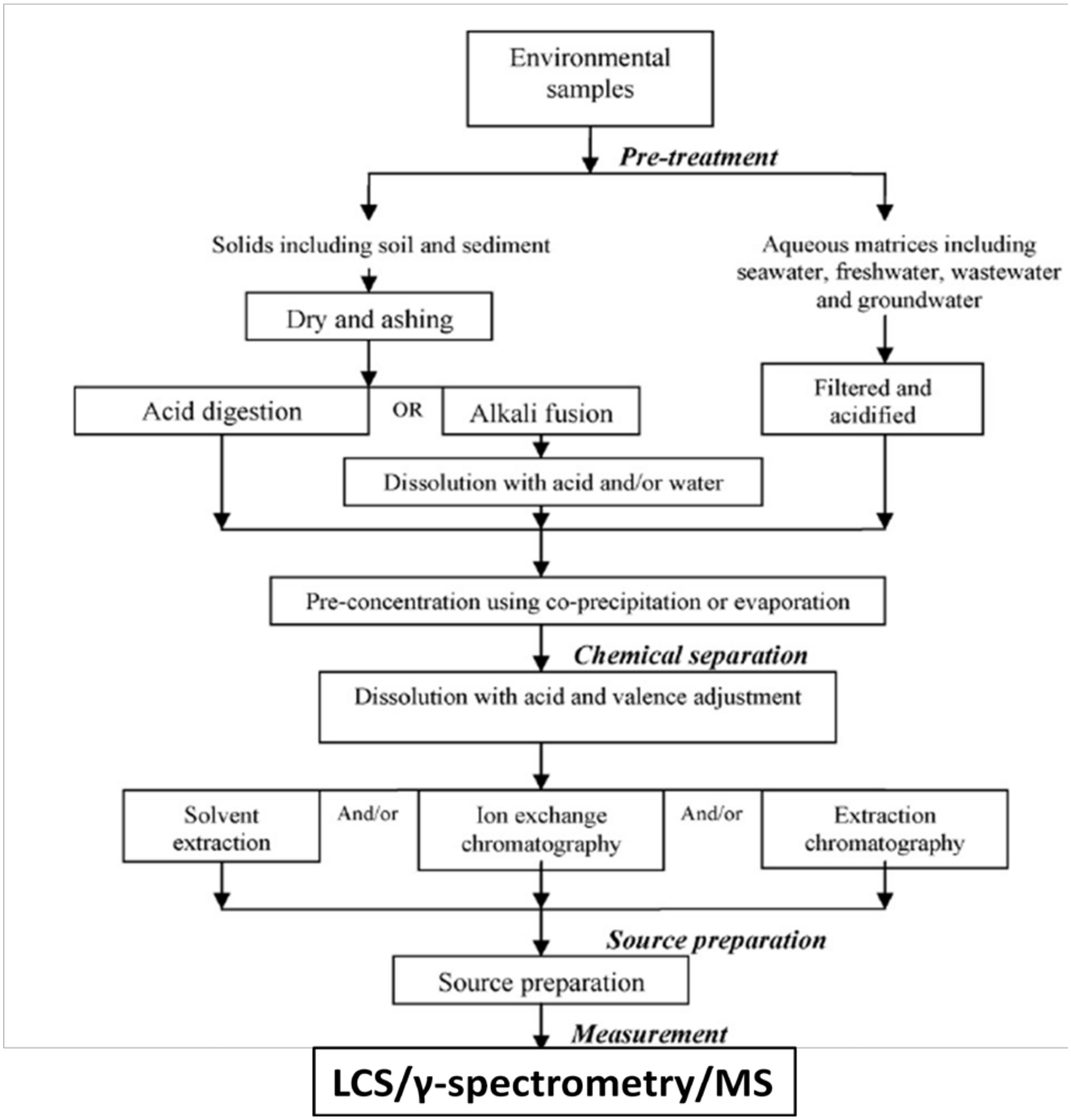

Scheme 1.1. Flow chart of the analytical procedure for determination of actinides in environmental sample

1.4.1. Coprecipitation

Preconcentration of actinides by coprecipitation is frequently used for large volume aqueous samples as well as for sample solutions obtained after destruction of solid samples. A well-selected coprecipitant concentrates the analyte in a small volume, removes most of the cationic and anionic interferences, and increases the decontamination factor (DF) of the radiochemical procedure. Bismuth phosphate was the first precipitant applied in large scale processing of Pu, and was used to separate Pu from U and other fission products [60, 61].

The most frequently used carriers of actinides are ferric and ferrous hydroxides [32, 62–65], lanthanide fluorides and hydroxides [34], alkaline earth oxalates [47, 66, 67], phosphates [68, 69], and fluorides [3, 19, 70, 71], barium sulfate, and manganese dioxide [72, 73]. Ferric hydroxide is known to coprecipitate actinides in all oxidation states, but sometimes recoveries are low and hence ferrous hydroxide, which can act as a reducing agent itself, is preferred. Hydroxide, phosphate, and carbonate precipitates can be easily dissolved with acids, whereas fluoride precipitates can be dissolved as borate complexes and carry only tri- and tetravalent actinides. Coprecipitations in acidic media, e.g., fluorides, are usually more selective than those in basic solutions, e.g., hydroxides. Am can be separated from many elements, including actinides and lanthanides, by selective oxidation of Am(III) to Am(VI) by ammonium peroxydisulfate, while all non-oxidizable lanthanides and actinides were precipitated as fluorides and filtered off. MnO_2 precipitated from $KMnO_4$ and $MnCl_2$ at pH 8-9 is used for the preconcentration of Am, Pu, and Np from seawater samples at the IAEA’s Marine Environmental Laboratory [72]. For preconcentration of actinides from large volume of aqueous or biological samples, special extraction chromatographic materials of extremely high distribution coefficients have also been developed and applied, e.g., TEVA, TRU, DIPHONIX and DIPEX resins [73–75].

1.4.2. Liquid-liquid Extraction (LLE)

Liquid–liquid extraction (LLE), also known as solvent extraction or partitioning, is a method of separation of the compounds in a mixture, based on their relative solubility in two different immiscible liquids, usually water and an organic solvent [76]. Figure 1.5 shows a typical example of solvent extraction where a solute contained in an aqueous phase, generally termed as the feed solution, is transferred to another immiscible organic phase when both liquids are thoroughly contacted and subsequently separated from each other again. The organic phase that is enriched in solute after separation is called extract and the feed solution that is depleted in solute is called raffinate. Solvent extraction is widely used in the nuclear reprocessing, ore processing, production of organic compounds, production of vegetable oils and biodiesel, processing of perfumes and other industries.

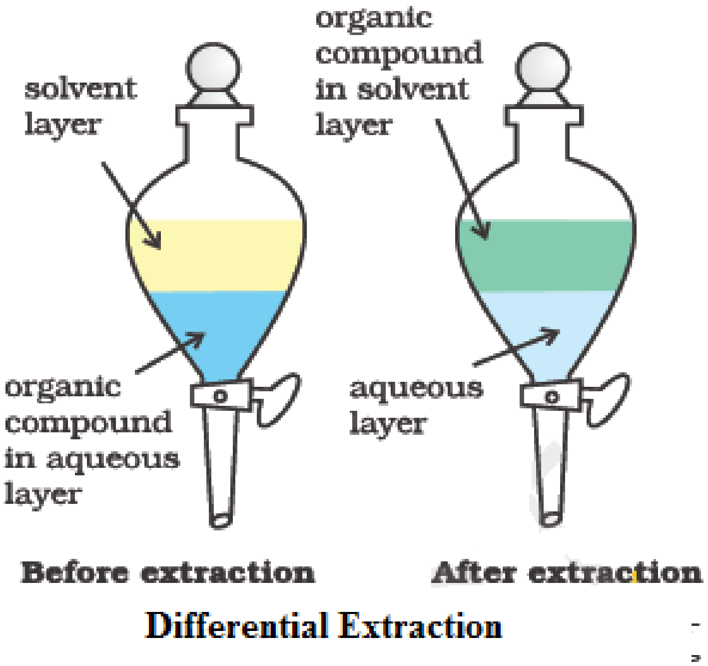

Figure 1.5. Liquid-liquid extraction of an organic compound

The efficiency of a solvent extraction process is expressed in terms of Distribution Ratio (D), which is defined as the ratio of the concentration of a solute in the organic phase to its concentration in the aqueous phase. Generally D is a function of temperature, concentration of chemical species in the system, and various other parameters. Sometimes, the distribution ratio is also referred as the Partition Coefficient, which is often expressed as the logarithm. The separation factor is distribution ratio of one solute divided by that of another and gives a measure of the ability of the solvent extraction process to separate two solutes. Decontamination factor is used to express the ability of a solvent extraction process to remove a contaminant from a product.

Extensive studies have been carried out on solvent extraction of U, Pu and Am in order to develop large-scale processes. Three types of extractants can be distinguished: (i) neutral extractants which form neutral complexes, generally by chemical bonding via electron donor atoms e.g. oxygen, phosphorus, sulfur, nitrogen etc., with the actinide ions involving the counter ions, very often nitrates or chlorides; (ii) basic extractants, generally long-chain alkyl or aryl tertiary or quaternary amines, where positively charged organic amines form complexes with anionic actinide complexes in a manner analogous to anion exchange, and (iii) acidic extractants which form chelate complexes with the actinide cations replacing the H^+ in the organic compound. The interaction of actinide with the neutral and basic extractants can be regarded as ion association complexation and can be applied in acidic media, where in general, the distribution coefficients are increased when acid concentration increases. On the contrary, the acidic extractants are used in low acidic medium because H^+ ions compete with the cations for the binding sites.

Originally reprocessing of actinides in the nuclear industry was accomplished by LLE, employing a wide range of organic acids, ketones, esters, alcohols and ethers. Methyl-isobutyl ketone (MIBK) and ether derivatives like triglycol dichloride and dibutyl carbitol were used for the extraction of U and Pu. Later all these processes were uniformly replaced by the PUREX process, which uses tributylphosphate (TBP), an organophosphorus compound that is less explosive and has higher distribution ratios, for the extraction of Pu(IV) and U(VI) from HNO_3

medium. Other than TBP, trioctylphosphine oxide (TOPO) [55, 77, 78] and octyl(phenyl)-N,N-di-isobutylcarbamoylmethylphosphine oxide (CMPO) [79, 80] has also been used for extraction of Pu, Am, U and Th from acidic solutions. Apart from organophosphorus compounds, tertiary and quaternary amines, like trioctyl amine (TOA), methyl-trioctyl amine (Aliquat 336), Alamin 336 (a mixture of n-octyl and n-decyl amines) etc., are also used for the extraction of nitrate or chloride complexes of tetra and hexavalent actinides from acidic medium [29, 81, 82]. Chelating extractant thenoyl-trifluoroacetone (TTA) is one of the most selective reagent for the separation of Np(IV) from Pu(III) and has been used to separate Pu from water, urine and sediment samples and from fission products [59, 83, 84]. The trivalent Am cation can also form stable chelate with TTA at a relatively high pH [83]. Bis-2-etylhexyl-phosphoric acid (HDEHP) is another chelate that shows selectivity for higher valent cations compared to lower valent ions, and is frequently used for the separation of tetravalent actinides or Am/Cm separations [7]. The separation of trivalent actinides from lanthanides by HDEHP is only possible in presence of strong complexing agents, like lactic acid or DTPA, in the aqueous phase.

Diamides is another promising group of extractants for partitioning of tri- and tetravalent actinide ions from solutions containing high concentrations of nitric acid [85]. The diamide bridges that chelate with the actinides are either alkyl groups (malonamides or succinamides), or ether oxygen (diglycolamides) or sulphur atom (thiodiglycolamides). The affinity of a diamide towards actinides is dependent not only on the molecular structure of the bridge between the two amide groups, but also on the nitric acid-induced aggregation of the diamideligands. Among several diglycolamides studied, *N,N,N′,N′*-tetraoctyldiglycolamide (TODGA) has been found to be the best extractant for the partitioning of minor actinides both in terms of the solubility in *n*-dodecane and the extraction of Ln(III) and An(III, IV) from highly acidic solutions.

1.4.3. Ion Exchange

Ion exchange is the process of exchange of ions between a solution and a solid substrate, leading to purification, separation, and decontamination of aqueous and other ion-containing solutions with solid inorganic or organic 'ion exchangers'. The ion-exchanger has fixed-charge sites and oppositely charged mobile counter ions. In a typical ion-exchange mechanism, the mobile counter ions are exchanged with the ions in solution having same charge but stronger electrostatic interactions with the fixed-sites or exchanged due to shift in ion-exchange equilibrium caused by change in the concentration of inter-changing counter ions in solution. Typical examples of ion exchanger are ion-exchange resins (functionalized porous or gel polymer), zeolites, montmorillonite, clay, and soil humus [86]. Ion exchangers are either cation exchangers that exchange cations or anion exchangers that exchange anions. There are also amphoteric exchangers that are able to exchange both cations and anions simultaneously. However, the simultaneous exchange of cations and anions can be more efficiently performed in mixed beds that contain a mixture of anion and cation exchange resins, or passing the treated solution through several different ion exchange materials. Ion exchange is a reversible process and the ion exchanger can be regenerated or loaded with desirable ions by washing with an excess of these ions.

Ion exchangers are widely used for water softening, water purification and water decontamination. Ion exchange chromatography is also used in chemical & petrochemical, pharmaceutical, food & beverage and a host of other industries. Ion-exchange processes are also extensively used in nuclear industry to separate uranium and plutonium from other actinides, including thorium, for the separation of various lanthanides, in reprocessing of spent fuel products of a nuclear reactor, for treatment of radioactive waste and zirconium-hafnium separation etc. Figure 1.6 represents the schematic of a typical ion exchange process employed for the recovery of radioactive liquid waste.

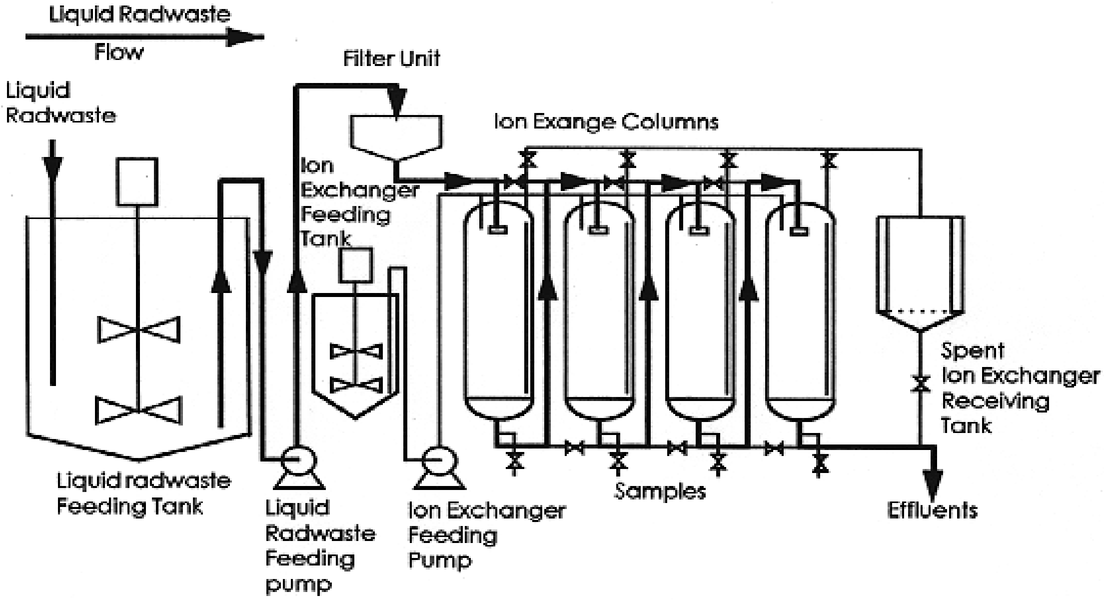

Figure 1.6. Typical ion exchange process for recovery of radioactive liquid waste

Cation exchanger resins, made of high-molecular weight organic polymers, like styrene and divinylbenzene copolymers, with either strongly acidic sulfonate groups, or less acidic phosphonate and carboxylate groups covalently bonded to the polymer network, are generally used for the separation of actinides. The ion exchange affinity of the cations is proportional to the respective ionic potentials. All Pu species, i.e., Pu^{4+}, Pu^{3+}, PuO_2^{2+}, hexavalent UO_2^{2+} and Am^{3+} are retained well at low acidities, and they are removed from the resin by concentrated acids, however no selectivity against other cations were observed. Cation exchangers have been used for the preconcentration of actinides from large volume dilute acidic solutions and from a variety of matrices including groundwater, liquid radioactive wastes, spent fuel leaching solution etc [87, 88]. A general flow sheet used for the ion-exchange separation of Pu ions from other actinides is shown in Scheme 1.2.

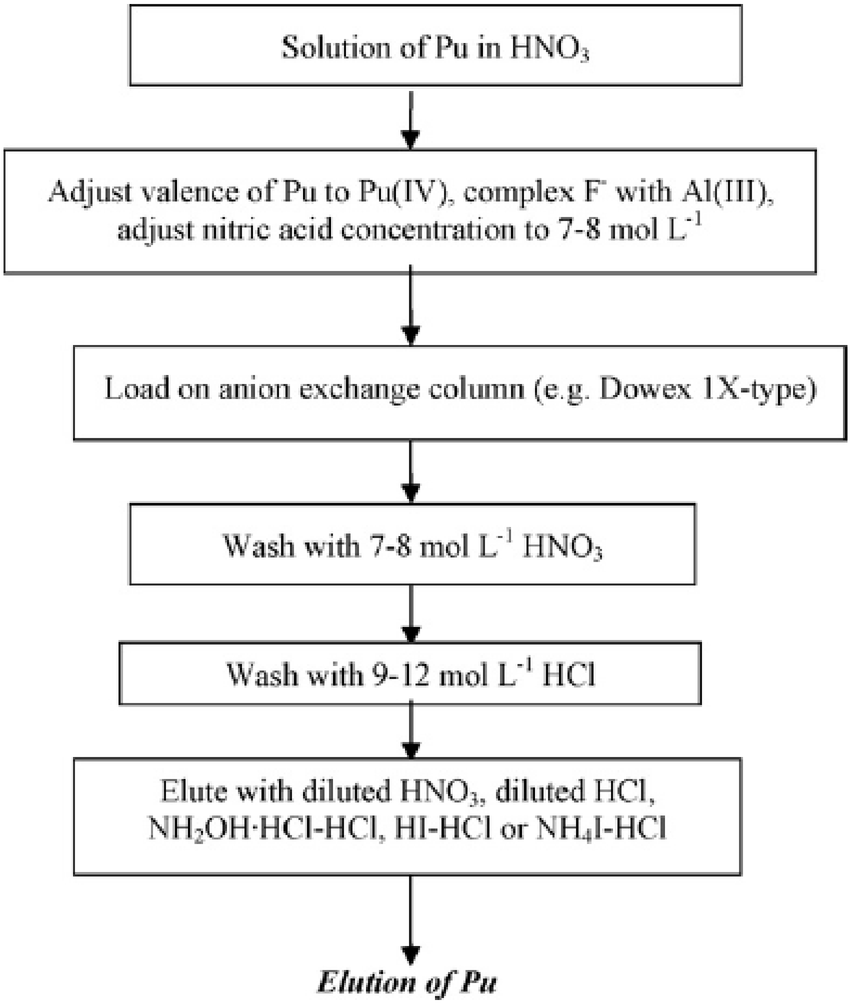

Scheme 1.2. General flow sheet for ion-exchange separation of Pu for analytical applications.

1.4.4. Extraction Chromatography

Extraction chromatography (EC) is a form of liquid-liquid chromatography, where the stationary phase is an organic liquid, sorbed onto a porous solid support, and the mobile phase an aqueous solution. EC is a technique that combines the selectivity of solvent extraction with the ease of operation of chromatographic methods. Figure 1.7 shows the surface of porous bead, acting as an inert support, impregnated with an extractive stationary phase in contact with the mobile phase, containing the target analyte to be extracted. In recent years, extraction chromatography (EC) has played an increasingly prominent role in radiochemical analysis, providing a facile means for the separation and preconcentration of a number of radionuclides, particularly actinides and selected fission products, from a wide variety of sample matrices [89].

The advantages of EC compared to solvent extraction and ion exchange are (i) the extraction process takes place on the thin surface layer, allowing good contact of the reagents and fast exchange kinetics compared to ion exchangers, (ii) chromatographic technique provides more effective separation than batch extraction techniques e.g. solvent extraction, (iii) less chemicals are used and less hazardous waste is produced and (iv) more economical process.

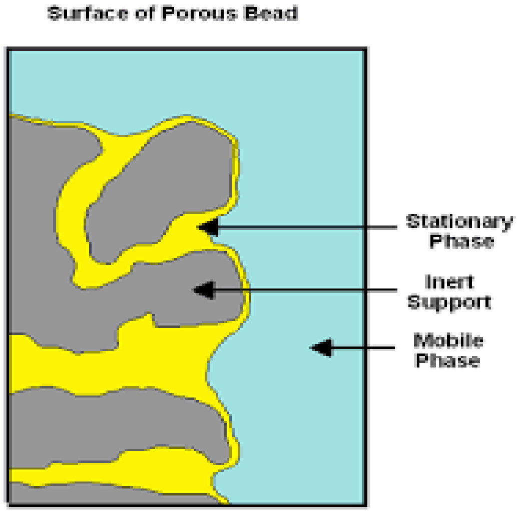

Figure 1.7. An extraction chromatographic stationary phase in contact with mobile phase

TRU resin [62], TOA on Icorene and TOPO supported on Microthene (microporous polyethylene) [83], HDEHP loaded onto the PTFE [90], has been used for the separation of Pu from urine samples followed by alpha spectrometric determination. In the 1990s, a new class of EC materials was developed for the separation of actinides by Horwitz et al at Argonne National

Laboratory, which are now commercially available from EiChrom Co. and Triskem SAS. The EC materials are well characterized in terms of physical and chemical properties, distribution coefficients, extraction kinetics and elution behavior. If a single resin is not capable of separating all the desired radionuclides because of limited selectivity, the use of tandem columns is recommended, where the effluent of one column serves as the load solution for the subsequent one as shown in Scheme 1.3. TEVA resin aimed to separate tetravalent (TEtraVAlent) actinides, is a supported quaternary amine-based (Aliquat 336) liquid anion exchanger, where the support material is Amberchrom CG-71 ms, and has got widespread application in Pu analysis [91].

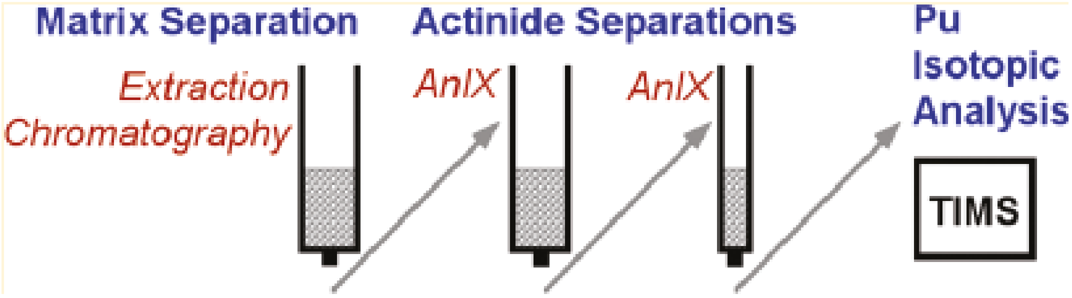

Scheme 1.3 Combination of extraction chromatography (EC) and anion-exchange (AnIX) columns used for separation of Pu prior to TIMS analysis.

1.5. Hyphenated techniques for determination of actinides

In recent years substantial studies were directed towards the development of hyphenated techniques, which includes a combination of a separation technique coupled with a sensitive detection method, for trace elemental analysis and speciation. Earlier, hyphenated techniques involved an offline separation and sample preparation step, followed by a subsequent detection technique. More recently, the online coupling of separation and detection techniques is gaining popularity. Hyphenated techniques provide a number of advantages including shorter analysis time, higher degree of automation, low sample throughput and less chance of contamination because sample manipulation and analysis is performed in a closed system. Also the enhanced selectivity of a hyphenated technique combined with better reproducibility, provides higher degree of information, and eliminates human errors and bias.

Hyphenated ICP-MS techniques, generally coupled to either high performance liquid chromatography (HPLC) or capillary electrophoresis (CE) or flow/sequential injection (FI/SI) for the separation of various analytes, including actinides, have been extensively studied [92]. For the determination of actinides by hyphenated ICP-MS techniques, generally commercially available actinide-specific resins like TRU, TEVA and UTEVA are used as the chromatographic phase, either individually or in combination and good detection limits are achieved for long-lived actinides. Leopold et. al. first reported the analysis of uranium, plutonium, neodymium and some other fission products in irradiated nuclear fuel by HPLC, employing lonPac CS5 or CS10 analytical column, coupled on-line with ICP-MS [93]. They have also demonstrated the application of multi-collector ICP-MS to eliminate isobaric interferences for the determination of the plutonium isotopic composition in irradiated fuel. In a recent study, Aldave et. al. have illustrated the use of an IonPac cation concentrator column as an additional concentration step, to improve the shape and width of the chromatographic peaks, to enhance the sensitivity and lower the detection limit to fg g^{-1} level [94]. CE coupled to ICP-MS is a technique extensively employed for the study of speciation of various actinides in aqueous systems like groundwater, riverwater, soil extracts etc. [95–97]. Interaction of actinides with nitrate or carbonate ligands were also investigated employing CE-ICP-MS and the stability constants of the respective actinide complexes were determined [98]. Aldstadt et al. have used a FI-ICP-MS for online determination of uranium in environmental samples where commercially available TRU^{TM} resin is packed into a glass separation column in a limited dispersion FI system [99];

potentially interfering environmental matrix was eliminated and a preconcentration factor of 30 was achieved by the separation module. Schaumloffel et al have recently reported a nanovolume FI-ICP-MS technique for the ultratrace determination of uranium and plutonium where 54 nanolitre sample was injected into a continuous flow of carrier liquid prior to ICP-SFMS [54].

Other than the hyphenated techniques, sorption preconcentration of actinides has been employed to develop combined and hybrid methods for their determination in complex environmental and biological matrices. Synthesis and designing of new sorbents with specified properties for quantitative recovery of actinides from diverse samples remains a challenging task. Ligands anchored on silica supports, superparamagnetic Fe_3O_4 nanoparticles and graphene oxide have been employed for sequestration of actinides and fission products from complex aqueous media [100-102]. However, these materials are more suited for the removal of matrix and separation of target actinide, rather than for analytical applications. Therefore, it would be interesting to investigate the possibility of directly subjecting a solid-phase sorbent to conventional analytical techniques such as α spectrometry and TIMS for quantification of the analyte preconcentrated in its matrix. Direct analysis of actinides from a solid phase sorbent would minimize the sample manipulation steps required for removal of the undesirable sample matrix without sacrificing the preconcentration factor.

1.6. Scope and aim of present work

The present work aims to develop bi-functional polymeric sorbents for a selective preconcentration of major actinides (U, Pu), followed by the direct quantification of the actinide sorbed the polymeric substrate by either alpha spectrometry or mass spectrometry. The extractive bifunctional layer was anchored on a thin membrane for alpha spectrometric determination of plutonium. For thermal ionization mass spectrometry, various polymeric substrates including bifunctional beads and the porous polymer supported liquid extractants were developed in the present work. The work presented in the thesis can be broadly summarized as follows: Two bi-functional polymers, HEMP-co-AMPS and HEMP-co-APTAC, were synthesized by photo-induced free radical polymerization using monomers phosphoric acid 2-hydroxyethyl methacrylate ester (HEMP) containing 25% diester, and 3-(acrylamido propyl) trimethylammonium chloride (APTAC), and2-acrylamido-2-methyl-1-propanesulphonic acid (AMPS). These bi-functional polymers, containing neutral phosphate groups and strong ion-exchange groups i.e. either sulphate or quaternary ammonium groups, were found to be selective for a particular actinide depending on the HNO_3 concentration of the medium. Both HEMP-co-AMPS and HEMP-co-APTAC had better extraction and stripping properties compared to HEMP polymer and were found to sorb Pu(IV) preferentially in the presence of large excess of U(VI) ions. The bi-functional HEMP-co-AMPS polymer was anchored as a thin film on the surface of a poly(ethersulphone) membrane, which served as a good source for quantification of Pu(IV) in complex aqueous matrices by alpha spectrometry. The two surfaces of PES membrane have different morphologies and the glossy surface served as a better alpha source than the rough surface. Membrane based alpha spectrometry was employed for determination of trace amounts of Pu(IV) in various biological & environmental samples and also in irradiated dissolver solution, containing large excess of U. Determination of Pu concentration by membrane based alpha spectrometry was carried out employing two independent methods, viz. efficiency calibration and isotope dilution. Single bead thermal ionization mass spectrometry (SB–TIMS) was developed for simultaneous preconcentration of plutonium using superparamagnetic bifunctional PES beads, followed by determination of Pu isotopic composition and concentration. SB–TIMS method was found to provide comparable accuracy & precision with respect to the conventional solution based loading technique for TIMS. The method significantly reduces the analysis time & the amount of solid/liquid waste generated is minimized. However analysis temperature of SB–TIMS was found to be considerably higher than the conventional solution based TIMS method. To overcome such problem, the polymeric material based reservoirs for actinide loading in TIMS were developed in the present work using UV-initiator induced grafting and physical immobilization of the extractant sin the poly(propylene) membrane. It was observed that HDEHP and TEHP immobilized in the poly(propylene) membranes are best suited for dual functions of the reservoir i.e. efficient preconcentration of Pu(IV) and U(VI) from a wide variety of aqueous matrices and TIMS loading with low vaporization temperature. The HDHP and TEHP immobilized in poly(propylene) were applied successfully for the quantification U(VI) and Pu(IV) in the synthetic urine sample, seawater and ground water using isotope dilution method with reasonable good accuracy and precision. U(VI) was preconcentrated in the reservoir was without adjusting the acidity of the aqueous samples, but require adjustment to 3 M HNO_3 for Pu(IV) preconcentration. The major advantage of the Reservoir-TIMS developed in the present work is that it is a single step sample manipulation and loading process that would greatly reduce the analysis time and prolong handling of the radioactivity causing possibility of contamination and exposure to radiations.

Chapter 2

Experimental Methods

2.1. Reagents and Materials

Analytical reagent grade chemicals/solvents, suprapure grade nitric acid (Merck, Mumbai, India), and deionized water with specific resistance of 18 MΩ cm^{-1}, purified by Quantum^{TM} from Millipore (Mumbai, India), were used throughout the present work. The stock solutions of ^{233}U, ^{241}Am, and Pu were obtained from Mass Spectrometry Section, Fuel Chemistry Division, BARC, Mumbai, India. A list of the chemicals used in the present study is given in Table 2.1. The chemical structures of the monomers and liquid extractants used are shown in Figure 2.1, and isotopic composition of stock solution of Pu is given in Table 2.2.

Table 2.1. List of chemicals used in the present work

Chemicals	**Specifications**	**Use**	**Suppliers**
Phosphoric acid 2-hydroxyethyl methacrylate ester (**HEMP**)	containing 25% diester, 90%	Monomer	Sigma-Aldrich
2-Acrylamido-2-methyl-1-propanesulfonic acid (**AMPS**)	98% pure	Monomer	Sigma-Aldrich
(3-Acrylamidopropyl)trimethyl ammonium chloride (**APTAC**)	98%, containing monomethyl ether hydroquinone inhibitor	Monomer	Sigma-Aldrich
2-ethylhexyl methacrylate (**EHM**)	(98%, containing ~50 ppm monomethyl ether hydroquinone)	Spacer monomer	Sigma-Aldrich
2,2′-Dimethoxy-2-phenylacetophenone (**DMPA**)	purity 99%	UV-initiator	Sigma-Aldrich
Fe_3O_4 nanoparticles	20-30 nm size	Beads	J.K. Impex, Mumbai
Tetraethoxysilane (**TEOS**)	-	Coating	Sigma-Aldrich
Poly(ethersulfone) (**PES**)	-	Polymer support	Goodfellow
Tris(2-ethylhexyl) phosphate (**TEHP**)	purity 96%	Liquid Extractant	Koch-Light Laboratories
bis(2-ethylhexyl)phosphoric acid (**HDEHP**)	purity 96%	Liquid Extractant	BDH, England
Polypropylene (PP) membrane	0.1/0.2 µm pore size	Porous support	Sterlitech Corporation, US
PES membrane	0.1/0.2 µm pore size	Porous support	Pall Science
Ultima Gold AB scintillation cocktail	-	Scintillation cocktail	Perkin Elmer

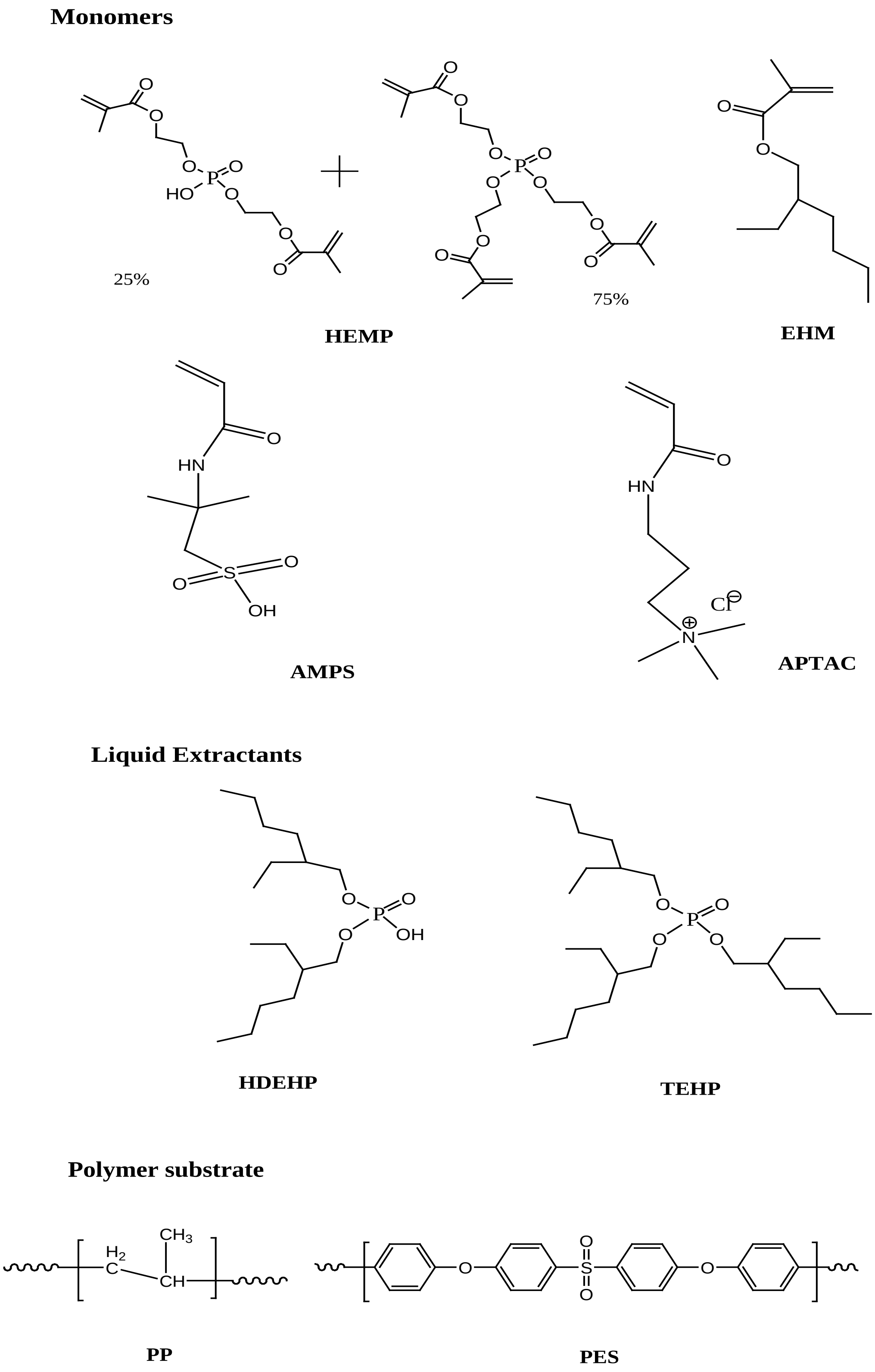

Figure 2.1. Chemical structures of monomers and liquid extractants used in making polymer supported materials for alpha spectrometry and TIMS.

Table 2.2. Isotopic composition of Pu stock solution used in the present study.

Isotope	Atom %
^{238}Pu	0.16 ± 0.006
^{239}Pu	68.79 ± 0.03
^{240}Pu	26.94 ± 0.03
^{241}Pu	2.09 ± 0.005
^{242}Pu	2.02 ± 0.006

2.2. Synthesis of polymeric substrates

Photo-induced polymerization involves absorption of ultraviolet radiation to produce an unstable excited species, followed by subsequent formation of a free radical by either rearrangement or fragmentation or energy transfer. The free radical thus generated attacks upon a monomer, initiating the polymerization. The process is similar to the polymerization initiated by ionizing radiation like gamma rays and can be represented the following scheme:

$$S + h\nu \longrightarrow S^* + \text{(radical formation)}$$

$$S^* + M \longrightarrow S + M^* \text{ (initiation)}$$

$$M^* + nM \longrightarrow (M)_nM^* \text{ (propagation)}$$

$$(M)_nM^* + R^* \longrightarrow (M)_nMR \text{ (termination)}$$

where S is the photo-initiator and M is the monomer. Photo-induced polymerization involves free-radical mechanism and therefore depends on various conditions like type of irradiation source and its wavelength, distance between the source and the reaction cell, nature and concentration of the photo-initiator and the monomer, temperature, solvent and presence of oxygen etc.

In the present work, the bifunctional polymers were synthesized by ultraviolet induced free radical polymerization method, using a UV multilamp photoreactor, procured from Heber Scientific, Chennai, India (model HML-SW-MW-LW-888), equipped with eight 8 Watt mercury UV lamps of 365 nm wavelength (Sankyo Denki, Japan) in a circle. The design of photoreactor is shown in Figure 2.2.

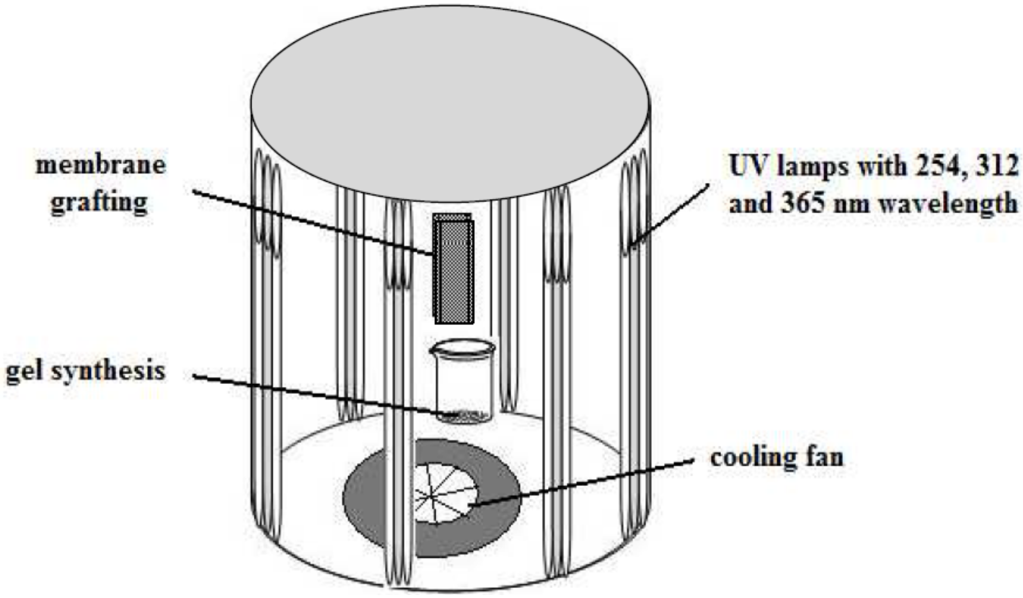

Figure 2.2. **Schematic setup of photoreactor used for synthesis of polymer gel and grafting of the monomers on a porous substrate.**

The present work involves the polymerization of three different monomers, viz. phosphoric acid 2-hydroxyethyl methacrylate ester (HEMP), 2-acrylamido-2-methyl-1-propanesulfonic acid (AMPS) and (3-acrylamidopropyl)trimethyl ammonium chloride (APTAC), all three being methacrylic acid monomers containing different functional groups. However, the rate of opening the C=C double bond in the methacrylic moiety to generate free radicals for polymerization is extremely low when exposed to 365 nm photons. Therefore, 2,2′-dimethoxy-2-phenylacetophenone (DMPA) was used to initiate the chain reaction for polymerization. Figure 2.3 illustrates the structure of DMPA and its dissociation when subjected to 365 nm UV radiation. The DMPA radical, once formed, accelerates the polymerization of the methacrylate monomers.

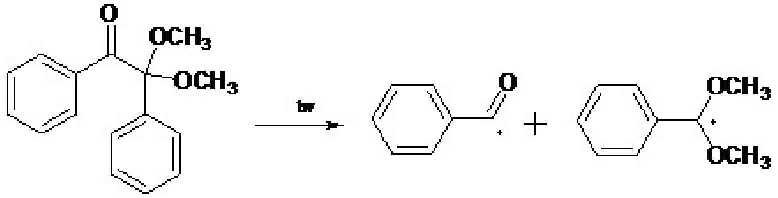

Figure 2.3. Photolysis of DMPA when subjected to UV radiation

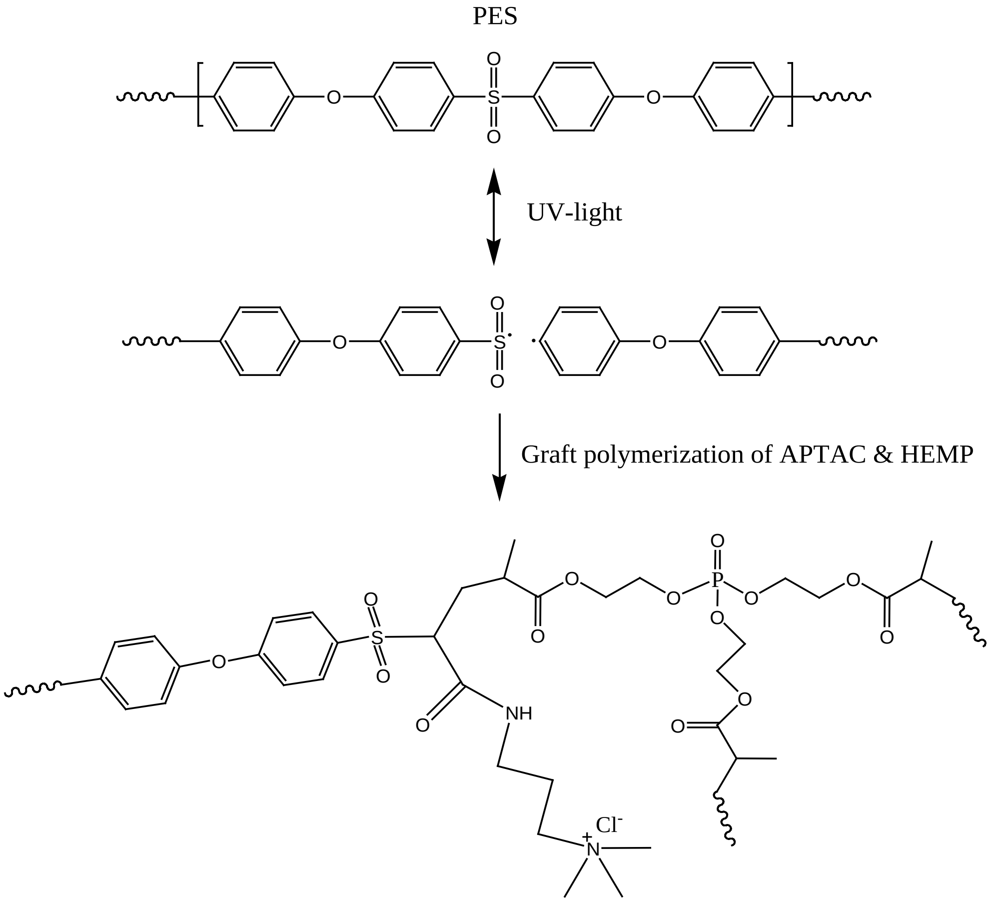

Poly(APTAC-co-HEMP-ES)

Figure 2.4. Photolysis of PES followed by grafting of HEMP and APTAC monomers.

The HEMP, AMPS and APTAC monomers were also anchored on polyethersulfone (PES) membrane and beads by UV induced free radical grafting. The graft polymerization of the monomers on PES support was based on the formation of free radicals due to photolysis of PES chains under UV light. Figure 2.4 shows UV induced photolysis of PES polymer chain to generate free radicals, which in turn reacts with the monomers. The fragments and growing polymer chains have tendency to abstract hydrogen from the host PES polymer to cause grafting.

2.3. Formation of Fe_3O_4 nanoparticles

The Fe_3O_4 nanparticles were prepared by the co-precipitation method using either $FeCl_2$ or a mixture of ($FeCl_2$ + $FeCl_3$). In a single salt co-precipitation method, 100 mL of de-ionized water was taken in a round bottom flask and deoxygenated by continuously purging N_2 followed by heating to attain a constant temperature of 70 ± 0.5^oC. To this, weighted amount of $FeCl_2.xH_2O$ (about 3 g) was added and homogenized for 20 minutes by stirring continuously at 600 rpm. The standardized ammonium solution was added drop-wise using a Soxhlet funnel without interrupting stirring. After addition of 100 mL ammonia, a sudden precipitation occurred which was allowed to cool at room temperature and settled at the bottom of flask. The precipitate was washed with water/ethanol repeatedly and dried in air for 24 hours. The chemical reactions involved in this process are given below.

$$3\,FeCl_2 + 6OH^- + 2H_2O \longrightarrow Fe(OH)_2 + 2Fe(OH)_3 + H_2$$

$$Fe(OH)_2 + 2Fe(OH)_3 \longrightarrow Fe_3O_4 + 4H_2O$$

In another method, 0.01 mol $FeCl_2$ and 0.02 mol $FeCl_3$ were dissolved in a 250 mL flask containing 100 mL of deionized and deoxygenated water. To this, 0.08 mol of NaOH dissolved in 100 mL was added slowly for 3 hours. The resulting precipitate was washed and dried as described above. Generally, a surfactant is also used to control the size of the Fe_3O_4 nanoparticles. In the present work, Fe_3O_4 nanparticles having 20-30 nm sizes were procured from J.K. Impex were prepared by double salt method. These nanoparticles were characterized by TEM and VSM, as shown in Figure 2.5.

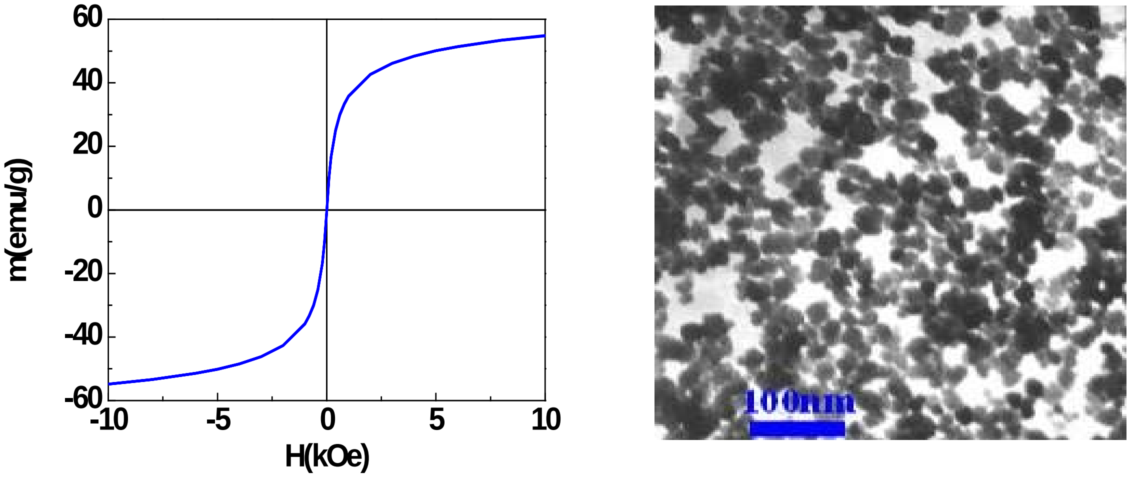

Figure 2.5. Vibrating sample magnetometry curve and TEM image of commercially available Fe_3O_4 nanoparticles.

2.4. Characterization techniques

The polymeric substrates synthesized in the present work were characterized by different methods. The principles of those characterization techniques are described as follows.

2.4.1. Scanning electron microscopy

In the present work, the polymers, PES bead and membrane samples were characterized for surface morphology and porosity by scanning electron microscope (SEM). SEM is a kind of electron microscope that produces images of a sample by scanning it with a focused beam of electrons, which interact with the atoms present in the sample and produces signals which provide information about surface morphology and composition of the sample. SEM can achieve resolution better than 1 nanometer. The most common mode of scanning is the detection of secondary electrons, emitted by atoms excited by the electron beam. The number of secondary electrons ejected, depends on the angle at which beam meets surface of sample i.e. on sample morphology – by scanning the sample and collecting the secondary electrons with a special detector, an image displaying the surface morphology is created. SEM can provide from about

10–500,000 times of magnification, which is about 250 times the magnification limit of the best optical microscopes. Back-scattered electrons (BSE) are beam electrons that are reflected from the sample by elastic scattering and can provide information about the distribution of different elements in the sample, as the intensity of the BSE signal is strongly related to the atomic number (Z) of the sample. Characteristic X-rays are also emitted when the electron beam removes an inner shell electron from the sample, causing a higher-energy electron to fill the shell and release energy. These characteristic X-rays along with BSE are often used in analytical SEM to identify and measure the elemental composition of the sample.

In a typical SEM, the electron beam is thermionically emitted from an electron gun fitted with a tungsten filament cathode. Tungsten is normally used in thermionic electron guns because of its low cost, highest melting point and lowest vapour pressure of all metals, thereby allowing it to be heated for electron emission. The electron beam, which typically has an energy ranging from 0.2 keV to 40 keV, is focused by one or two condenser lenses to a spot having 0.4–5 nm diameter. When the primary electron beam interacts with the sample, the electrons lose energy by repeated random scattering and absorption which results in the reflection of high-energy electrons from the sample by elastic scattering, emission of secondary electrons by inelastic scattering and the emission of electromagnetic radiation, each of which can be detected by specialized detectors. In the present work, the physical structures of the polymeric substrates were examined by SEM. For conventional SEM imaging, sample must be electrically conducting, at least at the surface, to prevent the accumulation of electrostatic charge at the surface. However, non-conducting/organic samples tend to charge when scanned by the electron beam, leading to scanning faults and other image artifacts. Therefore, in the present study, all polymeric samples were coated with an ultrathin layer of silver, deposited on the sample surface by low-vacuum sputtering.

Emitter type (Thermionic emitter and Field emitter, respectively) is the main difference between the Scanning Electron Microscope (SEM) and the Field Emission Scanning Electron Microscope (FE-SEM). Thermionic Emitters use electrical current to heat up a filament; the two most common materials used for filaments are Tungsten (W) and Lanthanun Hexaboride (LaB6). When the heat is enough to overcome the work function of the filament material, the electrons can escape from the material itself. Thermionic sources have relative low brightness, evaporation of cathode material and thermal drift during operation. Field Emission is one way of generating electrons that avoids these problems. A Field Emission Gun (FEG); also called a cold cathode field emitter, does not heat the filament. The emission is reached by placing the filament in a huge electrical potential gradient. The FEG is usually a wire of Tungsten (W) fashioned into a sharp point.

2.4.2. Secondary ion mass spectrometry

Secondary ion mass spectrometry (SIMS) is a technique used to analyze the composition of solid surfaces and thin films by sputtering the surface of the sample with a focused primary ion beam, followed by collection and analysis of the ejected secondary ions. The mass-to-charge (m/z) ratios of these secondary ions are measured with a mass spectrometer for determination of the elemental, isotopic, or molecular composition of the sample surface, to a depth of 1-2 nm. SIMS is generally considered to be a qualitative technique since large variation is encountered in the ionization probabilities among different materials; however quantification is also possible with the use of suitable standards. SIMS is the most sensitive surface analysis technique, with elemental detection limits ranging from ppm to ppb. Typically, a secondary ion mass spectrometer consists of: (i) primary ion gun which generating the primary ion beam which in turn is accelerated and focused onto the sample surface, (ii) high vacuum sample chamber holding the sample and the secondary ion extraction lens, (iii) mass analyser separating the ions according to their respective m/z ratio and (iv) ion detection unit.

SIMS requires a high vacuum, $<10^{-4}$ Pa, to ensure that the secondary ions do not collide with background gases on their way to the detector and to prevent surface contamination by adsorption of background gas particles during measurement. The choice of ion gun depends on the required current, pulsed or continuous, the required beam dimensions and on the type of sample to be analyzed. SIMS instruments are equipped with three different mass analyzers viz. sector field, quadrupole and time-of-flight. However, the time of flight mass analyzer, which separates the ions in a field-free drift path according to their velocity, is the only analyzer type able to detect all generated secondary ions simultaneously, and is the standard analyzer for static SIMS instruments. Detection limits for most trace elements are between 10^{12} and 10^{16} atoms/cm^3, depending on the type of instrumentation, the primary ion beam used and the analytical area. While only charged secondary ions emitted from the material surface through the sputtering process are used to analyze the chemical composition of the material, these represent a small fraction of the particles emitted from the sample. In the present work, ToF-SIMS was employed for depth profiling of the polymer grafted membrane samples. The ToF-SIMS experiments were carried out with 15 keV Ga^+ ion source as the primary beam, using a TRIFT V time of flight instrument.

2.4.3. Vibrating sample magnetometry

Magnetometer is an instrument used to measure the magnetization of a magnetic material or to measure the strength and direction of the magnetic field at a point in space. A vibrating sample magnetometer (VSM) measures magnetic properties of a sample by mechanically vibrating the sample inside of an inductive pickup coil. The sample is placed in a uniform magnetic field to magnetize the sample and then physically vibrated sinusoidally, generally using a piezoelectric material. The dipole field of the sample generates an electrical signal proportional to the sample's magnetic moment, but is independent of the strength of the applied magnetic field.

2.5. Detection and quantfication of actinides

2.5.1. Safety measures

All radioactive materials are potentially hazardous and should be handled with proper precaution. Prior knowledge of the activity of the sample is very important, while executing any experiment with radioactive material. In the present study, the major radionuclides handled were ^{241}Am, ^{233}U and a mixture of Pu isotopes having mass number 238–244. The radiotracers used in the present work primarily emits alpha particles and low energy beta particles. About 10–100 microCuries (µCi) of alpha activity was used in the radiotracer based experiments. The major gamma emissions were from ^{241}Am and ^{233}U and the gamma dose associated with the samples was less than 1mR/hour (milli Roentgens per hour) at about 1 ft distance from the source. The low level radioactivity was handled in a fume hood, connected to an exhaust system, using disposable latex gloves and personnel radiation monitoring badge was used during all the experiments.

2.5.2. Choice of radiotracer & their detection

The choice of radiotracers used in the present work was based on several factors. The radiotracer should have high specific activity so that the quantity required to trace any chemical process is very small. The half-life of the tracer should not be very long as it would result in less specific activity, but at the same time half-life must be long enough to have a constant activity during the course of experiment and detection. The tracer should be chemically compatible with the system to be studied under real experimental conditions. Also the tracer should be cost-effective, easily available and appropriate detector systems should also be available for the measurement of the radiation associated with the tracer. The penetrating power, effective dose and ease of measurement associated with the radiation emitted by the radiotracer should also be considered. The half-life, decay mode and specific activity of the radiotracers used in the present work are listed in Table 2.3.

Table 2.3. Nuclear properties of radionuclides of interest

Nuclide	Half-life (years)	Decay mode	Specific activity (Bq/g)
^{233}U	1.59×10^{5}	α (γ)	1.28×10^{12}
^{234}U	2.46×10^{5}	α (γ)	2.29×10^{8}
^{235}U	7×10^{8}	α (γ)	8.14×10^{4}
^{238}U	4.47×10^{11}	α (γ)	1.22×10^{4}
^{238}Pu	87.7	α (γ)	6.34×10^{11}
^{239}Pu	24,100	α (γ)	2.3×10^{9}
^{240}Pu	6,561	α (γ)	8.4×10^{9}
^{241}Pu	14.3	β (γ)	3.82×10^{12}
^{242}Pu	3.7×10^{5}	α (γ)	1.46×10^{8}
^{241}Am	432.6	α, γ	1.27×10^{11}

Power reactor grade plutonium was used throughout the present work, which is a mixture of five Pu isotopes with mass number ranging from 238 to 242. All these Pu isotopes are alpha emitters, except ^{241}Pu that emits a low energy beta; therefore Pu activity was measured by either liquid scintillation counter or alpha spectrometer. Similarly, studies involving uranium was monitored by the alpha activity of ^{233}U. A home-built liquid scintillation counter, equipped with a single channel analyser, was used for the measurement of gross alpha activity. For alpha spectrometry, a passivated ion-implanted planar silicon (PIPS) detector (Canberra, PD-450-16-100AM), with an area of 450 mm^2 and a resolution of 16 keV (FWHM) at 5.486 MeV of ^{241}Am, was used. For studies involving Am, ^{241}Am was used as tracer and the gamma ray emitted by ^{241}Am was measured using an HPGe detector (ORTEC, United States), coupled to a PC-based MCA, having a resolution of 550 eV (FWHM) at 122 keV of ^{57}Co.

2.5.3. Sorption efficiency & sorption kinetics

To study the sorption of actinides by the polymeric substrates, synthesized in the present work, about 100 mg of the polymer sample was equilibrated with 5 mL of well-stirred solution containing a tracer level concentration of Pu / ^{241}Am / ^{233}U. 25–50 μL of aliquot was taken out from the solution, before and after equilibration with the polymer samples. The amount of Pu or ^{233}U sorbed was determined from the difference in alpha activities. The schematic representation of the experiment for monitoring the sorption efficiency and kinetics is given in Figure 2.6. Similarly, sorption of ^{241}Am was monitored by the difference in gamma activities, before and after equilibration with the polymer samples. The actinide sorption efficiency in the polymer samples was obtained from the following equation:

$$\text{Sorption efficiency} = \frac{(\mathrm{A_i} - \mathrm{A_f})}{\mathrm{A_i}} \text{ X } 100 \qquad (2.1.)$$

where A_i and A_f are the alpha/gamma count rate of the actinide in solution, before and after equilibration with the polymer sample, respectively. The distribution ratios ($D_{Pu/U}$) of the polymeric sorbents, developed in the present work, were determined by measuring the alpha activity of a solution, containing 100:1 mole ratio of U(VI) and Pu(IV) ions at 3 M HNO_3 medium, before and after equilibration with the polymer sample. The $D_{Pu/U}$ values were obtained using the following equation:

$$D_{Pu/U} = \frac{(A_i - A_f)}{W} X \frac{V}{A_f} \qquad (2.2.)$$

where A_i and A_r represent the alpha activities of ^{233}U/Pu initially and after equilibration in the aqueous phase, W is the weight of the polymer sample and V is the volume of the equilibrating aqueous phase, respectively.

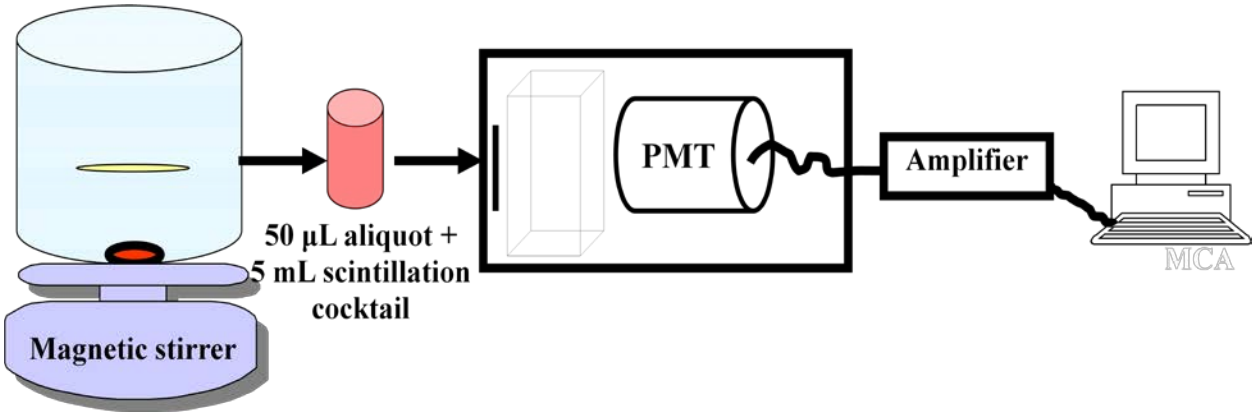

Figure 2.6. Schematic representation of experimental method used for measuring sorption efficiency and kinetics of alpha emitting radionuclide in the polymeric sorbent.

For studying the time required to obtain optimum sorption of actinides, about 200 mg of the polymer sample was added to 25 mL of aqueous solution containing trace levels of Pu(IV) with continuously stirring; 10 µL aliquot was taken out at regular intervals from the equilibrating solution for monitoring the Pu alpha activity. For desorption studies, about 100 mg of polymer sample was first equilibrated with 5 mL of aqueous solution containing a trace amount of actinide. After sorption of the actinide, the loaded polymer was filtered from the aqueous solution, washed with distilled water, and dried using filter papers to remove solution clinging on the polymer surface. The actinide-loaded polymer samples were then equilibrated with 5 mL of aqueous solution containing the appropriate concentration of the stripping agent. Stripping of Am and U from the polymers was carried out using 3 M HNO_3 and 1 M Na_2CO_3, respectively. For Pu, two separate stripping agents, viz., 0.1 M HNO_3 and 1 M $NH_2OH.HCl$, were used.

Chapter 3

Development of bi-functional polymeric sorbents for selective preconcentration of actinides

3.1. Introduction

The separation and extraction of plutonium from the irradiated uranium fuel was first studied by Glenn T. Seaborg and co-workers employing lanthanum fluoride process where plutonium was precipitated and extracted as PuF_3 [103]. However, due to the highly corrosive nature of fluorides, this process was not amicable for reactor cladding. Bismuth phosphate process was employed as an alternative to separate the insoluble Pu(III) and Pu(IV) phosphates, selectively and quantitatively, from the soluble UO_2^{2+} phosphates in acidic medium [60,61,104]. This was the initial use of phosphorus based ligands for the separation of actinides. But only plutonium could be extracted by $BiPO_4$ process while uranium remained in solution. Solvent extraction techniques were, thereafter, extensively studied and used for the separation of uranium and plutonium from the fission products and from each other, employing various reagents like methyl isobutyl ketone or hexone, dibutyl carbitol etc. [105]; although these reagents tend to decompose slowly in contact with nitric acid present in the aqueous phase. Among the solvent extraction techniques, PUREX process is the most widely accepted one, where an aliphatic hydrocarbon solvent containing tri-*n*-butyl phosphate (TBP) and kerosene is used to extract hexavalent and tetravalent nitrate complexes of uranium and plutonium and most of the fission products remain in the aqueous phase [106–108]. The Pu(IV) extracted in the organic phase is then reduced to Pu(III), generally adding either ferrous sulfamate, hydroxylamine or U(IV), to selectively strip plutonium from the organic phase to the aqueous phase, leaving the hexavalent uranium in the organic phase.

Apart from solvent extraction, the concept of immobilizing extractants/ligands onto a polymer support, for the recovery of metal ions, including actinides, from various aqueous or process streams, has also received a good deal of attention [77–80]. Principles that are applicable for liquid-liquid extraction processes can be extrapolated to solid-liquid extraction process too. Syntheses of polymers to which metal specific ligands are covalently bonded or in which extractants are physically entangled are reported in literature [76]. The objectives of the synthesis of polymer-supported extractants can be summarized as follows: (1) To develop an understanding of the role of the polymer in the extraction process and to optimize the conditions for enhanced selectivity displayed by the polymer supported extractant, (2) To develop bifunctional extractants which contain neutral and ionic moieties within the same polymer network and (3) To develop commercially applicable resins with good selectivity in acidic solutions. Aromatic substitution reactions allow the synthesis of a wide variety of high-capacity resins. The synthetic variables can be adjusted to allow modifications of the diffusion properties of the polymer network. In some solvent extraction systems, it has been reported that use of an ionic and another neutral extractant in the same solution allowed synergistic extraction, in which more metal is extracted than either extractant would complex alone [109, 110]. Development of an analogous polymeric system would be promising for polymer-supported synergistic extraction of metal ions.

Ion-exchange resins, such as Amberlite IR-120 (sulfonic resin), Duolite (phosphonic resin), Dowex A–1 (carboxylic resin) and Amberlite IRA-900 (quaternary ammonium ion resin), as well as neutral polymeric extractants such as poly(diallylphophonate) and poly(styrene-phenyltrimethylenephosphine oxide) are commercially available for the extraction of metal ions [111–114]. Ion-exchange resins have been widely used for various applications like recovery of metal ions from variety of matrices and as chromatographic supports [115]. The most common ion-exchange resins are polystyrene-based sulfonic acids and the acrylic acids [116]. Due to their highly acidic nature, metal extraction by the sulfonic acid functionalized resins can be carried out over a wide pH range but with less selectivity, especially when the metal ion of interest is in trace amounts relative to other common metals such as the alkali metal ions [115, 117, 118]. Selectivity can be enhanced by introducing a weakly acidic cation-exchange resin like acrylate groups are bonded to either a styrenic or ethylenic network. The acrylic acid functionalized resins show better selectivity towards metals, but can be employed over a limited pH range depending on their respective pK_a [117, 118]. Phosphate functionalized ligands or resins exhibit an important intermediate property in metal ion extraction, since they are more selective compared to the sulfonic acids and can be employed in solutions having lower pH compared to the carboxylic acids [115]. Phosphate functionalized resins have been reported to operate by a dual mechanism where metal ion exchange can be followed by reduction to the free atom if the metal ion has a suitable reduction potential allowing for the isolation of the pure metal from solution [119]. However the use of phosphonic acid in the analogous area of polymer-supported complexing agents has not been intensively studied.

Alexandratos et al. have developed and reported a series of dual mechanism bi-functional polymers (DMBP) which shows stronger selectivity towards metal ions compared to sulfonic acid and acrylic acid functionalized resins, through two different mechanisms, either by chemical reactivity like reduction or precipitation, or by strong coordination [115, 116, 118–122]. Alexandratos et al. have chosen polystyrene, an industrial polymer with an economical synthesis and resistant to chemical degradation under ordinary conditions, as the polymer support. The effects of the polymer backbone on the selectivity displayed by the extractant were also studied [121, 122]. It was also observed by Alexandratos et al. that bi-functionality could enhance the complexation kinetics of the selective resins [115, 121, 123, 124]. Phosphate functionalized polymers for selective extraction of actinides, like TEVA resin, are nowadays commercially available. However the studies carried out on phosphonic acid functionalized resins were primarily focused on the selective extraction of metals and did not consider the quantification of the extracted metal ions. The objective of the present work was focused to the development of phosphate functionalized polymeric sorbents that can selectively extract actinides and the actinide sorbed by the polymer can be directly quantified by some suitable techniques, like radiometry or mass spectrometry.

Two different extractive bi-functional polymers, each having neutral phosphate functional groups along with an ion-exchange group, either sulfonate or quaternary ammonium groups, were developed in the present study for the selective preconcentration of Pu(IV) and its subsequent quantification by either alpha spectrometry or thermal ionization mass spectrometry. The synthesis, characterization and actinide sorption properties of these bi-functional polymers are discussed in details in the present chapter. The neutral phosphate group is selective towards actinides due the coordinating ability of the P=O moiety with actinide ions. The sulfonic acid or quaternary ammonium groups have been incorporated in the bi-functional polymer for tuning the selectivity of P=O toward Pu(IV) and also for providing ion-exchange sites for charge balance. The self-supported bi-functional polymer discs were synthesized by photoinduced free radical copolymerization of two monomers, phosphoric acid 2-hydroxyethyl methacrylate ester (HEMP) with either 2-acrylamido-2-methyl-1-propanesulfonic acid (AMPS) or (3-acrylamidopropyl)trimethyl ammonium chloride (APTAC). The bi-functional polymers were characterized for chemical composition, physical structure and homogeneity. The actinide sorption efficiency as a function of HNO_3 concentration, sorption selectivity toward Pu(IV), and Pu(IV) sorption kinetics in the polymer matrices were also studied. The improvement in Pu(IV) sorption properties of the bi-functional polymer, compared to mono-functional polymer containing either sulfonic acid/ quaternary ammonium or phosphate groups, was also studied.

3.2. Experimental

The extractive polymers were synthesized in the present work by photo-induced free radical polymerization method, as described in the Chapter 2.2. For the synthesis of the self-supported bi-functional polymer discs, appropriate amount of the UV initiator DMPA (1 wt. %) was dissolved in minimum volume of DMF and an equimolar mixture of HEMP and AMPS/APTAC monomers in 1:1(v/v) H_2O:ethanol was added to it. The polymerization solution was homogenized by ultrasonication for 5 minutes, poured in a circular Teflon mould having 1 cm diameter, as shown in Figure 3.1 and irradiated in a UV photoreactor for 15 min. The bi-functional polymer discs, obtained after irradiation, were washed with water at 70-80°C to remove un-polymerized components and conditioned by successive equilibrations with 0.5M NaOH and 0.5M HNO_3. After washing, the discs were dried in oven for 3–4 hours at 70–80°C and stored in 0.5M NaCl. Similar procedure was employed for the synthesis of HEMP, AMPS and APTAC polymer discs.

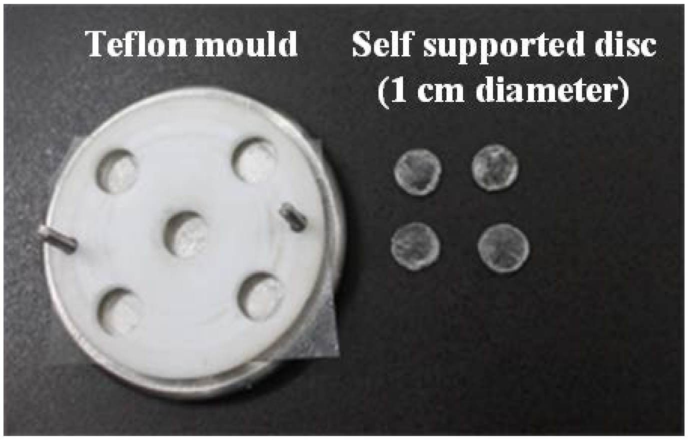

Figure 3.1. Teflon mould used for synthesis of bi-functional polymer discs by UV-initiator induced polymerization.

The swelling ratios of the polymers were determined from weight of a polymer disc before and after equilibration with Millipore water, using the following equation:

$$\text{Swelling ratio} = \frac{W_{\text{wet}}}{W_{\text{dry}}} \qquad (3.1)$$

where, W_{wet} and W_{dry} are the water equilibrated and dry weight of the same polymer disc, respectively. The porosity and effective surface area of the polymers discs were measured using a mercury porosimeter. The elemental analyses at randomly selected surface points of the polymer discs were carried out using SEM–EDS. The homogenous distribution of the functional groups in the HEMP–co–AMPS and HEMP–co–APTAC polymer discs was studied by exposing a Pu loaded polymer disc to CR-39 detector for recording alpha tracks. The alpha tracks were developed on the exposed CR-39 film by chemical etching in 6M NaOH at 70^0C for 4 hours and the track–etched film was subjected to alpha radiography using an optical microscope (model BX-63, Olympus, Japan). The sorption and desorption properties of both the mono- and the bi-functional polymers in acidic medium were studied by equilibrating the polymer discs with appropriate amount of Pu/^{241}Am/^{233}U radiotracers. The sorption efficiencies were determined by radioactivity balance method. The distribution coefficients of the polymeric sorbents for Pu(IV) and U(VI) were measured in competing mode, from a solution containing 100:1 mole proportions of U(VI): Pu(IV). The details of the sorption and desorption studies as well as sorption kinetic studies are discussed in Chapter 2.5.3.

3.3. Results & discussions

3.3.1. Syntheses and characterization of bi-functionalized polymers

The self-supported HEMP–co–AMPS and HEMP–co–APTAC polymer discs are required to have minimum change in dimensions with a sufficient porosity. The swelling ratios of HEMP–co–AMPS and HEMP–co–APTAC polymer discs were found to be 1.32 and 1.47, respectively, which indicated the structural rigidity of the bi-functional polymers. This may be attributed to the presence of HEMP monomer in these bi-functional polymers, which contains three polymerizable double bonds and provided a high degree of crosslinking in the polymer network. Figure 3.2 shows the SEM images of HEMP–co–AMPS polymer disc at different magnifications. Both HEMP–co–AMPS and HEMP–co–APTAC have dense, lamellar structures with no visible micropores. The porosity of these bi-functional polymers was found to be in the range 0.1–0.15 cm^{3}g^{-1}.

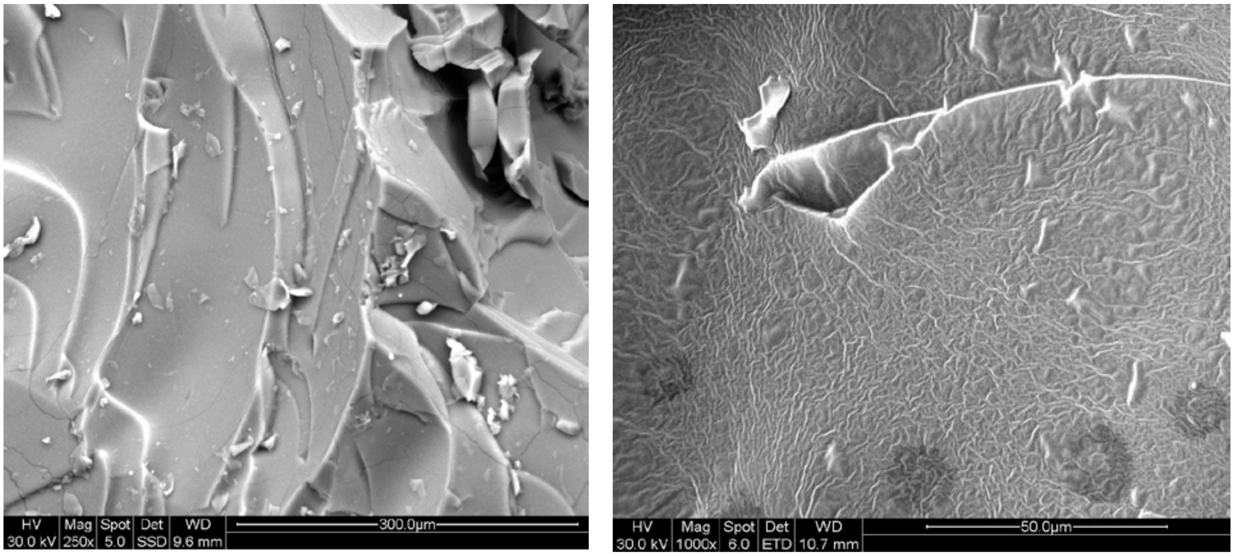

Figure 3.2. SEM images of HEMP–co–AMPS polymer disc at different magnifications.

The elemental analysis by EDS confirmed the homogeneous distribution of the phosphate and the sulfonate/quaternary ammonium groups in the HEMP–co–AMPS/APTAC polymers. Table 3.1. shows the proportions of HEMP and AMPS/APTAC in the bi-functional polymers obtained by measuring sulphur to phosphorus (S/P) ratio and nitrogen to phosphorus (N/P) ratio, respectively, by EDS. There was reasonably good agreement between the measured S/P or N/P ratio in the bi-functional polymer with that calculated based on the proportion of monomers used in the polymerizing solution. This indicated that the rates of polymerization of HEMP and

AMPS/APTAC monomers were equivalent, which can be attributed to the presence of methacrylate moiety in all the monomers. However, the measured atom ratio is a representative of the statistical distribution of the two functional groups in the polymer, and does not indicate the presence of alternate HEMP and AMPS/APTAC units in the polymer chain. To confirm the homogeneity of the functional groups in the bi-functional polymers, alpha track radiography of Pu loaded HEMP–co–AMPS disc was also carried out. The micrograph given in Figure 3.3, showed the uniform distribution of alpha tracks in the disc, which could be correlated to the homogenous distribution of binding sites in the bi-functional polymer.

Table 3.1. Elemental analyses of HEMP–co–AMPS and HEMP–co–APTAC polymer discs by Electron Dispersive Spectrometry.

Sample ID	Atom%		S/P ratio	
	S	P	Measured	Expected
HEMP-co-AMPS	56.13±0.38	43.85±0.37	1.28±0.02	1.34
	N	P	N/P ratio	
HEMP-co-APTAC	47.62±0.34	52.27±0.38	0.92±0.03	0.93

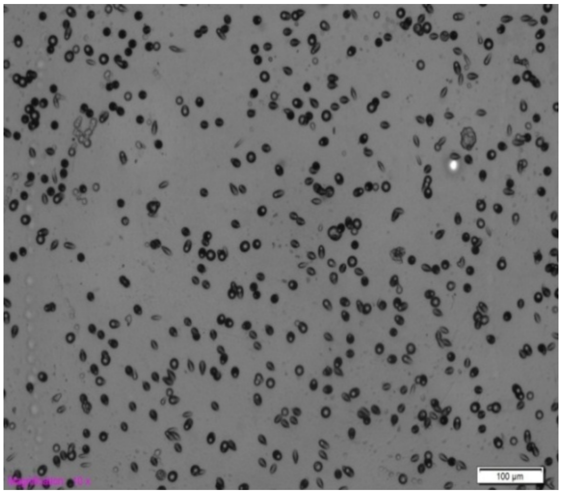

Figure 3.3. Alpha tracks in CR-39 detector exposed to Pu loaded HEMP–co–AMPS disc.

3.3.2. Actinide sorption and desorption studies

The sorption efficiencies of HEMP-co-AMPS polymer towards Am(III), Pu(IV) and U(VI) ions in aqueous solution were studied as a function of HNO_3 concentration and compared with that HEMP and AMPS polymers. Figure 3.4 illustrates the sorption profiles of the mono- and bi-functional polymers for the actinide ions, when concentration HNO_3 of in the equilibrating solution was varied from 0.1–4 M. From Figure 3.4(a), it can be seen that the sorption efficiencies of HEMP and HEMP-co-AMPS polymers for Pu(IV) increased with increasing HNO_3 concentration in the equilibrating solution, and attained a maximum of about 60±2% and 85±3%, respectively, in 3-4 M HNO_3. The sorption profiles of U(VI), shown in Figure 3.4(b), also followed a similar trend. The maximum sorption efficiency of HEMP and HEMP-co-AMPS polymers for U(VI) was found to be about 65±2% and 85±3%, respectively, in 3-4 M HNO_3. Figure 3.4(c) shows the sorption profiles of Am(III), representative of the trivalent actinides, in 0.1–4 M HNO_3, which followed a reverse trend and sorption efficiencies of all the three polymers for Am(III) decreased with increasing HNO_3 concentration.

(a)

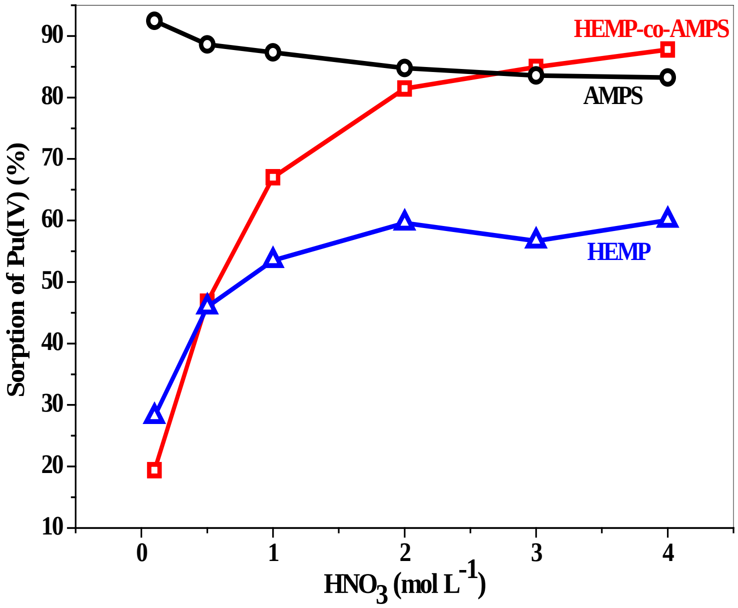

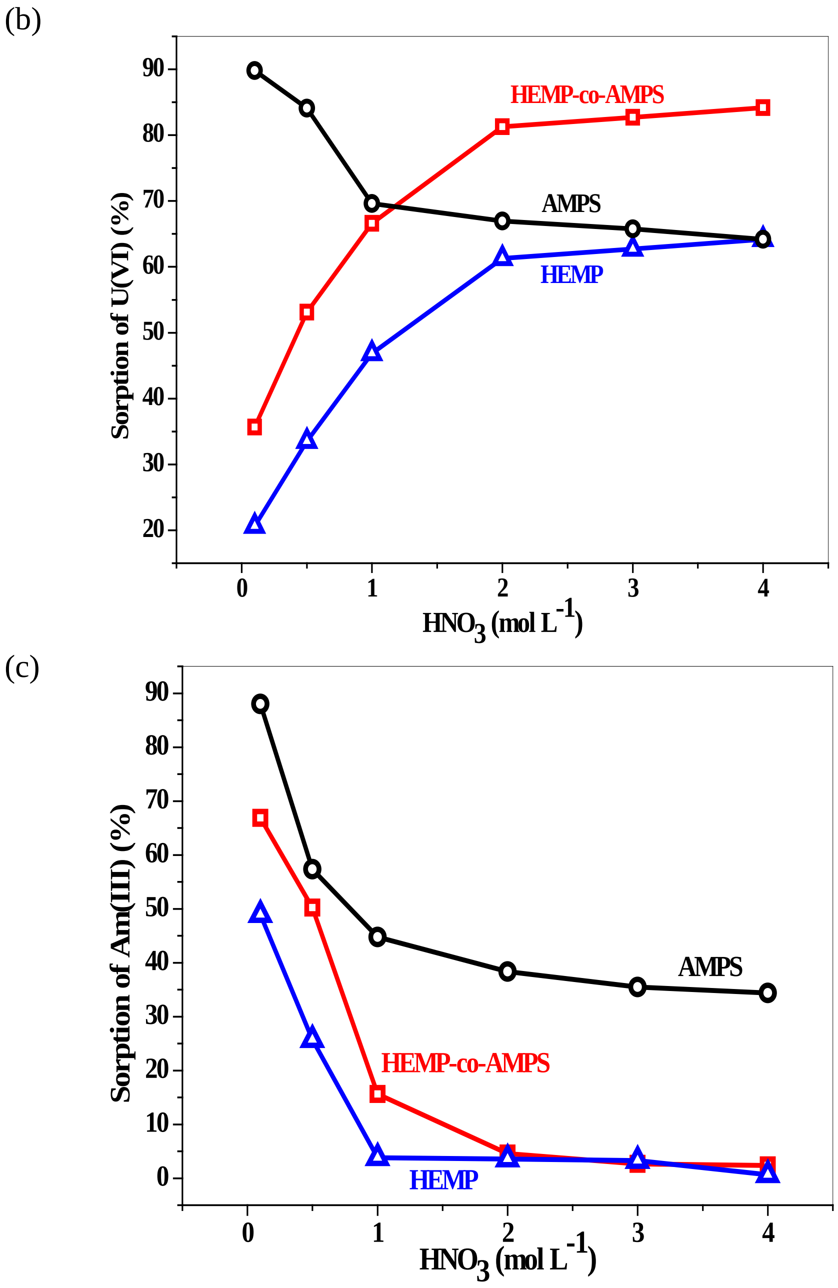

Figure 3.4. Sorption profiles of (a) Pu(IV), (b) U(VI) and (c) Am(III) in HEMP-co-AMPS, HEMP and AMPS polymers as a function of HNO_3 concentration in the equilibrating medium.

The increase in sorption efficiency of HEMP-co-AMPS and HEMP polymers for Pu(IV)/U(VI) ions with increasing HNO_3 concentration could be attributed to the complexation of Pu(IV)/U(VI) with neutral phosphate groups present in these polymers, which require sorption of nitrate ions for charge balance. Whereas sorption of Am(III) is through ion-exchange mechanism; therefore Am(III) sorption efficiency decreases with increasing HNO_3 concentration due to the increase in the concentration of H^+ ions which also compete for the ion exchange sites. In case of pure HEMP polymer, the presence of 25% diester form of HEMP monomer is responsible for ion-exchange mechanism. From Figure 3.4, it can be concluded that Pu(IV) can be discriminated from trivalent actinides like Am(III) in 3–4 M HNO_3 concentration. Also, at any given HNO_3 concentration, the bi-functional HEMP-co-AMPS polymer showed significantly higher sorption efficiencies for both Pu(IV) and U(VI) than the pure HEMP polymer. The better sorption efficiency of HEMP-co-AMPS for Pu(IV) and U(VI) could be attributed to the fact that AMPS unit provides anionic binding sites for charge neutralization of the Pu(IV)/U(VI) ions. Also the presence of sulfonate groups reduce the covalency in binding of actinide ions, which in turn enhances transfer of Pu(IV) ions from one binding site to another. This is important as porosity of disc is not sufficient to provide high accessibility of binding sites to actinide ions present in the equilibrating solution.

To understand the role of sulfonate groups in the sorption of actinide ions, the sorptions of Pu(IV), U(VI) and Am(III) by pure AMPS polymer were also studied as a function of HNO_3 concentration in the equilibrating solution. The Am(III)-sorption efficiency in the AMPS polymer decreased with HNO_3 concentration, which is similar to Am(III) sorption profiles in the HEMP and HEMP-co-AMPS discs. However, it is seen from Figure 3.4(a) that Am(III) sorption efficiency in the AMPS disc is better that that in the HEMP and HEMP-co-AMPS discs. For example, the Am(III) sorption efficiency in the AMPS disc is 30% at 3-4 M HNO_3 while Am(III) sorption is negligible in the HEMP and HEMP-co-AMPS discs under similar conditions.

Thus, the discrimination between Pu(IV) and Am(III) ions is improved in the HEMP-co-AMPS polymer compared to that in the AMPS polymer. The Pu(IV) sorption efficiency in the AMPS polymer did not vary with HNO_3 concentration but remained nearly constant at 87±3 %. The AMPS polymer contains sulfonate groups which are not selective towards Pu(IV) in the presence of competing actinides ions having higher oxidation states like U(VI).

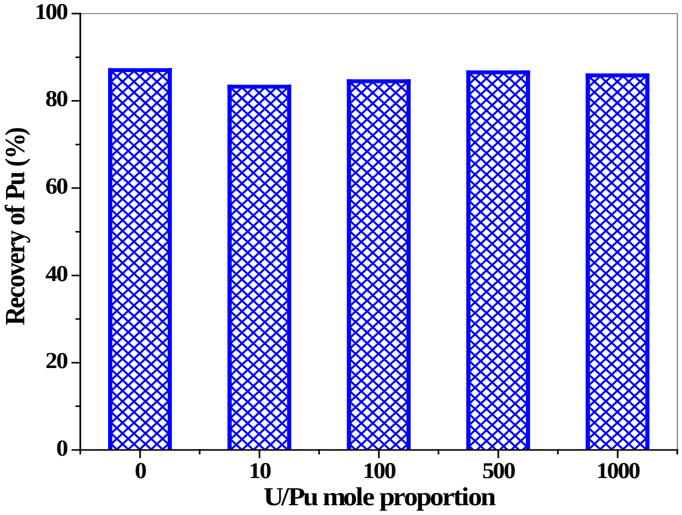

Figure 3.5. Sorption of Pu(IV) by HEMP–co–AMPS polymer from 3M HNO_3 as function U/Pu mole proportion; each solution contained 1 μg of Pu(IV) and 0-1000 μg of U(VI).

To study the selectivity of the bi-functional HEMP–co–AMPS polymer towards Pu(IV) in the presence of U(VI) in 3–4 M HNO_3, the Pu(IV) sorption efficiency was measured in a series of solutions containing 1 μg of Pu(IV) and varying amounts of U(VI), ranging from 0 to 1000 μg. It can be seen from Figure 3.5, Pu(IV) was preferentially sorbed by HEMP–co–AMPS polymer even in the presence of 1000 times excess of U(VI) i.e., Pu(IV) chemical recovery was unaffected from the solution containing 1:1000 wt. proportion of Pu(IV) to U(VI). This was confirmed by measuring the distribution coefficients for Pu(IV) (D_{Pu}) and U(VI) (D_U) ions in competing mode, by equilibrating the polymeric sorbents with a solution containing 1:100 mole proportion of Pu(IV):U(VI) in 4 M HNO_3. As can be seen from Table 3.2, the ratio of D_{Pu} to

D_U is higher for the HEMP-co-AMPS polymer than that for AMPS polymer. This suggests that HEMP-co-AMPS polymer can be employed for the selective sorption of Pu(IV) in presence of other competing actinides like U(VI) and Am(III).

Table 3.2. Distribution coefficients (D) of Pu(IV) and U(VI) ions in the polymeric sorbents from the solution containing 1:100 mole proportion of Pu(IV):U(VI) in 4 M HNO_3

Polymer sorbent	$D(Pu^{IV})$ (mL g^{-1})	$D(U^{VI})$ (mL g^{-1})	D_{Pu}/ D_U
Poly(HEMP)	227	25	9.09
Poly(AMPS)	113	58	1.95
Poly(HEMP-co-AMPS)	396	37	10.70
Poly(APTAC)	98	46	2.13
Poly(HEMP-co-APTAC)	462	40	11.53

The bi-functional HEMP-co-AMPS polymer is efficient for extraction of Pu(IV) from 2–4 M HNO_3 medium owing to the fact that in 2–4M HNO_3, Pu(IV) exists as cationic or neutral nitrato complexes like $[Pu^{IV}(NO_3)]^{3+}$, $[Pu^{IV}(NO_3)_2]^{2+}$, $[Pu^{IV}(NO_3)_3]^{+}$ and $[Pu^{IV}(NO_3)_4]$. However, Pu(IV) sorption efficiency of HEMP-co-AMPS polymer was found to decrease from 85±2% in 3 M HNO_3 to 70±2% in 8 M HNO_3. This could be attributed to the formation of anionic Pu–nitrato complexes like $[Pu^{IV}(NO_3)_5]^-$ and $[Pu^{IV}(NO_3)_6]^{2-}$ with the increasing HNO_3 concentration. This indicates that a bi-functional polymer containing a strong cation exchange group e.g. a quaternary ammonium chloride along with the complexing phosphate group would be more suitable for the extraction of Pu(IV) ions from solution having higher (>4 M) concentration of HNO_3. Therefore, the sorption efficiency of HEMP-co-APTAC polymer towards Am(III), Pu(IV) and U(VI) ions were also studied as a function of HNO_3 concentration in the range 2–8 M HNO_3 and compared with that of HEMP and APTAC polymers.

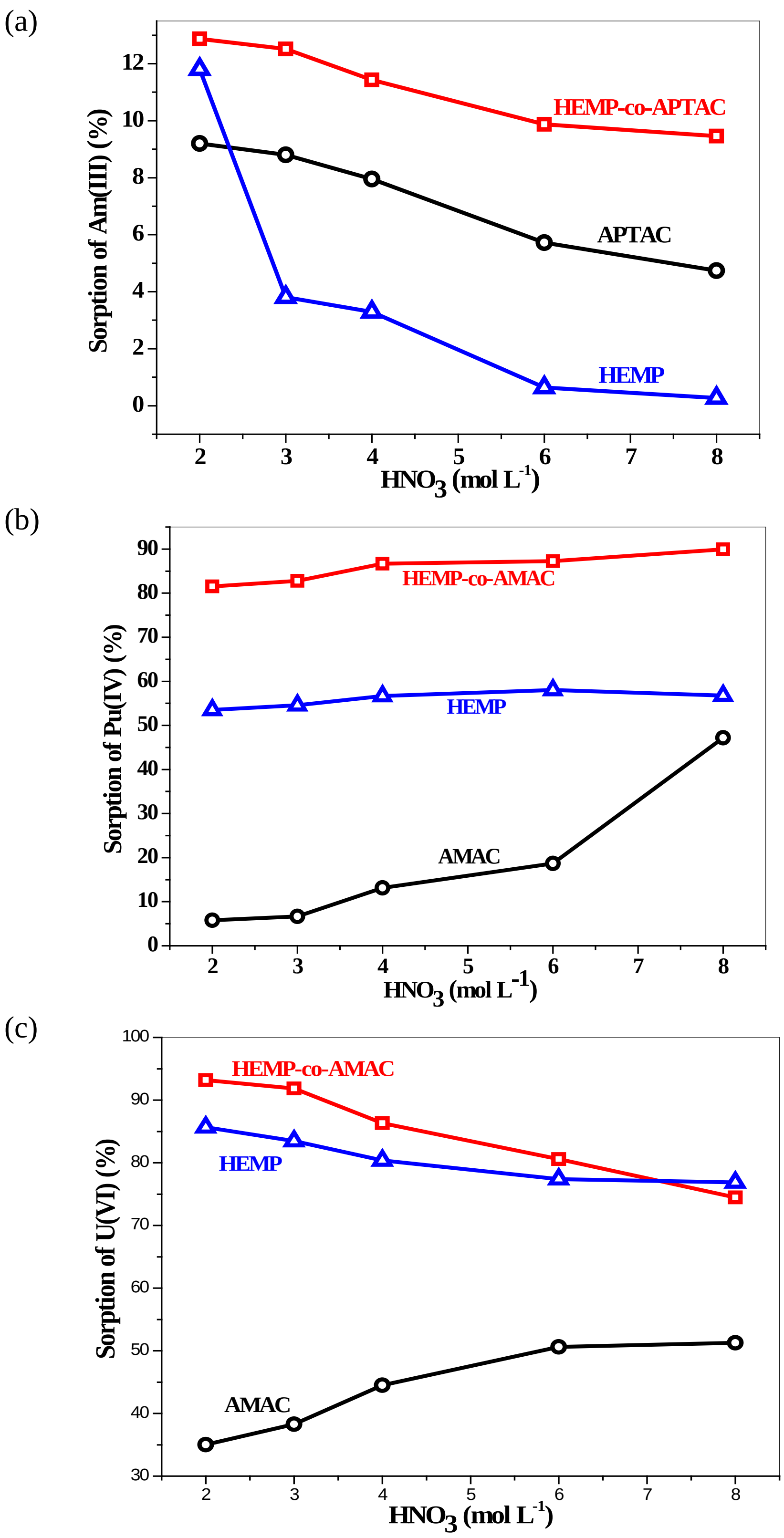

Figure 3.6. Sorption profiles of (a) Am(III), (b) Pu(IV) and (c) U(VI) in HEMP-co-APTAC, HEMP and APTAC polymers as a function of HNO$_3$ concentration.

Figure 3.6 illustrates the sorption profiles of the HEMP-co-APTAC, HEMP and APTAC polymers for the actinide ions. The sorption profiles in Figure 3.6 show that Am(III) is not sorbed with significant efficiencies in all the three polymers unlike Pu(IV) and U(VI) ions. It is interesting to observe from Figure 3.6 that, the Pu(IV)-sorption efficiency did not change significantly in the HNO_3 range of 2-8 M for both HEMP-co-APTAC and HEMP polymers. However, the Pu(IV)-sorption efficiency of HEMP-co-APTAC polymer was considerably higher (≈90%) than that in HEMP polymer (≈60%). This indicates that the presence of quaternary ammonium groups in HEMP-co-APTAC polymer improves the sorption efficiency of the anionic Pu-nitrato complexes that exist in high HNO_3 concentration. In case of U(VI) ions, the sorption efficiency of HEMP and HEMP-co-APTAC polymers remained high (80-90%), and decreased slightly with increase in HNO_3 concentration. Therefore, to study the selectivity of HEMP-co-APTAC polymer towards Pu(IV) and U(VI) ions in competitive mode, the D values were measured by using the solutions containing 100:1 mole ratio of U(VI) and Pu(IV) in 4 M HNO_3. It can be seen from the data given in Table 3.2 that, D_{Pu} value is higher in all the polymeric sorbents, in spite of 100 time excess of U(VI). However, it is seen from Table 3.2 that the D_{Pu} value for Pu(IV) and the ratio of D_{Pu} to D_U is maximum for the bi-functional HEMP-co-AMPS and HEMP-co-APTAC polymers, developed in the present work.

Desorption of actinide ions is important for the reusability of the polymeric sorbents. The desorption of trivalent actinides like Am(III) was possible from the HEMP, HEMP-co-AMPS and HEMP-co-APTAC polymers using high HNO_3 concentration, as indicated in the Am(III) sorption profile shown in Figure 3.4(c). U(VI) could be desorbed from the polymers using 1 M Na_2CO_3 and the extent of desorption was higher in HEMP-co-AMPS and HEMP-co-APTAC polymers (~90%) than HEMP polymers. Desorption of Pu(IV) from the polymers was studied using 0.5 M HNO_3 and 1 M $NH_2OH.HCl$. As can be seen from Figure 3.7, only 40–50% of the sorbed Pu could be stripped from the polymers using 0.5 M HNO_3. It was found to be possible to increase the extent of desorption of Pu(IV) from the HEMP-co-AMPS and HEMP-co-APTAC polymers upto 80% by single equilibration in 1 M $NH_2OH.HCl$ for overnight. This was attributed to the reduction of Pu(IV) to Pu(III) by hydroxylamine hydrochloride. However, Pu(IV) could be desorbed only 40% from the HEMP disc with 1 M $NH_2OH.HCl$. This indicates that the presence of sulfonate groups in the poly(HEMP-co-AMPS) not only improves the sorption properties of the polymer, but also enhances the desorption of Pu(IV). After desorption, Pu(IV) could be again loaded with the same efficiency indicating the reusability of the bi-functional HEMP-co-AMPS and HEMP-co-APTAC polymers.

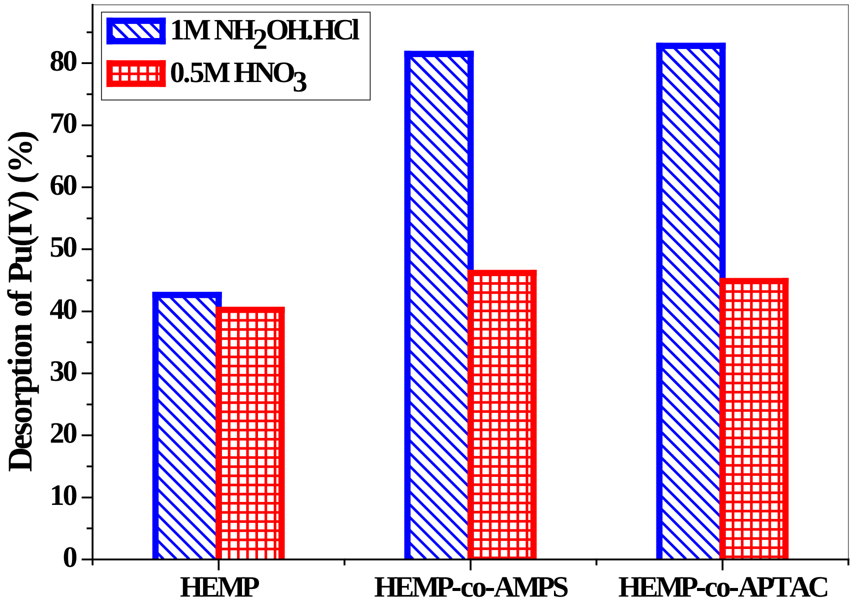

Figure 3.7. Desorption of Pu(IV) from HEMP, HEMP-co-AMPS and HEMP-co-APTAC polymers.

3.3.3. Plutonium sorption kinetics

The sorption rate kinetics for Pu(IV) by HEMP-co-AMPS polymer was studied in order to understand the role of sulfonate groups in the transfer of Pu(IV) ions from surface of the bi-functional polymer disc to its interior matrix. The Pu(IV) sorption rate profile from 3 M HNO_3 is shown in Figure 3.8. The sorption kinetics was studied in high HNO_3 concentration as Pu tends to hydrolyze and polymerize in low acidic conditions. Also at 3 M HNO_3, the ion-exchange mechanism would not have a major effect on the sorption rate profile. It can be seen from Figure 3.8 that the initial sorption of Pu(IV) is very fast and 50% of Pu(IV) sorption equilibrium was attained within 10 min of equilibration time. Thereafter, the rate of sorption decreased which could be attributed to the slow transfer of Pu(IV) ions, from surface of the HEMP-co-AMPS disc to its interior matrix. In case of pure HEMP, the Pu sorption efficiency did not increase beyond 60% due to strong binding of Pu(IV) that would hinder transfer of Pu(IV) ions from surface to interior matrix.

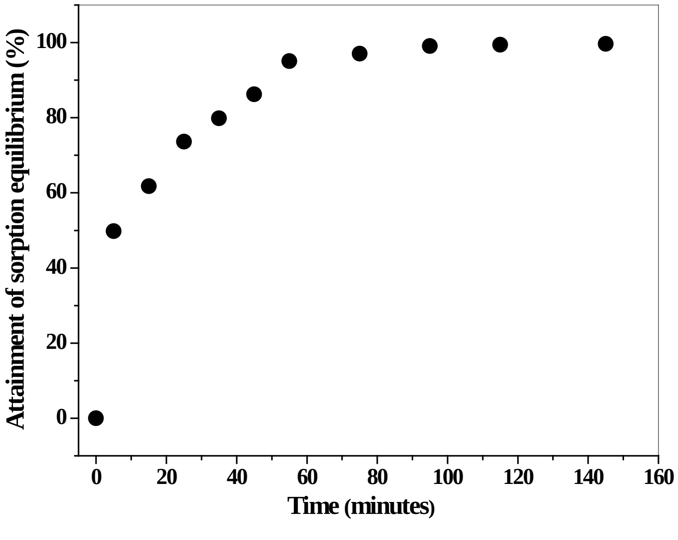

Figure 3.8. Attainment of Pu(IV) sorption equilibrium by HEMP-co-AMPS polymer in 3 M HNO_3 medium.

The rate profile of Pu(IV) sorption by the HEMP-co-AMPS polymer could be fitted to linearized pseudo-second order rate equation given below [125], which is normally observed in chemical sorption of ions in the sorbent at tracer concentration.

$$\frac{t}{Q_t} = \frac{1}{K_2 Q_e^2} + \frac{t}{Q_e} \qquad (3.2)$$

where Q_t and Q_e are the amounts of Pu(IV) sorbed per unit weight of the HEMP-co-AMPS polymer at time t and at equilibrium, respectively, and K_2 is the pseudo-second-order rate constant of sorption. Q_e also represents the Pu(IV) sorption capacity which is the maximum amount of Pu(IV) that could be sorbed per unit weight of the bi-functional polymer. Figure 3.9 shows pseudo-second order rate of sorption of Pu(IV) by the HEMP-co-AMPS polymer in 3 M HNO_3 medium. The value of Q_e, deduced from slope of the Pu sorption rate profile in Figure 3.9 fitted with eqn. 3.2, was 107 µg of Pu g^{-1}, which was found to be in good agreement with experimentally measured Pu loading capacity 108 µg of Pu g^{-1}. The value of pseudo-second order rate constant K_2 for HEMP-co-AMPS polymer was found to be 0.95 g $\mu mol^{-1} s^{-1}$.

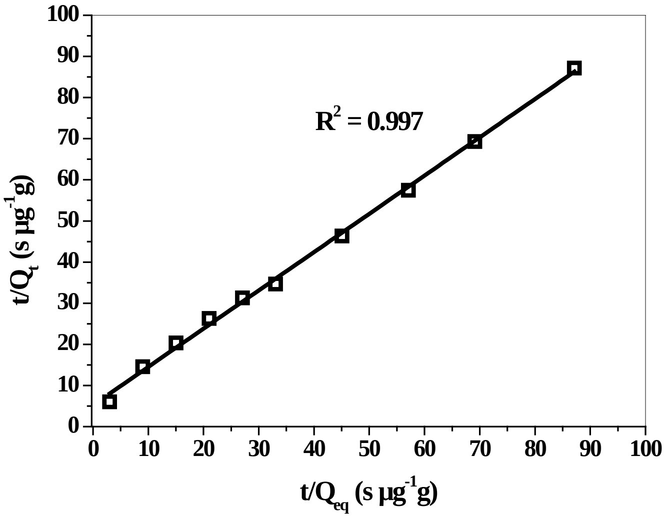

Figure 3.9. Pseudo-second order rate of sorption of Pu(IV) by the HEMP-co-AMPS polymer in 3 M HNO_3 medium.

3.4. Conclusion

The present work involves the development of bi-functional polymers containing neutral phosphate group and strongly ionic group, either sulfate or quaternary ammonium, for the selective and fast preconcentration of Pu(IV) from the aqueous samples. The bi-functional polymers were synthesized by photo-induced free radical polymerization of the HEMP monomers with either AMPS or APATAC monomers. The bi-functional HEMP-co-AMPS or HEMP-co-APTAC polymers were found to have a better Pu(IV) sorption efficiency compared to the monofunctional polymers such as HEMP, AMPS and APTAC polymers at any given HNO_3 concentration. Also, the bi-functional polymers have a better ability to discriminate Pu(IV) from trivalent actinides like Am(III), than the AMPS/APTAC in 3−4 M HNO_3. The bi-functional polymers were found to be selective towards Pu(IV), in the presence of excess U(VI) ions, with a high Pu(IV) recovery efficiency of 86±3%. The distribution ratios of the bi-functional polymers for Pu(IV), in presence of excess U(VI), were also found to be higher than that of either poly(HEMP) and poly(AMPS/APTAC) polymers. This indicated that the bi-functional HEMP-co-AMPS or HEMP-co-APTAC polymers could be promising for the selective extraction of Pu(IV) from complex matrices like various environmental, biological samples, and nuclear fuel dissolver/waste solutions. The amount of Pu(IV) sorbed by the bi-functional polymers can be quantified by alpha spectrometry or mass spectrometry. However, for quantification of the sorbed Pu(IV) directly from the polymer matrix, the bi-functional polymers should be suitably tailored according to the requirements of alpha spectrometric or mass spectrometric techniques.

Chapter 4

Anchoring of a thin layer of bi-functional polymer on membrane for alpha spectrometric determination of Pu(IV)

4.1. Introduction

Radiometric methods are simple yet sensitive techniques for the quantification of actinides in various complex aqueous matrices like environmental, biological and nuclear facilities samples. The simplest method for quantification of alpha emitting actinides is gross alpha counting by proportional or liquid scintillation counters, provided the target actinide emits monoenergetic alpha particles. However, the resolution of conventional proportional or scintillation counters is not sufficient to resolve multiple alpha energies. Pu cannot be quantified by proportional or scintillation counter as it is always associated with other alpha emitting actinides e.g. ^{241}Am etc. An alternative to gross alpha counting for the quantification of Pu is alpha spectrometry, using the high resolution semiconductor detectors. Though spectral interferences like ^{241}Am, ^{210}Po and ^{228}Th with ^{238}Pu, ^{224}Ra, ^{229}Th, ^{231}Pa, ^{232}U, and ^{243}Am with ^{239,240}Pu cannot resolved by the commercially available alpha detectors. Various chemical separation procedures are employed, prior to alpha analysis, to remove major and minor matrix interferences from the sample. Also, since alpha particles have very short range in matter, the thickness of an alpha source should not exceed a few micrometers in order to minimize the degradation of alpha energy and improve peak resolution in the alpha spectrum. Chemical separation of the target actinide from the other sample components is, therefore, necessary in order to avoid various interferences and obtain very thin alpha source. The commonly used separation methods for alpha spectrometry are co-precipitation, solvent extraction, ion-exchange, and extraction chromatography using TEVA, TRU and/or UTEVA resins as discussed in section 1.4.2 [3, 126–128]. Recently, Chamizo et al. have developed a method for the determination of Pu isotopes in environmental samples by alpha spectrometry, after separation of Pu from matrix by actinide specific extraction chromatography resin (TEVA®, Eichrom Industries, Inc.) [129].

A multi-dimensional separation method employing extraction chromatography for the analysis of actinides in environmental samples was reported for alpha spectrometry by Guérin et al, where Th, U, Np, Pu and Am were separated into individual fractions using TEVA and DGA resins, in order to remove interferences and enable their proper identification and quantification [89]. Cloud point extraction procedure, coupled to inductively coupled plasma mass spectrometry and alpha spectrometry, was also reported for the quantification of plutonium in a wide variety of aqueous and digested samples like synthetic urine, waste water, drinking water, seawater and soil [130]. Apart from the improvements of the separation techniques for matrix removal and preconcentration of actinides, attempts were also made for more accurate data analyses in alpha spectrometry. Marroyo et al. have applied corrections for an energy drift in the long-duration measurements and developed an efficient deconvolution method for complex alpha spectra [131].

Alpha source preparation is the next important step for analysis of Pu by alpha spectrometry after the standard separation procedures for the removal of matrix interferences. It is essential to prepare a thin and uniform alpha source in order to achieve sufficiently good resolution of at least 30–50 keV, as the full width at half maximum, in the alpha spectrum. The alpha source should be prepared in such a way that extent of deposition of the target actinide from the solution is quantitative and at the same time it is deposited as a very thin, uniform layer on the surface of a flat substrate. Alpha sources are prepared preferably on polished stainless steel or platinum discs, generally termed as planchettes. The common methods used for alpha source preparation are evaporation, micro-precipitation and electrodeposition. In evaporation method, 25–200 μL volume of the sample solution is evaporated under IR heating onto a planchette and then ignited in flame so that the actinides get adhered to the planchette. However, it is difficult to prepare a uniform source by evaporation method and there is no control over the thickness of source. Also, high salt content in the sample may create a deposit on the source which would result in degradation of the energy of the alpha particles, leading to low energy tailing of the characteristic alpha energy peaks in the spectrum. As a result, the spectral resolution would worsen. Micro-precipitation of actinides with rare earth fluoride like NdF_3 and filtration deposition on the smooth surface of a membrane are the alternative methods reported for alpha source preparation [132,133]. However, the most widely used method for alpha source preparation is electro-deposition of actinides onto a planchette, serving as the cathode in an electrolytic cell [134]. A standard protocol for alpha source preparation by the electro-deposition of actinides was reported in 2000 and reapproved in 2005 (ASTM C1284-00, 2000b). Recently, Novikov et al. have reported the use of an ionic liquid trihexyltetradecylphosphonium hexafluorophosphate to improve electro-deposition of americium from the organic medium [135].

The multistep separation and alpha source preparation associated with alpha spectrometry often introduce high uncertainty in the results. Such uncertainties can be minimized by the combination of alpha spectrometry with a standard addition technique, like isotope dilution with a suitable radiotracer [46, 136–138]. The long analysis time and tediousness of the multistep hybrid methods still remains a bottleneck, particularly when emergency preparedness or risk assessment of contaminated areas resulting from nuclear weapon tests, nuclear accidents, discharge of nuclear waste etc. are concerned. Automated flow injection (FI) or sequential injection (SI) techniques can partially improve the scenario, but the requirement of solid thin alpha source preparation still persists. A plausible alternative to the conventional, time consuming, multistep methods is thin extractive sorbent based direct alpha spectrometry [139–

141]. The methods reported till date for thin film based alpha spectrometry involve sophisticated synthetic routes which are not amenable to routine uses.

The objective of the present work was to develop a membrane based alpha spectrometric method for the determination of Pu(IV) using a surface grafted membrane that combines matrix removal, preconcentration of Pu(IV) and alpha source preparation in a single step. A thin bi-functional polymer layer, containing phosphate and sulphonate functional groups, was anchored on polyethersulfone (PES) membrane by photo–induced free radical grafting for a direct alpha spectrometry of Pu(IV). The formation of the thin bi-functional layer on the PES membrane was an easy, reproducible, one step process that is amenable for the routine applications of alpha spectrometric determination of Pu(IV) ions in the acidic solutions. Also, the membrane based alpha spectrometry provides a fixed and reproducible counting geometry necessary to achieve a constant efficiency factor for the quantification of Pu by alpha spectrometry. However, use of isotope dilution technique in the membrane based isotope dilution alpha spectrometry (Mem-IDAS) would account for the unforeseen errors during preconcentration and provide flexibility in mounting the membrane in the alpha counting chamber. In the present work, membrane based alpha spectrometry was employed for determination of Pu concentration in a various matrices, employing either efficiency calibration method or isotope dilution method.

4.2. Experimental

Commercially available PES membranes, having, 0.1 and 0.2 µm pore-sizes, were cut into 2X1 cm^2 pieces, washed thoroughly with methanol and dried. The functional monomers phosphoric acid 2-hydroxyethyl methacrylate ester (HEMP) and 2-acrylamido-2-methyl-1-propanesulphonic acid (AMPS) were dissolved in (1:1) water:ethanol to prepare the polymerizing mixture. The two sides, viz. rough surface and glossy surface, of the commercially available PES membrane have different morphologies and surface grafting of the PES membranes was carried out selectively on either rough or glossy surface. The PES membranes, having 0.1 and 0.2 μm pore-sizes, were cut into 2x1 cm^2 pieces, washed thoroughly with methanol and dried. To graft the bi-functional polymer on a desired surface (i.e. rough or glossy surface), the opposite surface of the membrane was blocked using tape. The polymerizing mixture consisting of saturated solution of HEMP and AMPS in 1:1 mol proportion, dissolved in 1:1 (v/v) water:ethanol, was homogenized with ultrasonication and poured on the unprotected surface of PES membrane and immediately exposed to 365 nm light in a photoreactor for 15 minutes. After photo-irradiation, the tape on membrane pieces was removed, washed thoroughly with methanol and water to remove un-grafted monomers, dried under vacuum, and hydrated with deionized water before use. The amount of bi-functional polymer grafted on the surface of PES membrane was obtained gravimetrically from the weight changes before and after grafting. The surface morphologies of PES membranes, before and after grafting, were examined by SEM and the homogeneity of the phosphate and sulfonic acid functional groups grafted on the membrane was studied by SEM–EDS analysis. Depth profiling of the grafted membrane was carried out by ToF-SIMS, using 15 keV Ga^+ ion source as the primary beam. The sorption efficiency of the bi-functional PES membrane towards U(VI), Pu(IV) and Am(III) ions in HNO_3 medium was studied by radioactivity balance method, as described in the section 2.5.3.

For determination of Pu(IV) by membrane based alpha spectrometry, 2x1 cm^2 pieces of bi-functional PES membrane was equilibrated for 1 hour with 5 mL of well-stirred 3M HNO_3 solution containing appropriate amount of Pu(IV). After equilibration, the membrane was taken out, washed thoroughly with 3M HNO_3, dried and placed directly in front of a semiconductor detector to record the alpha spectrum. Two different passivated ion-implanted planar silicon detectors were used in the present study. A small area detector (PIPS Canberra, PD-25-12-100AM, 25 mm^2 surface area, 100 µm active thickness, 12 keV FWHM at 5.486 MeV energy of alpha particles emitted by ^{241}Am) was used for the comparison of the quality of alpha spectrum obtained using the membrane with that obtained using planchetted source. For the determination of Pu concentrations in various matrices a large area detector (PIPS Canberra, PD-450-17-100AM, 450 mm^2 surface area, 100 µm active thickness, 17 keV FWHM at 5.486 MeV energy of alpha particles emitted by ^{241}Am) was used to obtain higher geometrical counting efficiency and reduce counting time. The Pu loaded PES membrane samples were placed at a distance of about 1 cm from the PIPS detector in a vacuum chamber and pressure inside the chamber was reduced to about 10^{-6} bar. The detector voltage was applied with a 100 Volt HV-unit (M/s ECIL, India) fixed in a 6-slot NIM Bin (M/s Gyanic Systems, India).The alpha spectra were recorded by a PC-based 8K-MCA coupled to the PIPS detector through a USB interface and the spectral analyses were carried out using PCA3 software. To achieve good counting statistics, the alpha spectra were recorded for sufficient time to accumulate minimum 10,000 counts under the characteristics alpha peaks of Pu isotopes.

The Pu activities in various complex aqueous matrices were determined by membrane based alpha spectrometry, employing efficiency calibration method. 5-100 mL of seawater and groundwater samples were treated spiked with known amount of Pu stock solution. The urine/seawater/groundwater samples were then treated with 3M HNO_3 to adjust the acidity and 30% H_2O_2 to convert Pu into Pu(IV). 2×1 cm^2 piece of HEMP-AMPS grafted PES membrane was equilibrated with each of the treated aqueous samples, for 1 hour (for 5−30 mL) and 24 hours (for 100 mL), with continuous stirring at room temperature. About 2 g soil sample was soaked with known amount of Pu stock solution and then evaporated to near dryness. Pu was leached from the soil by treating with 100 mL of 8M HNO_3 containing 2−3 mL of 30% H_2O_2 with heating under an IR lamp. The soil leach liquor was then equilibrated with 2×1 cm^2 piece of HEMP-AMPS grafted PES membrane. After equilibration, the membranes were washed thoroughly with water, dried, and placed directly in front of a PIPS detector to measure the alpha count rate at characteristic energies of the Pu isotopes. The absolute counting efficiency of the membrane sample with fixed dimensions and at a fixed counting geometry was obtained by loading known activities of Pu(IV) in the membrane. The Pu activity (Bq) in the membrane sample was obtained by correcting the measured alpha count rate for both the absolute counting efficiency and the Pu(IV) sorption efficiency of the HEMP-AMPS grafted PES membrane.

Pu concentration in dissolver solution and in (U, Pu)C solutions were determined by membrane based isotope dilution alpha spectrometry (Mem–IDAS). For isotope dilution, a known weight of pre-calibrated ^{238}Pu spike solution was added to a known weight of the sample and the mixture was first treated with conc. HNO_3 for homogeneous mixing of the spike isotopes with the sample, followed by 3M HNO_3 and 30% H_2O_2 to adjust Pu oxidation state to Pu(IV). The sample volume was made up to 5 mL after treatment and equilibrated with a 2×1 cm^2 piece of HEMP-AMPS grafted PES membrane for 1 hour with continuous stirring. HNO_3 concentration in the equilibrating solution was maintained at 3 M to ensure optimum sorption of Pu(IV) ions. After equilibration, the membrane samples were washed thoroughly with water, dried and placed directly in front of the PIPS detector to record the alpha spectra. The Pu concentrations determined by Mem–IDAS method were compared with conventional isotope dilution alpha spectrometry (IDAS) and thermal ionization mass spectrometry (TIMS) results. The sample, the pure spike and spiked mixture were purified using a 5 cm column of Dowex

1X8 (200–400 mesh) anion-exchange resin, where Am and other fission products were eluted with 8 M HNO_3 and U(VI) was eluted with 3 M HNO_3. Pu(IV) was eluted from the column using 0.3 M HNO_3. After purification, Pu alpha source was prepared by evaporating a few drops of solution on a polished stainless steel planchette. The purified Pu sample was loaded on a high purity rhenium double filament assembly for TIMS analyses.

4.3. Results & discussion

4.3.1. Surface grafting of bi-functional polymer layer

The choice of commercially available PES membrane as a substrate for membrane based alpha spectrometry was promising because PES undergoes radiolysis to generate free radicals when subjected to UV light and, therefore, was suitable for the grafting of the bi-functional polymer layer. Also, the porous structure of the PES membrane would provide high accessibility of binding sites to Pu(IV) ions in the solution and at the same time it would serve as a thin, flat source for the quantification of preconcentrated Pu(IV) by alpha spectrometry. Figure 4.1 shows the SEM images of the PES membrane, before and after grafting the bi-functional HEMP-AMPS polymer. Though grafting results in a slight change in the morphology, the grafted surface still possessed sufficient porosity to provide high accessibility for Pu(IV) ions to the binding sites. From Table 4.1, it can be seen that the distribution of sulfur and phosphorus atoms, obtained from EDS analysis, on the grafted PES membrane surface was found to vary within ±2% which indicated the homogeneity of distribution of the phosphate and sulphonate functional groups on the membrane. Also the S/P ratio in the grafted membrane was found to be in a good agreement with that calculated from the mole proportion of HEMP and AMPS in the polymerizing solution, after correction for the sulfur contribution from the host PES membrane.

This indicated the rates of polymerization of HEMP and AMPS were comparable, owing to the presence of methacrylate moiety in both the monomers.

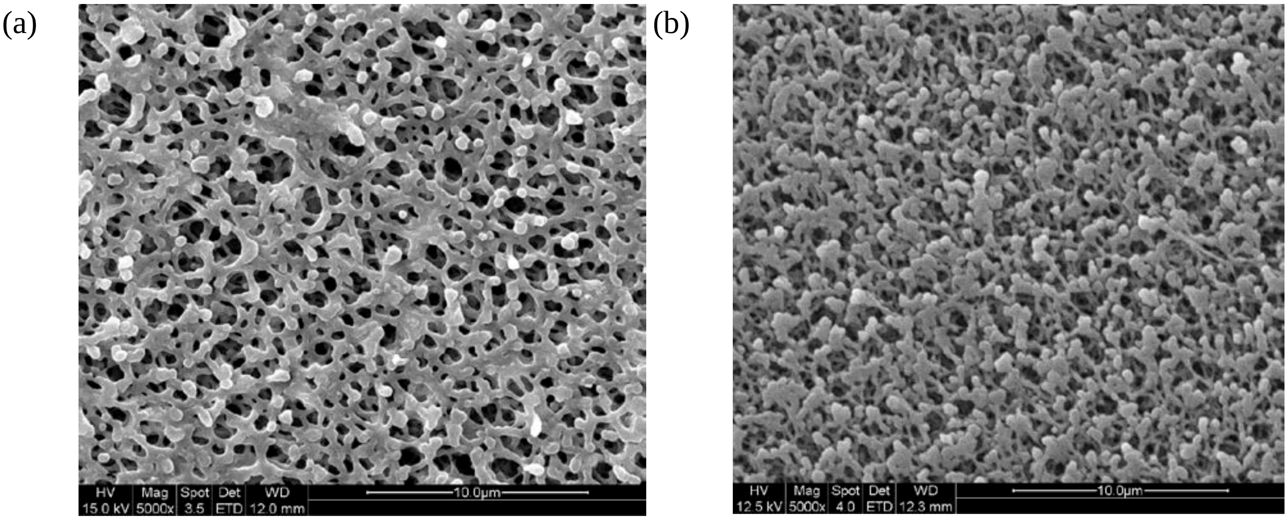

Figure 4.1. SEM images of (a) a pristine PES membrane having 0.2 μm pore-size and (b) same surface after grafting of HEMP-AMPS layer.

Table 4.1. Elemental analysis of the HEMP-AMPS grafted PES membrane by EDS

Concentration (Atom%)		S/P Ratio	
S	P	Measured	Expected
58.2	41.8	1.45 ± 0.03	1.47
58.6	41.4		
59.9	40.1		
59.7	40.3		

The commercially available PES membrane, produced by the phase inversion method, had rough and glossy surfaces having substantially different morphologies. Figure 4.2 shows the SEM images of the rough and glossy surfaces of the PES membranes, having 0.1 μm and 0.2 μm pore sizes. The porosity of the rough surface was significantly higher than that of the glossy surface of the PES membranes, having 0.1 μm and 0.2 μm pore sizes. The grafting yield and, therefore, the thickness of the bi-functional polymer grafted on the PES membrane would be highly dependent on the porosity of the membrane. Since the quality of an alpha spectrum is highly dependent on thickness of the alpha source, it was necessary to study the appropriate side of the PES membrane for grafting the bi-functional layer. Therefore, the HEMP and AMPS monomers were grafted selectively on the rough and glossy surfaces of the PES membrane. The amount of bi-functional layer grafted on a selected surface of the membrane could not be measured unambiguously. As an alternative, Pu(IV) loading capacities, which directly represented the available binding sites and hence could be correlated to the amount of bi-functional polymer grafted on the rough or glossy surface of the PES membrane, were measured.

The Pu(IV) loading capacities were measured by equilibrating 2×1 cm^2 piece of PES membrane, with the bi-functional polymer grafted selectively on the rough or glossy surface, with solutions containing excess of Pu(IV) in 3 M HNO_3 to assure saturation loading of Pu(IV) in the membrane samples. It is seen from Table 4.2, for a PES membrane having a fixed pore size, the rough side grafted membrane sample has higher Pu(IV) loading capacity compared to the glossy side grafted membrane. This clearly indicates that the extent of grafting of the HEMP and AMPS monomers is highly dependent on the porosity of the PES membrane and the glossy surface of a PES membrane, having fixed pore size, was grafted with lower amount of bi-functional polymer than rough surface of the same membrane.

The higher porosity of the rough surface provides larger effective surface area of PES chains for grafting of the monomers, than the glossy surface of the same membrane, leading to a higher grafting yield. Also, there is an increased probability recombination of the PES free radicals, generated during photolysis, in the densely packed glossy surface compared to the rough surface. The lower extent of grafting on the glossy surface of the PES membrane, having a fixed pore size, results in the lower Pu(IV) loading capacity than that of the rough surface of the same membrane. It is apparent from Table 4.2, that HEMP-AMPS grafted on the rough surface of PES membrane, having 0.1 μm pore size, would be the best choice for the determination of Pu(IV) be membrane based alpha spectrometry since it has the maximum Pu(IV) uptake capacity.

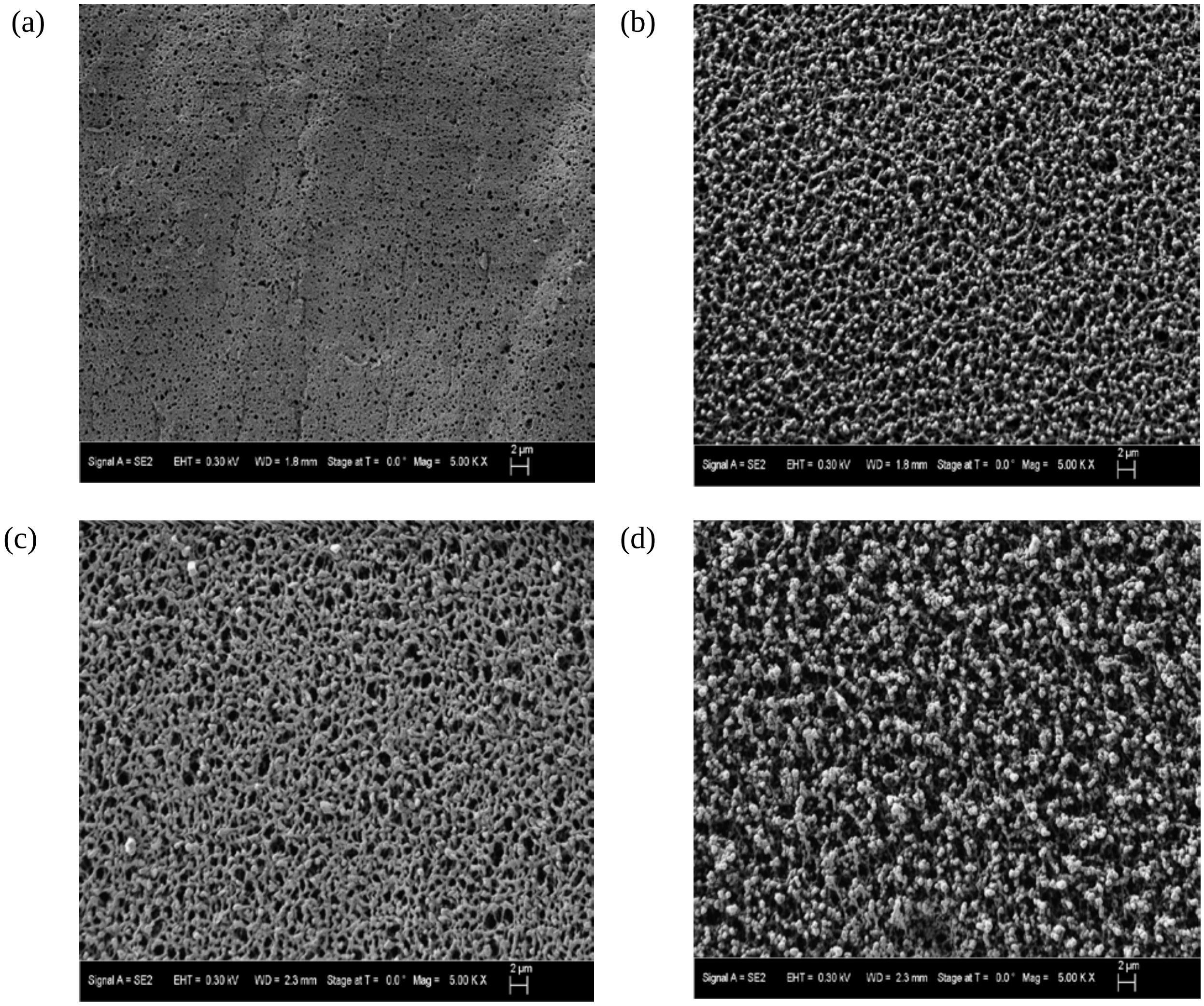

Figure 4.2. SEM images of glossy side (a) and rough side (b) of a pristine PES membrane having 0.1 µm pore-size, and glossy side (c) and rough side (d) of a pristine PES membrane having 0.2 µm pore-size.

Table 4.2. Pu(IV) loading capacity of 2×1 cm^2 piece of PES membrane, having different pore sizes, grafted with HEMP-AMPS selectively on either rough or glossy surface.

Pore size (μm)	Pu(IV) exchange capacity (μg)	
	Rough side	Glossy side
0.1	2.56 ± 0.06	1.83 ± 0.08
0.2	1.79 ± 0.09	1.08 ± 0.10

The quality of an alpha spectrum, in terms of alpha energy degradation and spectral resolution, should also be considered while choosing a substrate for alpha spectrometry, apart from Pu(IV) uptake capacity. Therefore, the alpha spectra were recorded from Pu(IV) loaded on HEMP-AMPS grafted rough side and glossy side of PES membrane samples having 0.1 μm and 0.2 μm pore sizes. It can be seen from Figure 4.3 that, for PES membrane having a given pore size, HEMP-AMPS grafted on a glossy side of the membrane serves as better substrate for obtaining a good quality alpha spectrum, with lesser energy degradation and better resolution. Since the degradation of alpha peaks is highly dependent on the thickness of the alpha source, it seems that the thickness of grafted HEMP-AMPS layer is more on the rough surface of a PES membrane, having a fixed pore size. As such, no measurable change in thickness of the HEMP-AMPS grafted membrane was observed by micrometer. Therefore, depth profiling of the rough and glossy surfaces of PES membrane was carried out using ToF-SIMS to measure the thickness of the bi-functional polymer layer grafted on either side of the PES membrane. Figure 4.4 shows the elemental profile of HEMP-AMPS grafted on the rough and glossy surface of PES membrane.

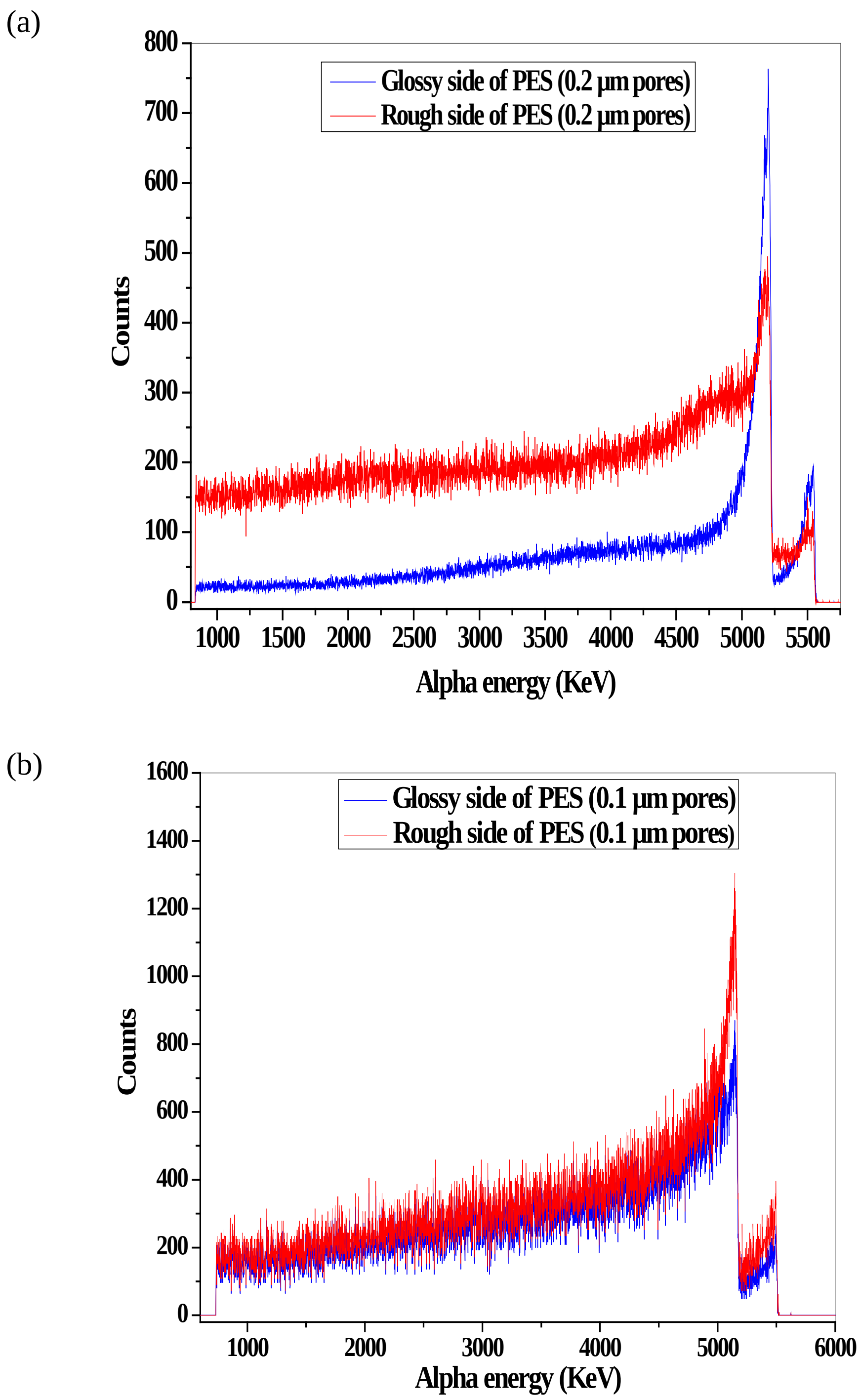

Figure 4.3. Alpha spectra obtained from Pu(IV) loaded on the HEMP-AMPS grafted PES membrane samples having (a) 0.2 µm pore size and (b) 0.1 µm pore size.

It can be seen from Fig. 4.4 that the fractions of phosphorus, from HEMP units, and sulfur, from AMPS units and PES polymer, with respect to total ions across the thickness of the glossy and rough surfaces are quite different. The PES polymer chains itself contain sulfur atoms and, therefore, sulfur concentration is expected to be higher on the glossy surface of the membrane due to a high packing density of the PES polymer chains, compared to the rough surface of the same membrane.

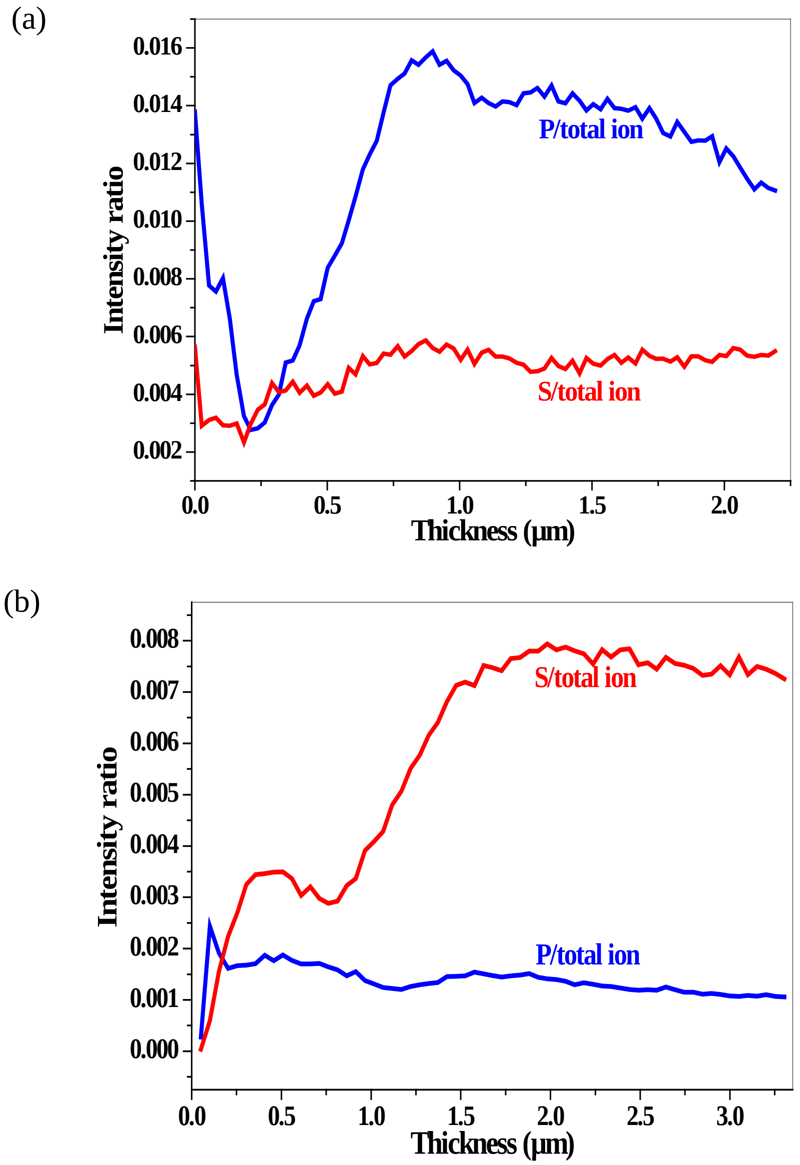

Figure 4.4. Depth profiling of phosphorus and sulfur contents in HEMP-co-AMPS grafted on (a) rough surface and (b) glossy surface of a PES membrane with 0.2 μm pore size.

Figure 4.4 shows an increase in the sulfur content of the glossy surface upto 1.5 μm thickness, which becomes nearly constant thereafter. The phosphorus content is lower than sulfur content on glossy surface and almost merges with the background above 1.0 μm thickness, suggesting that HEMP-AMPS polymer is confined to 1–1.5 μm thickness on the glossy surface. On the other hand, the phosphorous content along thickness of the rough surface of the same membrane was considerably higher than sulfur content up to 3 μm. Also, the phosphorus content in the rough surface initially decreases up to 0.5 μm and then again shows an increase, which may be attributed to the grafting of HEMP-AMPS polymer on the surface as well as on wall of the pores in the rough surface. This is expected as the higher porosity of the rough surface of PES membrane would allow UV radiations to penetrate a longer depth of the PES membrane. The alpha particles lose their kinetic energy while emerging from the interior of the thick HEMP-AMPS layer, >3 μm as observed from the depth profile, grafted on rough surface of the membrane, which results in the low energy tailing of the alpha peaks in the spectrum shown in Figure 4.3. Though Pu uptake capacity of the glossy side grafted 0.1 mm pore size PES membrane is more than that of the glossy side grafted 0.2 μm pore size PES, the alpha energy degradation appears to be more in the case of 0.1 μm pore-size PES due to higher thickness of the grafted layer. It can be concluded from the depth profiling data that that HEMP-AMPS grafted on glossy surface of 0.2 μm pore size PES membrane, where thickness of the grafted polymer layer is minimum, is better choice to obtain a good quality alpha spectrum. Therefore, HEMP-AMPS grafted on glossy surface of PES membrane, having 0.2 μm pore size, was better suited for determination of Pu concentration, in spite of its lower Pu(IV) loading capacity, and all further studies were carried out using this substrate.

4.3.2. Membrane based alpha spectrometry for Pu

The alpha spectra obtained from the HEMP-AMPS grafted PES membrane and from the conventional drop–evaporated planchetted alpha sources were compared in terms of various important parameters which affect the quality of alpha spectrum like FWHM, percentage tail contribution and peak to valley ratio etc. Figure 4.5 shows the energy spectra of alpha particles emitted by ^{239,240}Pu and ^{238}Pu, obtained from same amount of Pu loaded on HEMP-AMPS grafted PES membrane and deposited on a stainless steel planchette by drop-evaporation. Both samples were counted for the same time with identical counting geometry and a small surface area (25 mm^2) PIPS detector was used to obtain good resolution of the alpha peaks.

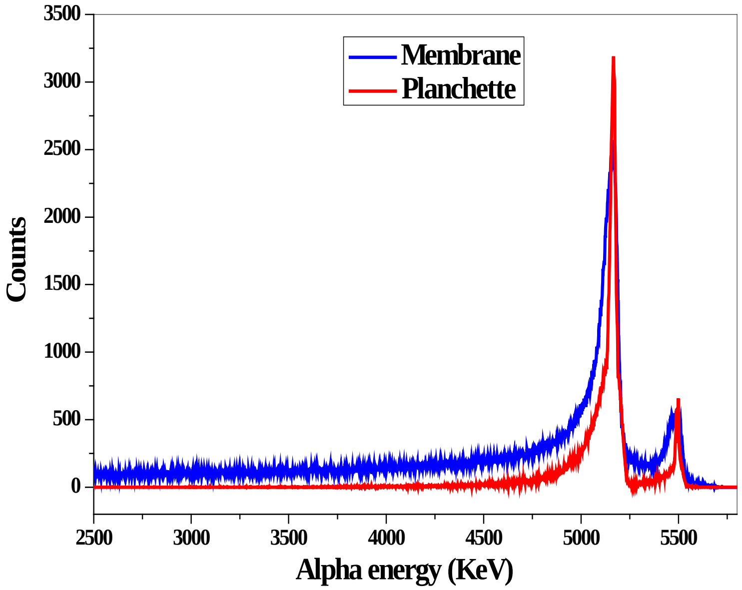

Figure 4.5. Comparison of alpha peak shapes obtained from Pu loaded on HEMP-AMPS grafted glossy surface of 0.2 µm pore size PES membrane and same amount of Pu deposited on a stainless steel planchette.

Figure 4.5 suggests that the alpha spectrum recorded from the membrane is comparable to that obtained from the planchette source. The resolutions at both 5.15 MeV and 5.5 MeV alpha energies were slightly better for the planchette than for the bi-functional PES membrane. The comparison of the FWHM, percentage tail contribution and peak to valley ratio for the alpha peaks obtained from the membrane and the planchette source, containing same Pu activity and counted in identical geometry for the same time, are given in Table 4.3. However, the tail contribution (%) per unit alpha activity ratio was significantly higher in the case of membrane as compared to that in the planchetted source. This can be attributed to the higher left-side tailing of the alpha peaks obtained from membrane than the planchette, due to the degradation of alpha energy within the 1−1.5 μm thickness of the bi-functional polymer layer, grafted on the glossy surface of PES membrane. The peak energies of alpha particles emitted by ^{239,240}Pu (5.157−5.168 MeV) are well separated from that of alpha particles emitted by ^{238}Pu (5.499 MeV). Therefore, the evaluation of ^{238}Pu/(^{239}Pu+^{240}Pu) alpha activity ratio requires correction for the low energy tail of 5.5 MeV (^{238}Pu) peak under the 5.1 MeV (^{239}Pu+^{240}Pu) peak as a result of the loss of alpha energy within the alpha source as well as at the detector window. The tail contribution of the higher alpha energy peak to the lower alpha energy peak cannot be measured directly and has to be evaluated mathematically.

Table 4.3. Comparison of typical alpha spectrometric parameters for drop evaporated planchetted sources and HEMP-AMPS grafted on the glossy surface of PES membrane.

Alpha spectrometry parameter	Alpha energy			
	5.16 MeV (^{239}Pu+^{240}Pu)		5.50 MeV (^{238}Pu+^{241}Am)	
	Planchette	Membrane	Planchette	Membrane
FWHM (in KeV)	20 – 25	28 – 35	15 – 20	18 – 24
Tail contribution (%) per unit alpha activity ratio[a]	1.28 – 2.19	5.11 – 11.43	-----	-----
Peak to valley ratio[b]	20 – 60	5 – 15	20 – 60	3 – 12

[a] Employing G. P. method and taking 300 keV width for each region.

[b] Valley as the mean of five data where the regions used in G. P. method for 5.16 MeV and 5.50 MeV peaks end.

Table 4.4. Comparison of ^{238}Pu/(^{239}Pu+^{240}Pu) alpha activity ratios obtained from drop evaporated planchette source and HEMP-AMPS grafted on glossy surface of PES.

Sample Id.	Alpha Source	^{238}Pu/(^{239}Pu+^{240}Pu) alpha activity ratio			
		Uncorrected	Corrected by GP method*	Error due to tail contribution (%)	A/B
Sample 1	Planchette	0.223	0.224	0.45	1.02
	Membrane	0.216	0.220	1.76	
Sample 2	Planchette	0.258	0.260	0.93	1.01
	Membrane	0.250	0.257	2.80	
Sample 3	Planchette	0.272	0.274	0.59	0.98
	Membrane	0.272	0.278	2.17	

*Tail contribution was corrected by GP method.

In the present study, geometric progression (GP) method was used for tail contribution at lower alpha energy [142]. The prime assumption in GP method is that the counts in the tail region of the 5.5 MeV alpha peak decrease in a geometric progression. In GP method, each alpha spectrum is divided into four regions, viz. A, B, C and D, such that each region has equal number of channels and two consecutive regions are separated by an equal number of channels. ^{238}Pu/(^{239}Pu+^{240}Pu) alpha activity ratio (R) is then calculated by the following equation 4.1:

$$\mathbf{R} = \frac{\mathbf{A}}{\mathbf{B}-\frac{\mathbf{AC}}{\mathbf{B}+\frac{\mathbf{AD}}{\mathbf{C}}}} \qquad (4.1)$$

Since the energy difference between the alpha peaks of ^{238}Pu and ^{239}Pu+^{240}Pu is about 300 keV, the width of each region in the alpha spectrum was taken as 300 keV. The two consecutive regions were separated by a width of 30 keV, which corresponds to 10% of the width of each region. Table 4.4 shows the ^{238}Pu/(^{239}Pu+^{240}Pu) alpha activity ratios calculated from the intensities of the characteristic alpha energy peaks of the Pu isotopes, along with respective relative standard deviations, obtained from the membrane and planchetted sources. It can be seen from Table 4.4, though the uncorrected ^{238}Pu/(^{239}Pu+^{240}Pu) alpha activity ratio, obtained from the membrane differs significantly from that obtained from the planchetted sources, the two ratios were found to agree within 1–2% after correction for a tail contribution by the GP method.

4.3.3. Analytical applications of membrane based alpha spectrometry

4.3.3.1. Absolute efficiency calibration

In the present work, membrane based alpha spectrometry (Mem–AS) was employed for the determination of ppb to sub-ppb level of Pu in complex aqueous matrices using absolute efficiency. Pu(IV) was preconcentrated from the complex aqueous matrices like seawater, groundwater, soil leach liquor and synthetic urine samples using HEMP-AMPS grafted PES membrane and the amount of Pu(IV) sorbed on the membrane was determined by applying absolute efficiency correction for a given size of the membrane and a fixed counting geometry. The absolute efficiency of an alpha spectrometry system is defined by the following equation:

$$\text{Absolute efficiency} = \frac{\text{Alpha count rate (cpm)}}{\text{Alpha disintegrations rate (dpm)}} \text{X100} \qquad (4.2)$$

To determine the absolute efficiency for the bi-functional PES membrane samples, the membrane samples were equilibrated with a series of 5 mL 3M HNO_3 solutions spiked with 0.025 – 0.45 µg of Pu(IV). After equilibration, the membrane samples were washed, dried and the alpha count rate in each membrane was measured in a fixed counting geometry. Since the size of the membrane sample is not a point source, a large surface area (450 mm^2) PIPS detector was used to obtain better counting efficiency and minimum counting time. The alpha disintegration rate in each membrane sample was calculated form the amount of Pu(IV) sorbed in that membrane, obtained from the difference in alpha activity of the equilibrating solution before and after equilibration. The absolute efficiency, for a given size of the bi-functional PES membrane and a given counting geometry, was determined from the alpha count rate and the alpha disintegration rate using equation 4.2. Due to the nearly constant Pu(IV) sorption efficiency and highly reproducible geometry of the bi-functional PES membrane samples, the variation of the alpha counts in the membrane sample with the amount of Pu present in the membrane was found to be linear. The absolute counting efficiencies for the 2×1 cm^2 membrane, 1×1 cm^2 membrane, and planchetted point alpha source were found to be 14.8%, 27.9%, and 29.7%, respectively. The absolute alpha counting efficiency of the 1×1cm^2 bi-functional PES membrane was comparable with that of the planchetted alpha source and could be used for the quantification of Pu(IV) sorbed in the membrane, without affecting the count rate significantly.

To determine Pu concentration in the large volume aqueous samples by Mem–AS, it was necessary to study the effect of the volume of the equilibrating solution on the sorption efficiency of the bi-functional PES membrane. A series of aqueous solutions, with volumes in the range of 5−100 mL were spiked with the same amount of Pu tracer and then equilibrated with a 2×1 cm^2 piece of the bi-functional PES membrane. It was observed that the efficiency of preconcentration was nearly constant when the volume of the equilibrating solution was varied from 5 to 100 mL. However under continuous stirring conditions, 5−30 mL samples required 1h to achieve equilibrium sorption of Pu(IV), whereas for 100 mL sample 24 hours was required for the same. Therefore, for the quantitative determination of sub-ppb to ppb amount of Pu in the synthetic urine, groundwater, seawater, and soil leach liquor samples by Mem–AS, upto 30 mL samples were equilibrated for 1 h and 100 mL samples were equilibrated for 24 h . The alpha spectrum for each sample was recorded for sufficient time to accumulate enough counts above the background. From Table 4.5, it can be concluded that HEMP-AMPS grafted PES membrane based alpha spectrometry offers good precision and accuracy for quantifying trace amounts of Pu(IV) in the complex environmental samples. The HNO_3 concentration in all the samples was 3 M, except for the soil leach liquor where HNO_3 concentration was 8 M. The Pu concentrations in the samples were corrected for the sorption efficiency, 85 ± 2% in 3M HNO_3 and 70 ± 2% in 8M HNO_3.

Table 4.5. Determination of Pu concentration in aqueous samples by HEMP-AMPS grafted PES membrane based alpha spectrometry using absolute counting efficiency.

Sample	Sample volume (mL)	Pu spiked		Pu measured	
		Bq mL^{-1}	ppb	Bq mL^{-1}	ppb
Synthetic urine	5	20	4.11	20.2 ± 1.0	4.16 ± 0.21
Seawater	5	15	3.08	14.9 ± 0.9	3.06 ± 0.18
	100	0.06	0.012	0.054 ± 0.004	0.011 ± 0.001
Groundwater	30	0.32	0.067	0.31 ± 0.02	0.065 ± 0.004
Soil sample	100	0.11	0.022	0.092 ± 0.009	0.019 ± 0.002

4.3.3.2. Membrane based isotope dilution alpha spectrometry

Membrane based alpha spectrometry, employing absolute efficiency, cannot be applied for the samples where chemical recovery Pu(IV) is not constant or Pu concentration is higher than Pu(IV) loading capacity of the bi-functional PES membrane. Also, any variation in the dimensions of the membrane or the counting efficiency, inefficient conversion of the Pu oxidation state to Pu(IV) or unknown chemical composition of the sample may introduce unforeseen errors in the determination of Pu concentration. To overcome such problems, the membrane based isotope dilution alpha spectrometry (Mem–IDAS) can be easily adopted, as an alternative to absolute efficiency calibration, for the quantification of Pu. In isotope dilution technique, Pu concentration in a given sample is determined from the change in ^{238}Pu/(^{239}Pu + ^{240}Pu) alpha activity ratio of the sample with respect to the same in a mixture of the sample and the spike solution [142, 143]. If a known weight W_{sp} of the pre-calibrated spike solution, having Pu concentration C_{sp}, is added to a known weight W_{sa} of the sample, then Pu concentration C_{sa} in the sample can be correlated with a change in ^{238}Pu/ (^{239}Pu+^{240}Pu) alpha activity ratio in the spiked mixture (R_m) with respect to that in the sample (R_{sa}) and spike (R_{sp}) using following equation:

$$C_{sa} = \frac{C_{sp} W_{sp}}{W_{sa}} \frac{(R_{sp} - R_m)}{R_{sp}(R_m - R_{sa})} \frac{(\lambda_{238} \mathrm{A.F.}_{238})_{sp}}{(\lambda_{239} \mathrm{A.F.}_{239})_{sa} + (\lambda_{240} \mathrm{A.F.}_{240})_{sa}} \frac{<\mathrm{At.Wt.}>_{sa}}{<\mathrm{At.Wt.}>_{sp}} \qquad (4.3)$$

where λ_i represents the decay constant of the isotope “i” [144], <A.F.> and <At. Wt.> represent the atom fraction and the average atomic weight of Pu, respectively.

Mem–IDAS method is independent of the sample composition, chemical recovery of Pu(IV) from the sample matrix or the loading capacity of the membrane. However, the choice of an appropriate spike is very crucial for isotope dilution technique. ^{240}Pu cannot be used as a spike for IDAS experiments since the alpha energy peak of ^{240}Pu at 5.168 MeV cannot be resolved from that of ^{239}Pu at 5.155 MeV, using commercially available alpha detectors. But the alpha energy peak of ^{238}Pu at 5.499 MeV is well separated from that of ^{239}Pu and ^{240}Pu isotopes, indicating the possibility of using ^{238}Pu as a spike for the quantification of Pu in an unknown sample. IDAS using ^{238}Pu as a spike and reverse-IDAS using ^{239}Pu as a spike were reported for the determination of Pu concentration [143, 145]. It is also necessary to have prior knowledge of the isotopic composition of Pu in the sample. If isotopic composition is not known, Pu in the sample can be loaded in a membrane, without spike, and subjected to alpha spectrometry to determine the Pu isotope ratios. In the present work, Pu concentrations in irradiated UO_2 fuel dissolver solution and in three (U, Pu)C samples were determined by Mem–IDAS, using a ^{238}Pu enriched spike.

The isotopic composition of Pu, obtained by TIMS, in the dissolver solution and the three different (U, Pu)C samples used in the present work as well as the ^{238}Pu enriched spike are given in Table 4.6. All the three samples were having Pu isotopic compositions similar to the PHWR grade Pu having ^{239}Pu (68– 69 atom %), and ^{238}Pu in the range 0.13–0.17 atom %. Hence, a ^{238}Pu-enriched spike used for isotope dilution alpha spectrometry was justified. The average atomic weight and atom fraction of various isotopes in each sample as well as in the spike were deduced from the isotopic composition data given in Table 4.6.

Table 4.6. Isotopic compositions of dissolver solution, (U, Pu)C samples and ^{238}Pu–enriched spike used for Mem–IDAS method.

Isotope	Atom Fraction of Pu				
	Spike	Dissolver solution	(U,Pu)C samples		
			Sample 1	Sample 2	Sample 3
^{238}Pu	0.9388	0.0294	0.0013	0.0015	0.0017
^{239}Pu	0.0584	0.9263	0.6989	0.6853	0.6870
^{240}Pu	0.0025	0.0672	0.2521	0.2667	0.2694
^{241}Pu	0.0002	0.0059	0.0316	0.0272	0.0216
^{242}Pu	---	0.0004	0.0162	0.0192	0.0203

The alpha activity ratio in the ^{238}Pu spike was also calculated from the isotopic composition given in Table 4.6, since it could not be measured directly from the alpha spectrum with a reasonable accuracy due to very high count rate at 5.5 MeV alpha peak, which results in very large tail contribution to 5.1 MeV alpha peak that had very low count rate because of low abundances of ^{239}Pu and ^{240}Pu in the spike. The Pu concentrations in the four aliquots of dissolver solution were determined independently by the Mem-IDAS method and the results were compared with the conventional IDAS and ID-TIMS methods. As can be seen from Table

4.7, the results obtained by the Mem-IDAS method were in good agreement with those obtained by other two methods. The relative standard deviation (RSD) was within 1% indicating a reasonably good precision of Mem-IDAS method.

Table 4.7. Concentration of Pu in dissolver solution determined by Mem-IDAS method using ^{238}Pu/(^{239}Pu+^{240}Pu) alpha activity ratio.

Sample Id.	Pu Concentration (µg/g)						
	Mem–IDAS[a]	Avg.	RSD (%)	IDAS[a]	Avg.	RSD (%)	ID-TIMS
Aliquot–I	12.88	13.01	0.85	13.09	13.07	0.78	13.05±0.04
Aliquot–II	12.96			12.93			
Aliquot–III	13.11			13.18			
Aliquot–IV	13.09			13.09			

[a]Result of analysis of duplicate aliquots

Table 4.8. Concentration of Pu in (U,Pu)C samples determined by Mem-IDAS using ^{238}Pu/(^{239}Pu+^{240}Pu) alpha activity ratio and biamperometry method.

Sample No.	Pu Concentration in (U, Pu)C (mg/g)						
	Mem–IDAS[a]	Avg.	RSD (%)	IDAS[a]	Avg.	RSD (%)	Biamperometry
1	4.09	4.11	0.56	4.13	4.12	0.26	4.16 ± 0.02
	4.12			4.12			
2	2.75	2.77	0.82	2.72	2.701	0.76	2.74 ± 0.01
	2.78			2.69			
3	3.61	3.64	0.88	3.69	3.71	0.68	3.68 ± 0.02
	3.66			3.73			

[a]Result of analysis of duplicate aliquots

Pu concentrations in three different (U, Pu)C samples, determined by the Mem-IDAS method as well as conventional IDAS method and biamperometry method, are given in Table 4.8. The Pu concentrations in the (U, Pu)C samples obtained by Mem-IDAS were found to be in good agreement with those obtained by other conventional methods. Therefore, from the present study it can be concluded that, Mem-IDAS based method could be used for the quantification of Pu in the different complex aqueous samples with good accuracy and precision.

4.4. Conclusions

In the present work, membrane based alpha spectrometry was developed for the determination of Pu concentration in the aqueous samples having 3 M HNO_3 concentration. A 1–1.5 μm thin, bi-functional HEMP-AMPS layer was anchored on PES membrane by UV–induced surface grafting. The bi-functional membrane was found to be effective for the selective preconcentration of Pu(IV) in the presence of a large excess of U(VI). The advantage of membrane based alpha spectrometry is that source preparation is not required as good quality alpha spectrum can be obtained from the Pu loaded membrane. The method involves minimum sample manipulation that is essential for handling high dose samples, encountered in nuclear plant process streams. Also, secondary waste generated could be minimized since the HEMP-AMPS grafted membranes can be regenerated and reused. Membrane based alpha spectrometry was tested for the quantification of ultratrace concentrations of Pu in a variety of matrices, including seawater, groundwater, soil leach liquor and synthetic urine, using absolute efficiency calibration. For the quantification of Pu in irradiated fuel dissolver solution, isotope dilution membrane based alpha spectrometry (Mem-IDAS) was employed to improve the accuracy and precision of the results. Since isotope dilution technique is independent of any incomplete chemical recovery, the Mem-IDAS can also be applied for samples having high Pu concentrations and high salt concentration. However, with the existing alpha detectors, it is not possible to determine the isotopic composition of Pu. Also, mass spectrometric techniques can provide more precise results for the determination of Pu isotopic composition and concentration as compared to alpha spectrometry. Therefore, the possibility of direct mass spectrometric analysis of Pu sorbed on the bifunctional polymer matrix was also explored in the present work.

Chapter 5

Magnetically retrievable bi-functional bead for thermal ionization mass spectrometry of Pu

5.1. Introduction

The relative contents of Pu isotopes are used as a finger print to identify the source of origin since the abundances of different isotopes of plutonium are highly dependent on the type of nuclear reactor, nuclear fuel burn-up etc. Precise isotope ratio measurements of plutonium in the environment or in body fluids can help to distinguish different sources of nuclear contamination such as global fallout from nuclear weapons testing, nuclear power plants or nuclear accidents. Therefore, the knowledge of Pu isotopic composition as well as concentration is important for the nuclear energy utilization, nuclear safeguards, nuclear forensics and environmental monitoring. Mass spectrometric methods, especially thermal ionization mass spectrometry (TIMS) coupled with isotope dilution, is the most suited technique for precise and accurate determination of Pu isotope ratio and concentration [146-148]. Recently, Lee et al. have reported a continuous heating TIMS method for the determination of ultra-trace concentration of Pu without chemical separation [149]. However, the bottleneck in Pu analyses by TIMS is the elaborate sample preparation procedure that involves dissolution/leaching of the sample to bring Pu into solution, matrix elimination and selective preconcentration of Pu, followed by manual deposition of a very small volume of about 10 μL of the preconcentrated Pu solution onto a filament. In general, several methods such as co-precipitation, solvent extraction, cloud point extraction, anion-exchange chromatography or extraction chromatography are employed for the sample preparation for TIMS [125,126,130]. For the separation and purification of Pu in the aqueous samples, anion-exchange and extraction chromatography are the most widely used methods [146]. In anion-exchange chromatography, the hexanitrato anionic complexes of Pu(IV), that exist in solution having a high concentration of HNO_3, are separated from most of the cationic impurities as well as from anionic uranium complexes using an anion-exchange column like Dowex 1X8 resin [86].On the other hand in extraction chromatography, Pu is separated based on its complexation with ligand impregnated or grafted resins like TEVA, TRU, DGA, DIPEX and DIPHONIX [129,133,146,150]. Automated TIMS techniques coupled with on-line ion-exchange and/or extraction chromatography employing flow injection or sequential injection have also been reported for reduced manual handling and analysis time [11,49,151,152].

To avoid the conventional tedious and time consuming sample preparation methods, resin bead based TIMS method was developed in Oak Ridge National Laboratory for the isotopic analysis of U and Pu in the safeguarded nuclear materials [153-156]. The Pu(IV) ions were loaded in a single anion-exchange bead either directly from the sample or after purification of the sample using anion-exchange or extraction chromatography. Then Pu-loaded-bead was then fixed on a Re filament and pyrolyzed in TIMS. The resin bead in one hand acts as the matrix for chemical separation and helps in secure transport of the analyte reducing the possibility of contamination of instrument or sample, and at the same time serves as a point source for thermal ionization. Sequential mass spectrometric analysis of uranium and plutonium has been carried out in our laboratory employing a single Dowex 1X8 resin bead loaded with about 10 ng of plutonium [153]. To enhance the Pu(IV) sorption kinetics in a single bead for TIMS, the acoustic streaming has been used for the small volume sample. However, it is difficult to collect the commercially available resin beads, generally micron sized particles, from large volume sample solutions and subsequently load them on the thin Re filament for TIMS.

The present work involves the synthesis of superparamagnetic Fe_3O_4 nanoparticles (NPs) embedded bi-functional poly(ethersulfone) (PES) beads for the single bead based TIMS (SB–TIMS) analysis of Pu in acidic aqueous samples. The PES polymer was used as a base matrix due to its amenability for UV grafting and easy formation of the porous beads by the phase inversion method [157,158]. The PES beads were grafted with functional monomers HEMP and APTAC, containing neutral phosphate and quaternary ammonium groups respectively, by UV–induced grafting. As described in section 3.3.2, the choice of phosphate groups was based on the fact it has high affinity towards Pu(IV) ions and quaternary ammonium groups would facilitate the sorption of anionic Pu(IV) complex that exist at higher HNO_3 concentration. The bi-functional PES beads can be easily retrieved from a large volume sample using an external magnet due to the presence of superparamagnetic Fe_3O_4 NPs immobilized within the beads. This concept is similar to magnetically assisted chemical separation [159-163]. For single bead TIMS analyses of Pu, the isotope dilution method was used for the quantification to make the results independent of chemical recovery and also unknown variations in the experimental parameters [136,138,164].

5.2. Experimental

The Fe_3O_4 nanoparticles (NPs) were coated with tetraethoxysilane (TEOS) dissolved in ethanol with constant shaking at room temperature for 12 hours. The magnetic PES beads were synthesized by solvent induced phase inversion method. Typically, PES granules were dissolved in appropriate volume of DMF to get a saturated solution and TEOS coated Fe_3O_4 NPs (Fe_3O_4@SiO_2) were dispersed homogeneously in this solution using sonication for 30 min. The Fe_3O_4@SiO_2 dispersed PES solution was added drop-wise to water with continuous stirring to produce nearly spherical magnetic PES beads having diameter ranging from 0.5-1 mm. Figure 5.1 shows the experimental setup for synthesis of PES beads. The Fe_3O_4@SiO_2 loaded PES beads were then equilibrated with a solution containing an equimolar mixture of two monomers HEMP and APTAC in 1:1 (v/v) water: ethanol. After equilibration the magnetic PES beads, filled with the polymerizing solution, were irradiated for 15 min in a UV reactor (λ_{max} = 365 nm) for grafting of the HEMP and APTAC monomers. The poly(HEMP-co-APTAC) grafted magnetic PES beads obtained after irradiation were washed with ethanol to remove un-reacted monomers, dried and stored in ethanol. The HEMP/APTAC grafted magnetic PES beads were synthesized in a similar manner, equilibrating the magnetic PES beads with HEMP or APTAC dissolved in ethanol, followed by UV irradiation. The various steps involved in the formation of the bi-functional magnetic PES bead is given in Scheme 5.1.

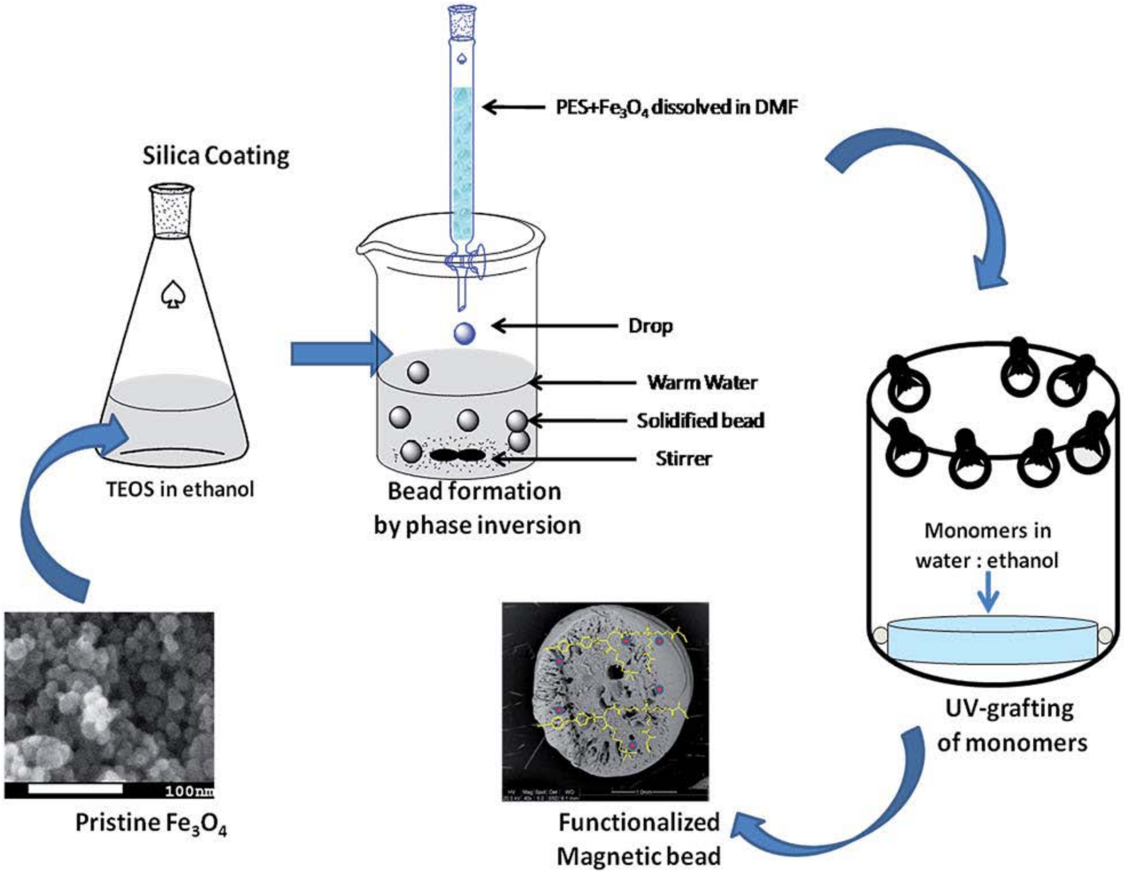

Scheme 5.1. Schematic of the synthesis of bi-functional magnetic PES beads by phase inversion and UV-grafting method.

The sorption and desorption studies of Pu(IV), Am(III) and U(VI) ions from the functionalized super-paramagnetic PES beads were carried out using same procedure as described in section 2.5.3. Pu(IV) sorption kinetics for the poly(HEMP-co-APTAC) grafted magnetic PES beads and the poly(HEMP-co-APTAC) gel were compared. To study Pu(IV) sorption kinetics, about 200 mg of PES beads/ poly(HEMP-co-APTAC) gel was equilibrated with 100 mL of 3 M HNO_3 solution spiked with appropriate amount of Pu radiotracer with continuous stirring. The alpha activity in 25µL aliquot of the equilibrating was measured as a function of equilibration time.

For Pu isotopic composition (IC) analysis in the samples by single bead thermal ionization mass spectrometry (SB-TIMS), 5 mL of well–stirred 3 M HNO_3 solution, spiked with ~1 µg of Pu, was equilibrated with a single bi-functional magnetic PES bead for 1 h. After equilibration, the bead was collected from the solution using a magnet, washed with 3 M HNO_3, dried and directly loaded onto a high purity rhenium filament for the TIMS analysis. All mass spectrometric analyses were carried out under static mode of multi-collection of thermal ionization mass spectrometer using double filament assembly for sample loading. Prior to Pu analysis, the temperature of the ionization filament (IF) was optimized to obtain ~200 mV equivalent of $^{187}Re^+$ ion current. Thereafter, the vaporization filament (VF) was heated from 0 to 2A in 900 seconds and degassing was carried out at 2A for 1800 seconds. After degassing, VF temperature was increased to obtain optimum Pu^+ ion current. To compare the results of Pu isotopic analysis by SB-TIMS method with the conventional solution based TIMS method, the standard solution was treated with 30% H_2O_2, purified from ^{241}Am, daughter product of ^{241}Pu, using DOWX 1X8 resin and the purified Pu(IV) was eluted using 0.3 M HNO_3. The purified Pu fraction was evaporated and then 10 µL of the concentrated solution was loaded on the Re filament for TIMS analysis. The various steps involved in Pu analysis by the SB-TIMS method are depicted in Scheme 5.2.

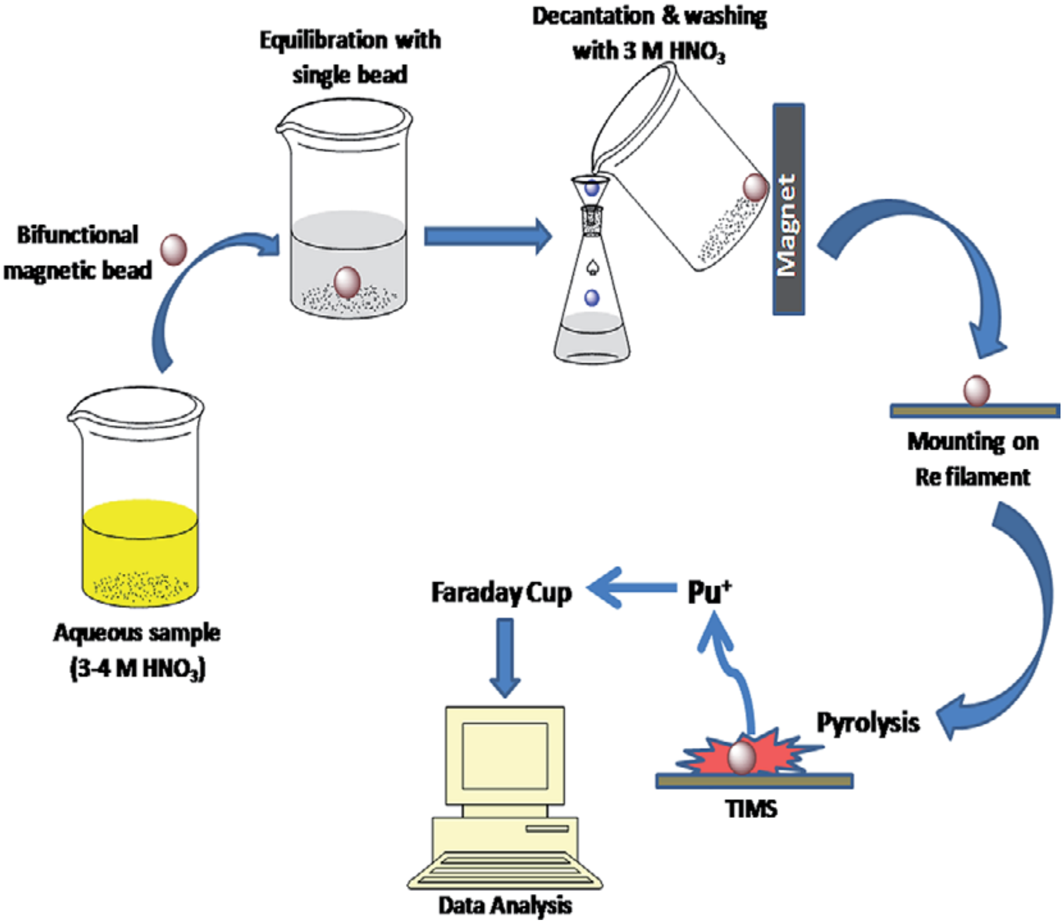

Scheme 5.2. Schematic of the synthesis of bi-functional magnetic PES beads by phase inversion and UV-grafting method.

For the determination of Pu concentration in dissolver solution of irradiated UO_2 fuel and in soil leach liquor samples, spiked with known amount of $Pu(NO_3)_4$, single bead isotope dilution thermal ionization mass spectrometry (SB–ID–TIMS) technique was employed. For determination of Pu concentration in dissolver solution (U:Pu mole ratio ~1000:1), a single bi-functional magnetic PES bead was equilibrated with 3 mL of dissolver solution and its spiked mixture, separately, for 1 h with continuous stirring for selective preconcentration of Pu(IV) ions. After equilibration, the single bead was washed and loaded onto Re filament for IC analysis of Pu in the dissolver solution and its spiked mixture. A known Pu activity and its spiked mixture was added to 50 mL of aqueous sample separately and equilibrated with a single bi-functional magnetic PES bead for 24 h with continuous stirring for Pu(IV) ions preconcentration. Similarly, a known Pu activity and its spiked mixture was soaked in about 2 g of soil sample and was evaporated to near dryness.; Pu was then leached from soil by 50 mL of 8 M HNO_3 containing 2-3 mL of 30% H_2O_2 with heating under IR lamp. Then, 50 mL of leach liquor was equilibrated with a single bi-functional magnetic PES bead for 24 h with a continuous stirring. After preconcentration of Pu(IV) ions, the bead was collected using a magnet, washed, dried and loaded onto Re filament for Pu isotopic composition analysis by TIMS. The Pu concentrations in various samples were calculated from the change in isotope ratios in the spiked mixture with respect to those in the sample and the spike.

5.3. Results and discussion

5.3.1. Synthesis & characterization of magnetic bi-functional beads

The PES beads were synthesized by solvent–induced phase inversion technique. Since PES is insoluble in water, the PES polymer at the water–DMF interface immediately solidified when PES dissolved in DMF was added drop-wise to water, and a nearly spherical PES bead with very dense outer surface was formed. The DMF solvent, trapped inside the PES droplet, then migrated slowly out creating a highly porous structure inside the PES bead. The size of the PES bead was primarily controlled by the size of the droplet of the PES in DMF solution that was added to water. In the present work, PES beads having 0.5–1 mm diameter were synthesized. The $Fe_3O_4@SiO_2$ dispersed in the PES solution remained physically trapped within the porous PES bead. The presence of superparamagnetic Fe_3O_4 nanoparticles makes the PES beads magnetically retrievable from the large volume aqueous samples and the SiO_2 coating on the Fe_3O_4 nanoparticles prevents any degradation when subjected to harsh chemical conditions. The grafting of the functional monomers, HEMP and APTAC, was based on the formation of free radical in the PES polymer chains when subjected to UV radiation as described in Chapter 2.2.

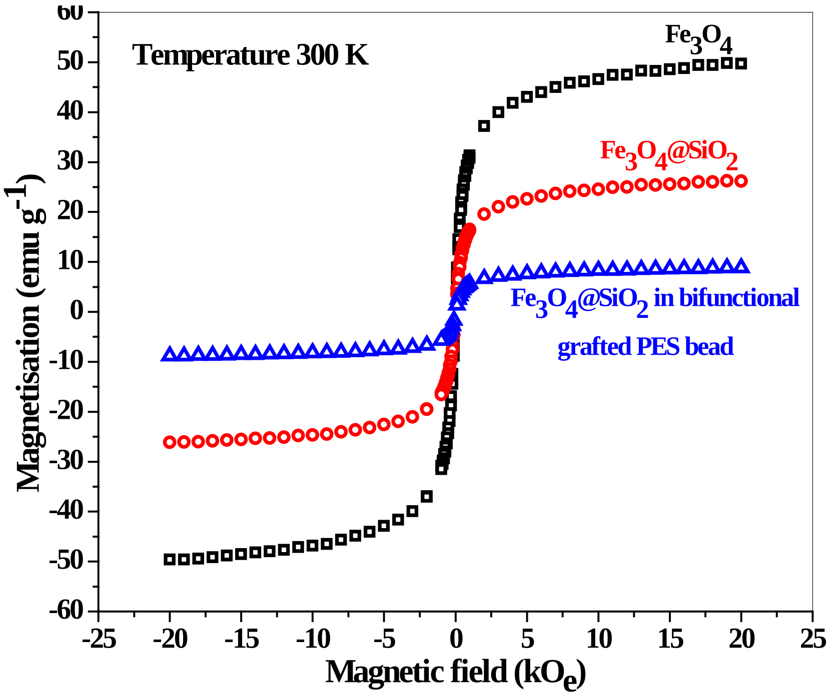

Figure 5.1. Changes in super-paramagnetic properties and saturation magnetization at different steps during the synthesis of bifunctional magnetic PES beads.

The changes in the magnetic properties of Fe_3O_4 nanoparticles, after coating with silica and immobilizing in the bi-functional beads, were studied by VSM. Figure 5.1 gives a comparison of the magnetization curves of bare Fe_3O_4 nanoparticles, $Fe_3O_4@SiO_2$ and the bi-functional magnetic beads. It can be seen from Figure 5.1 that Fe_3O_4 NPs retained their superparamagnetic properties when embedded in the poly(HEMP-co-APTAC) grafted PES beads, except that the saturation magnetization decreased in the beads due to shielding. The saturation magnetization of Fe_3O_4 particles decreased from 50 emu g^{-1} to 26 emu g^{-1} after silica coating and to 9 emu g^{-1} after embedding them in the bi-functional PES beads. However, the saturation magnetization of beads was found to be sufficient enough for withdrawing a single bead from aqueous samples using an external magnet.

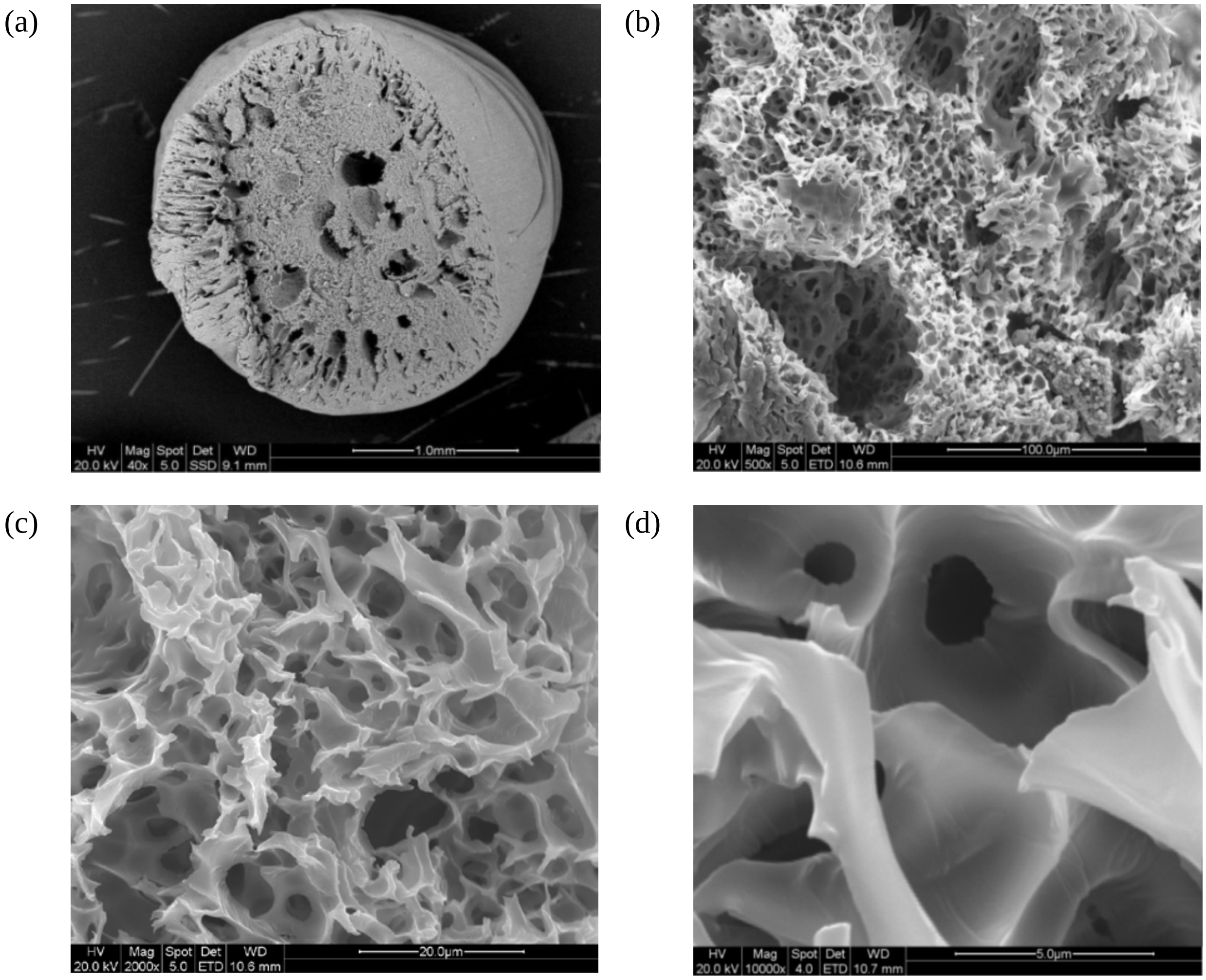

Figure 5.2. SEM images of HEMP-co-APTAC grafted magnetic PES bead at different magnifications.

Both the monomers HEMP and APTAC, grafted in the magnetic PES beads, are acrylate based and have comparable efficiencies for the graft–polymerization as described in Chapter 3.3.1. However, the poly(HEMP-co-APTAC) layer is expected to be primarily confined near the surface of the PES bead since 365 nm UV light would not be able to penetrate deep inside the PES matrix. The presence of three double bonds in the HEMP monomer may lead to the formation of a dense and cross-linked poly(HEMP-co-APTAC) layer on the surface layer of PES beads. The physical and elemental characterization of the bi-functional magnetic PES bead was carried out by SEM in combination with energy dispersive spectrometry. It can be seen from the SEM images given in Figure 5.2 that the PES beads prepared in the present work had a dense outer surface and highly porous interior. The highly porous structure of the PES bead was crucial for providing better accessibility of the binding sites during the sorption of actinides from aqueous solutions. The physical structure of the beads did not change during grafting of the HEMP or APTAC monomers.

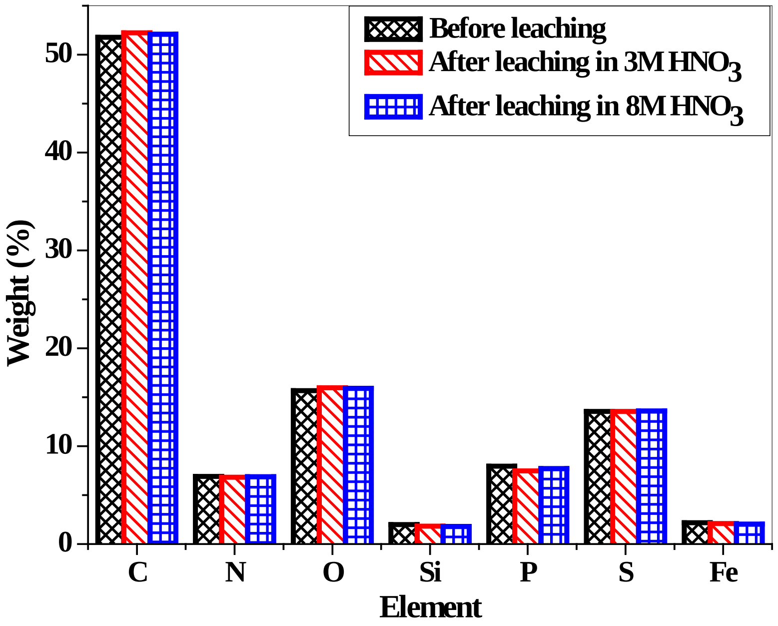

Figure 5.3. Comparison of elemental profiles of poly(HEMP-co-APTAC) grafted magnetic PES beads before and after subjecting to the equilibrations with 3 and 8 M HNO_3.

The phosphorus mappings at different locations of the cross section of a bi-functional magnetic PES bead showed that grafting of the HEMP and APTAC monomers was uniform across the diameter of the interior matrix. In Figure 5.3, the presence of elements such as S from base PES matrix, Fe and Si from $Fe_3O_4@SiO_2$, phosphorus and nitrogen from grafted poly(HEMP-co-APTAC) confirmed the expected elemental composition of the bi-functional beads. Also, the nitrogen content due to the two N atoms in APTAC and phosphorous content due to one P atom in HEMP) are comparable in Figure 5.3, which indicated that the HEMP and APTAC monomers had polymerized with a similar efficiency.

The bi-functional magnetic beads, developed in the present work, were intended to be used for the preconcentration of actinides from acidic solutions. However, the beads may tend to lose their magnetic properties in solutions containing high concentration of HNO_3, since the superparamagnetic Fe_3O_4 nanoparticles incorporated within the bead may leach out when in contact with HNO_3. Therefore it was important to study the effect of HNO_3 on the chemical composition and magnetic properties of the beads. So the bi-functional magnetic PES beads were subjected to the elemental analyses after equilibration with 3 and 8 M HNO_3 for 24 h. It can be seen from Figure 5.3 that the elemental composition of the beads, especially the atom% of Fe and Si, did not change during equilibration with 3 and 8 M HNO_3. This could be attributed to the fact that the silica coating on the superparamagnetic Fe_3O_4 nanoparticles prevented the leaching of Fe^{3+}/Fe^{2+} ions from Fe_3O_4 nanoperticles when subjected to high acid concentration. Thus, all components of the bi-functional magnetic PES beads, including silica coated Fe_3O_4 nanoparticles, are highly stable against leaching in the high concentration of HNO_3.

5.3.2. Pu sorption by magnetic bi-functional beads

The actinide sorption properties of the poly(HEMP-co-APTAC) grafted magnetic PES beads in HNO_3 medium, were similar to that of HEMP-co-APTAC polymer as described in Chapter 3.3.2. The recovery efficiency of the magnetic bi-functional beads in 3-8 M HNO_3 for Pu(IV) was found to be 85–90%, which could be attributed to the existence of anionic $[Pu(NO_3)_5]^-$ and $[Pu(NO_3)_6]^-$ complexes. Am(III) recovery by the bi-functional beads was negligible in high HNO_3 concentrations. But for U(VI) recovery efficiency was about 95% in 3 M HNO_3, which reduced to about 85% in 8 M HNO_3. As described in Chapter 3.3.2, the HEMP-co-APTAC polymer is selective for Pu(IV) in presence of up to 1000 times higher concentration of U(VI).

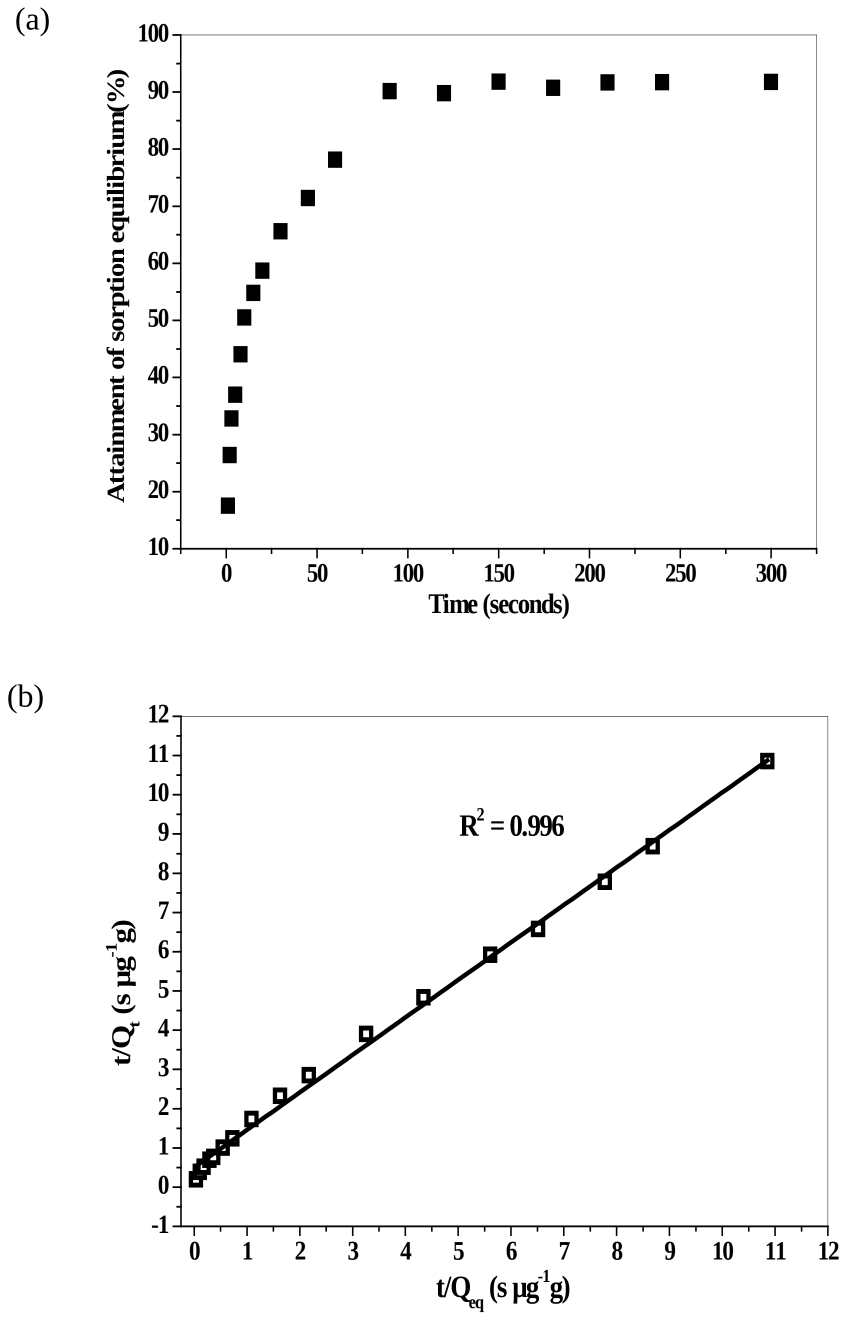

Figure 5.4. (a) Attainment of sorption equilibrium of Pu(IV) and (b) pseudo-second order rate of sorption of Pu(IV) by poly(HEMP-co-APTAC) grafted magnetic PES bead in 3 M HNO_3.

However for analytical purposes, it was important to study the kinetics of Pu(IV) sorption by the bi-functional magnetic PES beads in order to ensure complete recovery of Pu from the sample during equilibration. Figure 5.4 shows the rate of Pu(IV) sorption by the beads from 3 M HNO_3 as a function of equilibration time. It can be seen from Figure 5.4(a), that Pu(IV) sorption equilibrium was attained within 90 minutes. The sorption rate was found to follow a pseudo-second order equation, given in Chapter 3.3.3, and the initial rate sorption of Pu(IV) was fast and the rate eventually reduces during the transfer of Pu(IV) ions from surface to interior matrix. The sorption capacity of the bi-functional magnetic PES beads, determined from slope of the plot of t/Q_t vs. t/Q_{eq} in Figure 5.4(b) was found to be 93 µg of Pu g^{-1} which was in good agreement with the experimentally measured Pu loading capacity 92 µg of Pu g^{-1}.

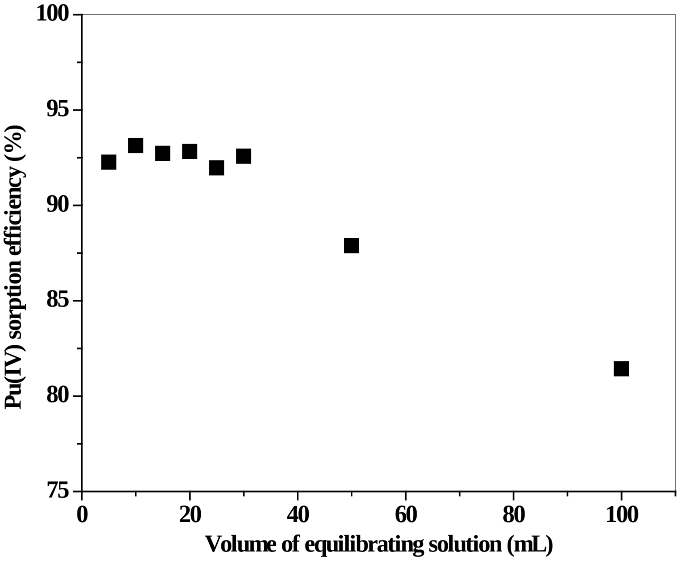

Figure 5.5. Effect of volume on extraction efficiency of Pu(IV) by HEMP-co-APTAC grafted magnetic PES bead in 3 M HNO_3 medium.

The effect of the volume of equilibrating solution on the Pu(IV) sorption efficiency of the bi-functional magnetic PES beads was also studied. It can be seen from this Figure 5.5 that the Pu(IV) sorption efficiency was nearly constant (92±2%) for equilibration volume up to 30 mL. For sample volume higher than 30 mL, the sorption efficiency reduced 80±2%, which could be attributed to the slower diffusion of Pu(IV) ions in large volume equilibrating solution. Therefore, the preconcentration of Pu(IV) ions from a large volume sample, higher than 30 mL, would require a longer equilibration time or better equilibration method like flow cell etc.

5.3.3. Single bead thermal ionization mass spectrometry (SB–TIMS)

For single bead thermal ionization mass spectrometry (SB-TIMS), the bi-functional magnetic bead loaded with Pu(IV) was fixed on a Re filament and subjected to high temperature for pyrolysis of the bead, thermal desorption of Pu and subsequent ionization. The extent of ionization of Pu is governed by Saha-Langmuir equation [26]. Due to the high ionization potential of Pu (6.06 eV), it was not possible to produce Pu^+ ions from a single filament. Therefore, in the present work, all analyses were carried out using high purity rhenium double filament assembly, where the bead was loaded on the vaporization filament (VF) and the Pu atoms evaporated from the bead were ionized at the ionization filament (IF). To achieve the optimum evaporation and ionization during TIMS analysis, the analyte should be in its chemically purest state. The rate of evaporation of Pu atoms, which is proportional to the Pu^+ ion current, from the bead loaded on the VF is important for the optimum analytical signal in TIMS. Therefore, the variations in Pu^+ ion current as a function of VF temperature were studied in single bead based TIMS and compared with conventional solution based TIMS. Since ^{239}Pu is the most abundant isotope in the samples analyzed in the present work, $^{239}Pu^+$ ion current was monitored with increasing VF temperature. Figure 5.6 shows the ^{239}Pu evaporation profiles obtained from solution and single bead based loading techniques. With increasing VF heating current, $^{239}Pu^+$ ion current was found to increase according to Saha-Langmuir equation. However, due to the reducing atmosphere provided by the PES polymer present on the filament surface, no PuO$^+$ ion current was observed during analysis. The optimum VF heating current for the Pu isotopic analysis by SB-TIMS was found to be about 4 Amp, at which about 1V ^{239}Pu$^+$ ion current was obtained. Though the ionization efficiency of SB-TIMS method was less than the conventional solution based loading method, the ion collection efficiency was comparable for both the techniques.

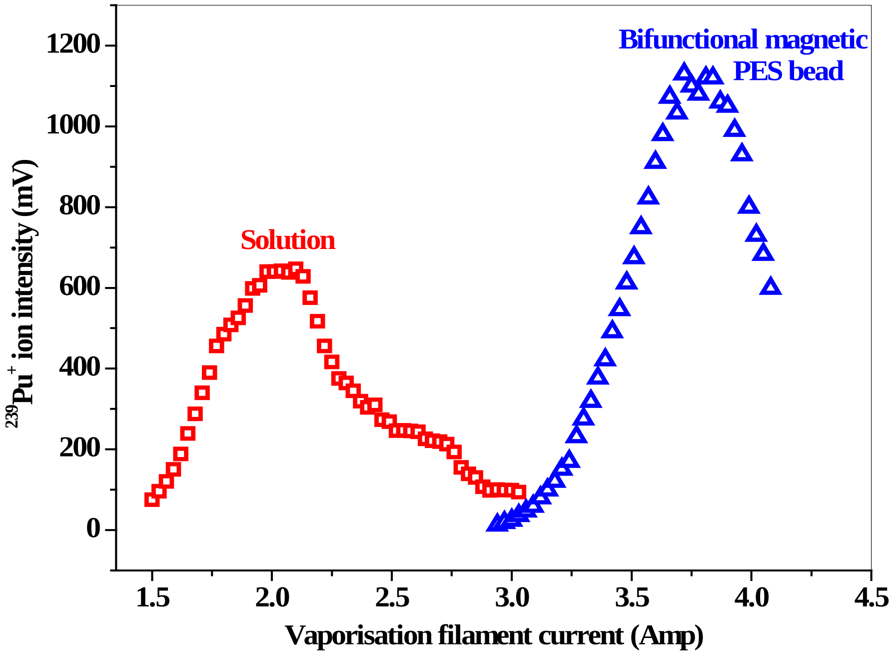

Figure 5.6. Variations of ^{239}Pu$^+$ ion current from solution and bi-functional magnetic PES bead based Pu loadings as a function of vaporization filament temperature.

The magnetic PES bead on the VF did not decompose completely. Therefore, prior to TIMS analysis, it was important to carry out degassing of the bead loaded on the VF to remove volatile impurities and obtain stable Pu$^+$ ion current. The effect of degassing on the precision of Pu isotopic ratio obtained from single magnetic PES bead loaded on the VF was studied. Figure 5.8 gives a comparison of the standard deviations associated with Pu isotope ratios, obtained from SB-TIMS and conventional TIMS method employing solution loading. The standard deviation of ^{240}Pu/^{239}Pu ratio was less compared to that of ^{241}Pu/^{239}Pu and ^{242}Pu/^{239}Pu ratios, since ^{240}Pu and ^{239}Pu were the major isotopes and ^{241}Pu and ^{242}Pu were the minor isotopes in the sample. It can be seen from Figure 5.7, the standard deviation associated with any given isotope ratio was found to improve with increasing degassing time. Therefore, the degassing was carried out for1800 seconds prior to the analysis of each sample for obtaining stable current.

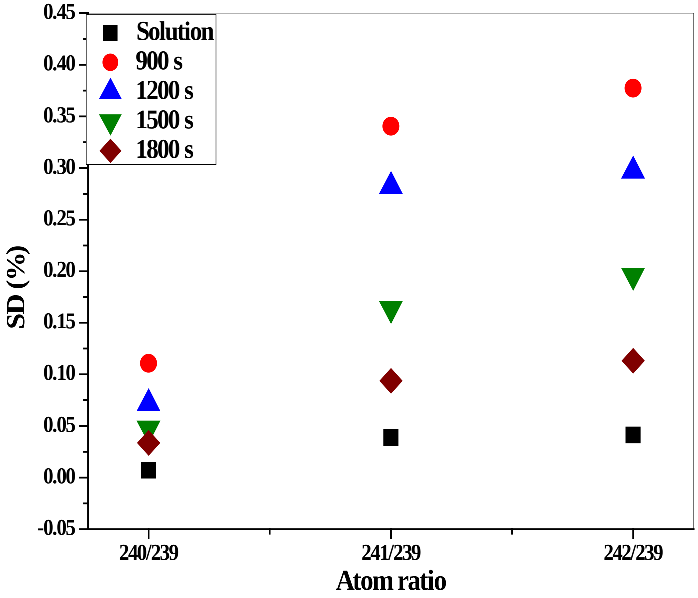

Figure 5.7. Effect of degassing time prior to TIMS analysis on the standard deviation of observed isotope ratios.

Table 5.1. Determination of Pu isotopic composition in SRM-947 Pu standard by TIMS using single bifunctional magnetic PES bead and solution based loadings.

Isotope	Atom% of Pu		
	Certified value	Bead loading	Solution loading
^{239}Pu	79.03 ± 0.02	78.96 ± 0.04	78.96 ± 0.03
^{240}Pu	19.02 ± 0.02	19.04 ± 0.012	18.99 ± 0.03
^{241}Pu	0.808 ± 0.006	0.735 ± 0.006	0.723 ± 0.006
^{242}Pu	1.238 ± 0.004	1.243 ± 0.008	1.225 ± 0.006

The analytical performance of SB-TIMS for Pu isotopic composition (IC) analysis was studied using NIST SRM–947 Pu isotopic standard. The comparison of Pu IC in NIST SRM–947 obtained by SB-TIMS and conventional TIMS employing solution based loading is given in Table 5.1. The atom% of the two major isotopes, viz. ^{239}Pu and ^{240}Pu, determined by the two methods were found to agree within 0.2% whereas atom% of ^{241}Pu and ^{242}Pu, which are less abundant isotopes, were found to agree within 0.5%.

5.3.4. Analytical applications of single bead thermal ionization mass spectrometry

The quantitative determination of trace concentrations of Pu(IV) in the aqueous solution, irradiated fuel dissolver solution and soil leach liquor samples was carried out by SB-ID-TIMS method. Determination of Pu concentration by isotope dilution (ID) involves addition of a known weight W_{sp} of a pre-calibrated spike solution, having Pu concentration C_{sp}, to a known weight W_{sa} of the sample solution. Pu concentration C_{sa} in the sample can be correlated with change in either ^{240}Pu/^{239}Pu or ^{242}Pu/^{239}Pu atom ratio in the spiked mixture (R_m) with respect to those in the sample (R_{sa}) and spike (R_{sp}) using the following equation:

$$\boldsymbol{C_{sa} = \frac{C_{sp}W_{sp}}{W_{sa}} \frac{(R_{sp}-R_m)}{R_{sp}(R_m-R_{sa})} \frac{AF_{sp}^{240/242}}{AF_{sa}^{239}} \frac{<At.Wt.>_{sa}}{<At.Wt.>_{sp}}} \qquad (5.1)$$

where, AF_{sp}^{i} and AF_{sa}^{i} are the atom fractions of ith isotope in the sample and spike, respectively, and $<At.Wt>_{sa}$ and $<At.Wt>_{sp}$ are the atomic weights of sample and spike, respectively. As described in Chapter 4.3.2.1, isotope dilution technique is suitable for the determination of Pu in matrices like nuclear fuel dissolver solution as it is independent of any matrix interferences and incomplete chemical recovery of the analyte. However, the choice of a suitable spike for isotope dilution is very crucial to get accurate and precise results. Ideally, a spike should be an isotope which is either not contained or present in minimum abundance in the sample. The isotopic composition of Pu in the samples analyzed in the present work and the spike solutions used for isotope dilution, determined by conventional TIMS, are given in Table 5.2.

Table 5.2. Pu isotopic composition in the sample and the spike solutions used in SB-ID-TIMS method.

Isotope	Dissolver solution	^{240}Pu Spike used for Dissolver solution	Aqueous samples spiked with Pu	^{242}Pu Spike used for (U, Pu)C
^{238}Pu	0.022 ± 0.001	0.192 ± 0.005	0.150 ± 0.005	0.02 ± 0.001
^{239}Pu	89.92 ± 0.04	67.73 ± 0.03	69.20 ± 0.03	1.54 ± 0.006
^{240}Pu	9.119 ± 0.009	27.35 ± 0.03	26.23 ± 0.03	2.97 ± 0.005
^{241}Pu	0.861 ± 0.003	2.574 ± 0.005	2.568 ± 0.005	0.66 ± 0.003
^{242}Pu	0.070 ± 0.001	2.15 ± 0.006	1.846 ± 0.006	94.81 ± 0.04

Each aliquot of dissolver solution, generally in 3-4 M HNO_3 medium, was equilibrated with a single bi-functional magnetic PES bead, for one hour with continuous stirring, and the bead was directly analyzed by TIMS after equilibration. It can be seen from Table 5.2, the dissolver solution contained 89.9% of ^{239}Pu isotope and 9.12% of ^{240}Pu isotope. The abundances of the other three isotopes ^{238}Pu, ^{241}Pu and ^{242}Pu are less than 1%. Therefore, a spike enriched in either of ^{238}Pu, ^{241}Pu or ^{242}Pu isotope would be ideal for the determination of Pu in dissolver solution by isotope dilution. However owing to the high cost and restricted availability of enriched Pu spikes, choice of an indigenously available power reactor grade Pu, from an Indian PHWR (average burn-up ~10,000 MWD/TU), as spike for isotope dilution was considered more economically viable. It can be seen from Table 5.2, the PHWR grade Pu spike contained 27.35 atom% of ^{240}Pu and the change in ^{240}Pu/^{239}Pu atom ratio in the spiked mixture of the dissolver solution with respect to that in the pure dissolver solution and in the spike was monitored. A known quantity of Pu was added to 50-100 mL of aqueous and soil leach liquor samples, equilibrated with a single bi-functional magnetic PES bead, for 24 h with continuous stirring and the bead was analyzed by TIMS after equilibration. The isotopic composition of Pu, which was added to these samples, was similar to PHWR grade Pu as given in Table 5.2. It contained 69.20% of ^{239}Pu and 26.23% of ^{240}Pu isotopes and, therefore, a ^{242}Pu–enriched spike was used for isotope dilution of these samples and Pu concentration was determined from the change in ^{242}Pu/^{239}Pu atom ratio in the mixture with respect to that in the sample and the spike.

Table 5.3. Determination of Pu concentrations by SB-ID-TIMS method and by conventional ID-TIMS.

Sample	Pu concentration (μg g^{-1})	
	SB-ID-TIMS	ID-TIMS
Dissolver solution	11.8 ± 0.3	11.9 ± 0.2
4 mol L^{-1} HNO_3	3.37 ± 0.02	3.39 ± 0.02
Soil leach liquor	2.31 ± 0.02	2.32 ± 0.02

The Pu concentrations in all samples were determined by both SB–ID–TIMS and conventional solution based loading ID–TIMS methods and the results, given in Table 5.3, were found to agree within 1%. Thus, SB-ID-TIMS has good analytical performance with respect to conventional solution based TIMS. SB-ID-TIMS provided matrix elimination, purification and preconcentration of Pu in a single step by equilibrating the samples with a single magnetic poly(HEMP-co-APTAC) grafted PES bead, thereby considerably reducing analysis time and minimizing secondary waste compared to the conventional ID-TIMS technique.

5.4. Conclusions

A method was developed for simultaneous preconcentration of Pu using a magnetic bi-functional PES bead grafted with poly(HEMP-co-APTAC), followed by determination of Pu isotopic composition and concentration by SB-TIMS method. SB-TIMS method provides a single step purification and preconcentration of Pu from 5-100 mL of solution with fast kinetics. Thus the cumbersome ion-exchange column based separation and purification steps can be avoided. The PES bead based loading technique was found to provide comparable accuracy and precision with respect to the conventional solution loading technique. The presence of superparamagnetic Fe_3O_4 NPs in the bi-functional PES beads allows easy retrieval of the bead from large volume of aqueous solution. Also, the poly(HEMP-co-APTAC) grafted magnetic PES beads are selective towards Pu(IV) in presence of other competitive ions like U(VI) and, therefore, provide a possibility of using SB-ID-TIMS analyses for Pu(IV) determination in complex aqueous samples. The SB-ID-TIMS method was successfully employed for the determination of ppm level of Pu in dissolver solution, containing large excess of uranium, and also from the soil leach liquor solution. However, the vaporization filament temperature required to get optimum Pu^+ ion current in SB-TIMS method was 4 Amp, which is considerably higher than the conventional solution based TIMS method. This can be attributed to the fact that the magnetic bi-functional PES bead only partially decomposed during analysis. During analysis, the effective thermal energy available for the evaporation of Pu ions was less as the VF temperature was distributed in the residual matrix left on the filament. Therefore, it is necessary to search for better polymeric substrates for the simultaneous preconcentration and TIMS analyses of Pu, with analysis temperature comparable to the conventional solution based TIMS method.

Chapter 6

Porous polymer matrix supported liquid extractants for thermal ionization mass spectrometry

6.1. Introduction

A new emerging, viable alternative to solution handling is a solid phase extraction which offers number of advantages such as high preconcentration factor, minimization of liquid analytical waste, easy storage and transportation, and possibility of direct quantification of analyte preconcentrated on the solid matrix [168]. For the analyses of radioactive elements, a single step solid phase extraction would also provide secure physical transportation reducing the possibility of contamination of instrument, cross contamination of samples, and minimize the radiation exposure by eliminating undesirable radioactivity. A single anion-exchange bead based TIMS methods have been developed for Pu(IV) and U(VI) ions [153-155,164]. However these beads are very small and difficult to mount on the filament. Recently, King et al. suggested a novel method using the 1% glucose w/v solution as an adhesive for mounting the beads on to rhenium TIMS filaments, which were then dried under a heat lamp to set the glucose and fix the beads [164]. The acoustic streaming has been used for the small volume sample to improve sorption kinetics of Pu(IV) [156]. However, the beads in these method has been used as the reservoir for Pu(IV) ions in the already purified aqueous sample, and no attempt has been made to use it for dual functions like elimination of matrix as well as selective preconcentraion of the analyte ions. In previous Chapter 5, the poly(HEMP-co-APTAC) grafted magnetic PES beads have been studied for SB-ID-TIMS analyses of Pu(IV) in the complex aqueous samples. The optimum vaporization filament (VF) heating current for the Pu isotopic analysis by SB-TIMS has been found to be about 4 Amp, at which about 1V $^{239}Pu^{+}$ ion current is obtained. The ionization efficiency of SB-TIMS method has been found to be lower than the conventional solution based loading method.

To address higher VF temperature problem in poly(HEMP-co-APTAC) grafted magnetic PES bead based ITMS, a systematic study has been carried out to explore the polymeric material based loadings of U(VI) and Pu(IV) ions in TIMS. These polymeric materials have been developed using two routes – one is grafting of the phosphate bearing monomer and the other one is physical immobilization of the phosphate based ligands in the microporous poly(propylene) and poly(ethersulfone) substrates. The liquid extractants immobilized in the microporous polymeric substrate is also known as a supported liquid membrane in the field of separation science and has been explored for analytical applications [168, 169]. The selection of phosphate functional group bearing reagent has been based on the fact that phosphate groups have strong affinity towards the actinides. These polymeric materials have been studied for their efficiency for selective preconcentration of U(VI) and Pu(IV) ions from a variety of environmental and nuclear fuel reprocessing samples, and used for the quantification of U(VI) and Pu(IV) ions using isotope dilution method based TIMS.

6.2. Experimental

For synthesis of the pore-grafted substrates, 1:1 mole proportion of the monomers, HEMP and ethylhexyl methacrylate (EHM), were dissolved in ethanol and 1 wt. % of photo-initiator DMPA in DMF was added to it. The polymerizing solution was homogenized by ultrasonication for 5 min and the microporous PP and PES membranes were immersed in it for overnight when the monomers along with the photo-initiator filled in the pores of PP and PES membrane. After overnight immersion, the pore-filled substrates were taken out; excess solution clinging on the surface was removed and then irradiated in a UV reactor for 15 min. The grafted polymer substrates were thoroughly washed with ethanol and water before use. The ligand impregnated polymer substrates were prepared in the same procedure as used for the preparation of supported liquid membranes [168-169]. The mixture of HDEHP and TEHP in 1:0, 3:1, 1:1, 1:5, 1:10 and 0:1 mole proportions were prepared. The PES beads, prepared by phase inversion technique as described in Chapter 5.2, and PP membranes were equilibrated with these mixtures for overnight, and then taken out solution and excess of solution was dripped out and gently washed the extractant-filled membranes with water. The details of the study of sorption efficiency and sorption kinetics of Pu, ^{241}Am and ^{233}U by the polymer substrates are given in Chapter 2.5.3.

Polymeric substrates reservoir based thermal ionization mass spectrometry (PolymRes-TIMS) was studied employing NIST SRM–947 Pu isotopic standard. NIST SRM–947 solution (2 mL) was treated with 30% H_2O_2 in 3 M HNO_3 to convert all oxidation states of Pu to Pu(IV), and then equilibrated with a 0.5x0.2 cm^2 piece of the polymer reservoirs developed in the present work for 1 h with a continuous stirring. After equilibration, the polymer reservoir was collected from the solution using a pair of tweezers, washed with 3 M HNO_3 to remove the surface adsorbed Pu(IV) ions, dried and directly loaded onto a high purity rhenium filament for the TIMS analysis. The polymer reservoir loaded filament was served as the vaporization filament (VF) and the other filament served as the ionization filament (IF). The loading techniques for the various polymeric reservoirs developed in the present study were different. The liquid extractant impregnated PES beads were wetted in 3M HNO_3 and placed at the center of the Re filament which was then slowly heated to decompose the polymeric reservoir partially. The 0.5x0.2 cm^2 pieces of pore grafted PP and PES membranes were wetted in 3M HNO_3 and placed along the length of the Re filament. For loading the liquid extractant impregnated PP membrane, a 0.5x0.2 cm^2 piece of the membrane was held vertically with a tweezers in such a way that one end of the piece touches the center of the Re filament; the filament was then slowly heated when the membrane gradually melted and deposited at the centre of the filament.

All analyses were performed under static mode of analysis of a thermal ionization mass spectrometer equipped with multiple Faraday cups, using double rhenium filament assembly. Prior to the isotopic analysis, the temperature of the IF was increased to obtain about 200 mV ^{187}Re$^+$ ion current. The temperature of the VF was slowly increased from 0 to

2A in 600 seconds and degassing was carried out at 2A for 1800 seconds. After degassing, VF temperature was increased to obtain optimum Pu^+ ion current of 200 mV or more. Pu isotopic analyses were also carried out by conventional solution based TIMS method after purifying the Pu sample by Dowex 1X8 anion–exchange resin, details described in Chapter 5.2, and the results of conventional TIMS and PolymRes-TIMS were compared.

The PolymRes-TIMS method was employed for the determination of Pu(IV) ions concentration in the dissolver solution of irradiated UO_2 fuel and also in other aqueous samples like seawater and synthetic urine samples spiked with known amount of $Pu(NO_3)_4$. Pu concentrations in the samples were determined by isotope dilution (ID) technique as described in Chapter 5.3.4. For determination of Pu concentration in dissolver solution (U:Pu mole ratio ~1000:1), a 0.5x0.2 cm^2 piece of liquid extractant impregnated polymer substrate (TEHP+HDEHP) was equilibrated for 1 h with a continuous stirring with 3 mL of dissolver solution and its spiked mixture, separately. After equilibration, the polymer substrate was collected, washed and loaded onto the VF for isotopic composition (IC) analysis of Pu in the dissolver solution and its spiked mixture. A known Pu activity and its spiked mixture was added to 50 mL of seawater/ synthetic urine separately, and equilibrated with a 0.5x0.2 cm^2 piece of liquid extractant impregnated polymer substrate (TEHP+HDEHP) for 24 h with a continuous stirring. After preconcentration of Pu(IV) ions, the polymer pieces were loaded for TIMS as described above, and Pu concentrations in the various samples were calculated from the change in isotope ratios in the spiked mixture with respect to those in the sample and the spike. Seawater has a uniform concentration of about 3.3 ppb of uranium, however the groundwater sample used in the present study did not contain any uranium. Therefore, a known weight of natural uranium in the form of $UO_2(NO_3)_2$ was added to the groundwater sample. For isotope dilution, known weight of a pre-calibrated ^{233}U spike solution was added to 50 mL of the sample and the spiked sample was equilibrated with 0.5x0.2 cm^2 piece of

HDEHP impregnated polymer reservoir for 24 h with continuous stirring. After preconcentration of U(VI) ions, the polymer reservoir were subjected to U isotopic analysis by TIMS, and U concentrations in various samples were obtained from the change in $^{233}U/^{238}U$ ratios in the spiked mixture with respect to those in the sample and the spike.

6.3. Results and discussion

6.3.1. Development of polymeric materials for thermal ionization mass spectrometry

In the present work, the polymeric materials were developed using two commercially available microporous membranes, PES and PP. Two different types of polymeric materials, viz. pore grafted polymer and ligand impregnated polymer substrates were synthesized using the base matrices PES and PP. For the pore grafted polymeric reservoirs, the monomer HEMP was anchored in the PES and PP membranes along with EHM. The polymeric reservoirs grafted with 1:1 mole proportion HEMP and EHM were termed as poly(HEMP-co-EHM)-PP and poly(HEMP-co-EHM)-PES reservoirs. In poly(HEMP-co-EHM)-PP, HEMP and EHM were polymerized using UV-initiator DMPA induced graft polymerization within the pores of the membrane. EHM did not contain any functional group and, therefore, had no direct role in the sorption of actinides; rather it acted as a spacer that reduced the extent of cross-linking polymer network created by HEMP having three polymerizing double bonds, which in turn improved the sorption efficiency. The Pu(IV) sorption efficiency of the polymer substrate formed by grafting pure HEMP in PP membrane was only about 20% in 3 M HNO_3. However, the Pu(IV)-sorption efficiency was increased to 80% under similar conditions when the spacer EHM was grafted along with HEMP in 1:1 mole proportion. This could be explained by the fact that a heavy cross-linking of HEMP restricted the accessibility of phosphate groups for binding with Pu(IV) ions. The presence of EHM provides flexibility to the grafted polymer chains that increases the Pu(IV)-

sorption efficiency. Figure 6.1 shows the SEM images of pristine PP membrane and poly(HEMP-co-EHM)-PP. It is seen from Figure 6.1 that the pores of PP membrane were only partially filled though the grafting yield was 70 wt.%. Thus, poly(HEMP-co-EHM)-PP still retained sufficient porosity after grafting HEMP with EHM that would improve the sorption kinetics.

The other of polymeric reservoir developed in the present study was ligand impregnated polymeric materials which involved the physical immobilization of hydrophobic liquid extractants in the pores of the PP membrane and PES beads. These polymeric reservoirs were termed as TEHP:HDEHP@PP and TEHP:HDEHP@PES. The choice of PP membrane or PES beads was based on the fact that these are hydrophobic polymers that would be best suited for immobilizing the hydrophobic ligands and their pore size was suitable for providing sufficient capillary force to hold the ligands. The amount of liquid extractants HDEHP+TEHP in the PP membrane was found to be 70–80 wt. %. The ligands TEHP and HDEHP were selected to retain the same phosphate functional group used in the pore grafted membrane. TEHP and HDEHP have similar chemical structures of phosphate groups as in the diester and triester components of HEMP as shown in Figure 2.1 in Chapter 2.1.

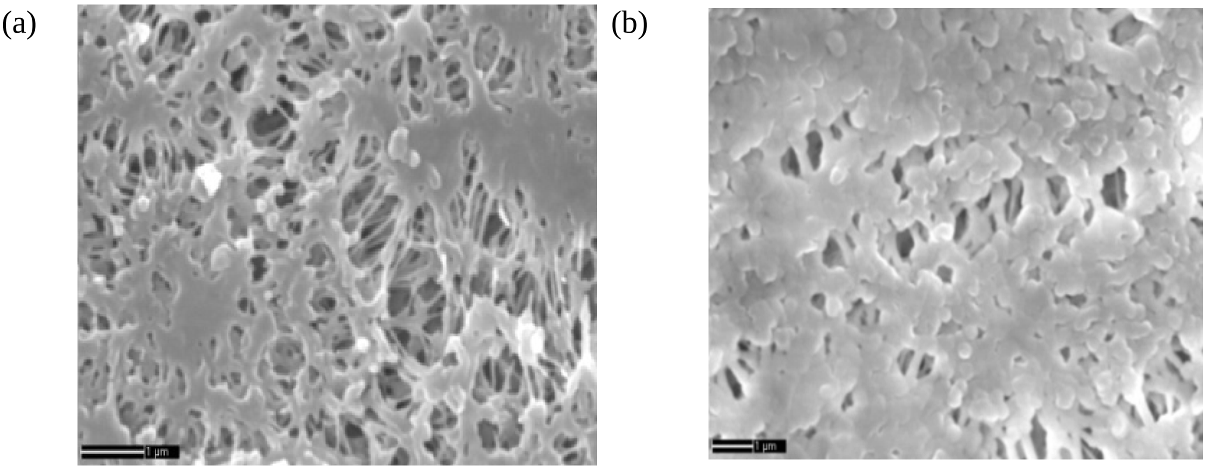

Figure 6.1. SEM images of (a) pristine PP membrane and (b) poly(HEMP-co-EHM)-PP membrane.

Different mole proportions of TEHP and HDEHP were used in ligand impregnated polymers to obtain optimum sorption efficiency for the actinides. The liquid extractants were held in the 0.1–0.2 μm pores of PP membrane or PES beads by capillary force and require a considerable pressure to eject out of pores. Thus, the immobilized hydrophic ligands have reasonably good stability in the host PP membrane or PES beads for one time use as a reservoir.

6.3.2. Actinides sorption studies of polymeric reservoirs

The sorption efficiency of the poly(HEMP-co-EHM)-PP reservoir for actinides was studied as a function of HNO_3 concentration and the Figure 6.2 shows the sorption profiles for Pu(IV), U(VI) and Am(III). It can be seen from Figure 6.2, the Pu(IV) and U(VI) sorption in the poly(HEMP-co-EHM)-PP reservoir increased with increasing HNO_3 concentration and attained a maximum of about 70% and 85% extraction of U(VI) and Pu(IV), respectively, in HNO_3 concentration more than 2 M. However, Am(III) sorption above 2 M HNO_3 concentration was negligible (< 5%) which is typical behavior of neutral phosphate based extractants. It can be concluded from Figure 6.2 that the poly(HEMP-co-EHM)-PP reservoir has good selectivity towards Pu(IV) ions, and slightly lower affinity for U(VI) ions.

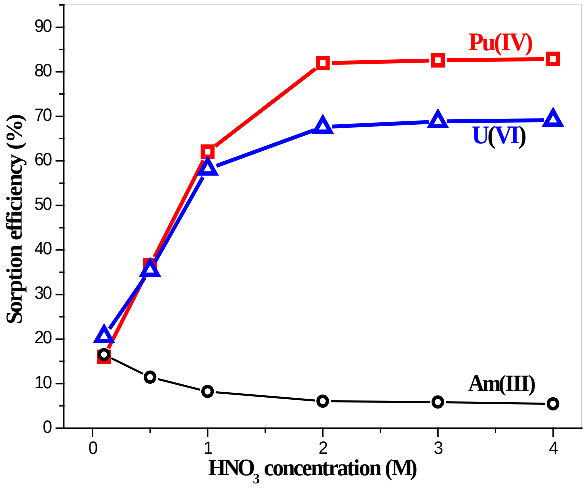

Figure 6.2. Sorption efficiency of the poly(HEMP-co-EHM)-PP reservoir for Am(III) (o), U(VI) (Δ) and Pu(IV) (□) ions as a function of HNO_3 concentration.

The actinides sorption studies were also carried out in the TEHP:HDEHP@PP polymer reservoirs, containing different mole proportions of HDEHP and TEHP viz. 1:0, 1:1, 1:3 and 0:1, as a function of HNO_3 concentration. The sorption profiles of Am(III), U(VI) and Pu(IV) are shown in Figure 6.3. It is seen from Figure 6.3(a) that Am(III) sorption efficiency of TEHP:HDEHP@PP was not quantitative and varied between 15-8 % in the HDEHP@PP below 2 M HNO_3. However, Pu(IV) and U(VI) were sorbed with a high efficiency in the all the TEHP:HDEHP@PP and HDEHP@PP reservoirs, but not in the TEHP@PP reservoir. Pu(IV)-sorption efficiency was optimum (95%) in the HDEHP@PP as shown in Figure 6.3(b). The U(VI)-sorption efficiency in the TEHP:HDEHP@PP reservoirs were independent of the HNO_3 concentration of the equilibrating solution or mole proportions of TEHP:HDEHP.

(a)

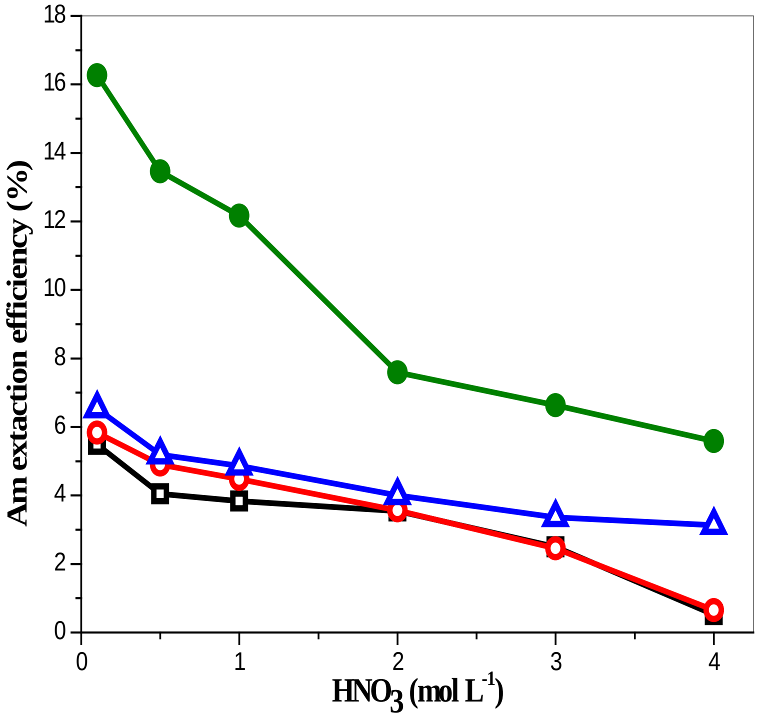

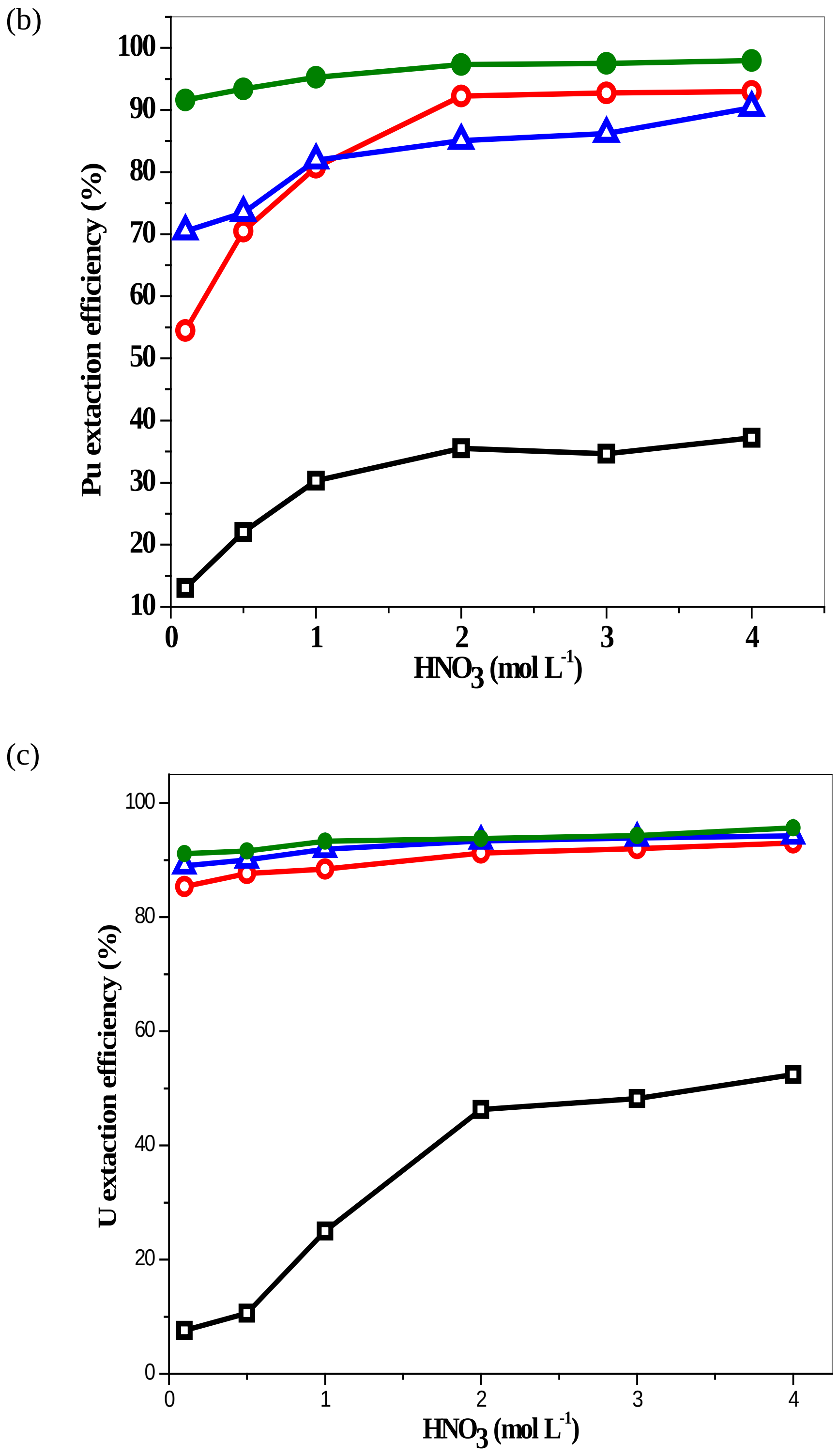

Figure 6.3. Sorption profiles of (1:0)TEHP:HDEHP@PP (□), (3:1)TEHP:HDEHP@PP (o), (1:1)TEHP:HDEHP@PP (Δ) and (0:1)TEHP:HDEHP@PP (●) for (a) Am(III), (b) Pu(IV) and (c) U(VI) as a function of HNO_3 concentration

In case of seawater and ground water samples, having pH in the range 7–8.5, the U(VI) sorption efficiency was found to be optimum in (1:10) TEHP:HDEHP@PP and HDEHP@PP reservoirs, as shown in Figure 6.4. For the determination of trace amount of uranium in natural water samples, it was also necessary to remove the matrix apart from preconcentration of the analyte. Energy dispersive X-ray spectrometry was employed to study the extent of matrix elimination during the preconcentration of U(VI) from seawater samples. It can be seen from Figure 6.5, only U(VI) ions were sorbed in the HDEHP@PP reservoir from seawater when U(VI) concentration was high enough to saturate the binding sites. However, other ions were also sorbed when the binding sites in the polymer reservoir were not saturated with U(VI) ions. In such conditions, all other ions, except U(VI), sorbed in the HDEHP@PP could be removed by equilibrating it with 3 M HNO_3 as only U(VI) and Pu(IV) are sorbed at this acidity.

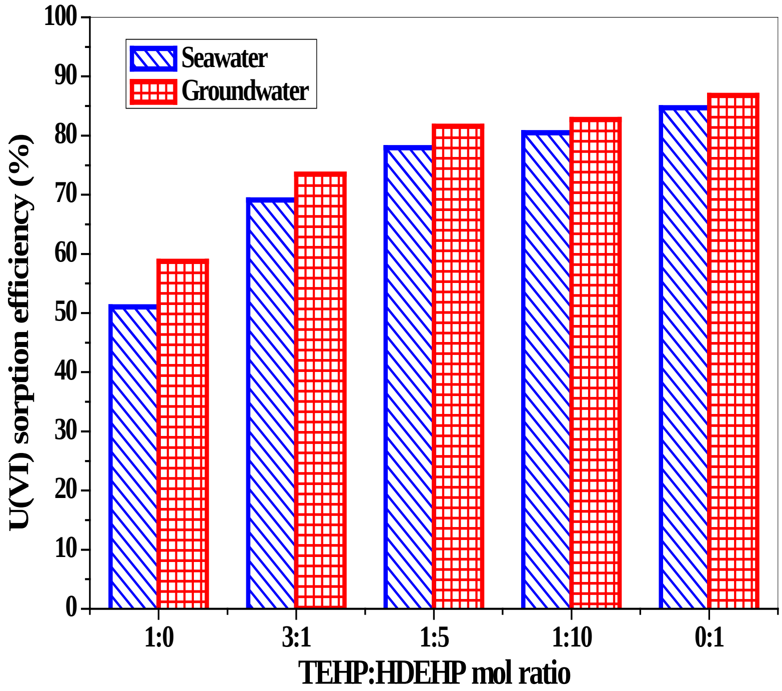

Figure 6.4. Sorption of U(VI) from seawater and groundwater by TEHP:HDEHP@PP, having different mole proportions of TEHP and HDEHP.

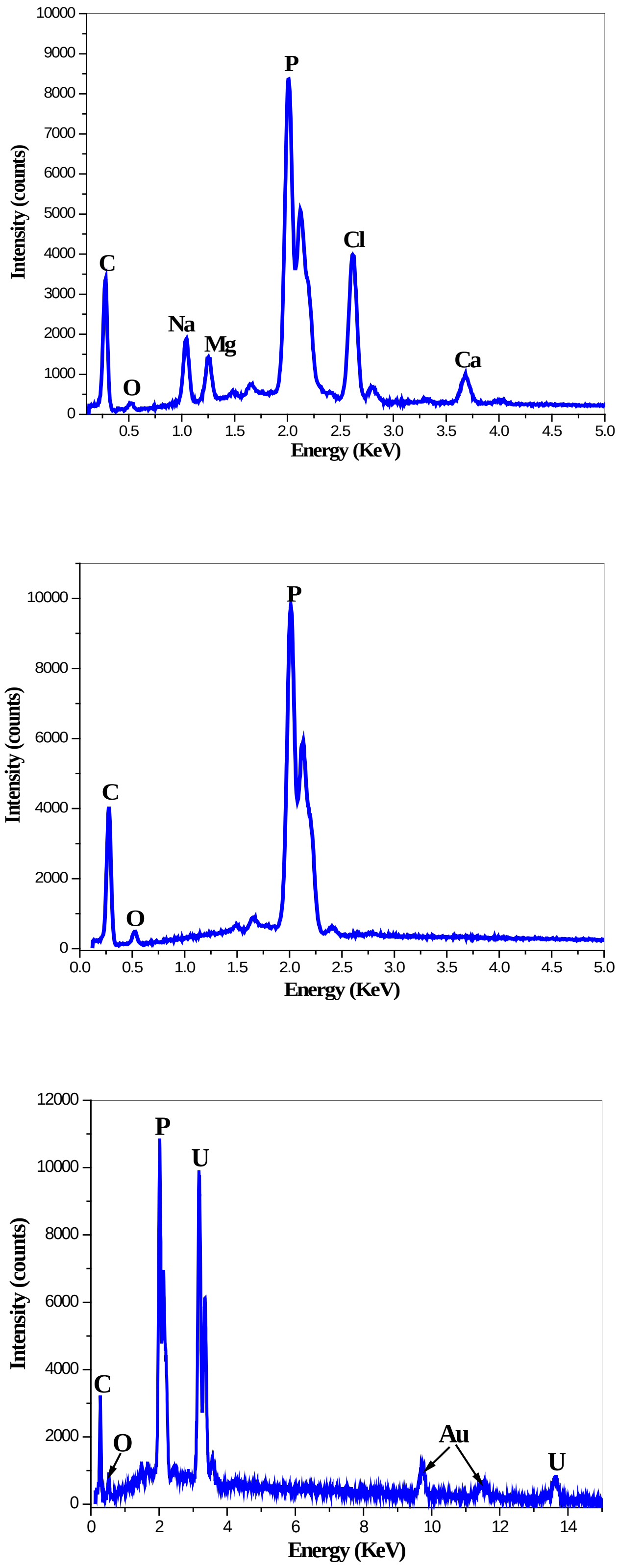

Figure 6.5. EDX analyses of HDEHP@PP membrane (a) equilibrated with seawater, (b) washed with 3 M HNO_3 after equilibration with seawater and (c) equilibrated with seawater spiked with 1.7 ppm U(VI).

It was interesting to observe from the data given in Table 6.1 that, the distribution ratios (D) of Pu(IV) and U(VI), determined in competing mode using a solution containing 100:1 mole proportion of U:Pu, were strongly dependent on the composition of TEHP and HDEHP in the TEHP:HDEHP@PP reservoir. The higher selectivity of the (3:1)TEHP:HDEHP@PP reservoir, as indicated by the $D(Pu^{IV})/D(U^{VI})$ ratio given in Table 6.1, could be attributed to the fact that P=O has higher affinity towards Pu(IV) as compared U(VI). Thus, $D(Pu^{IV})$ was higher in dynamic competition and increased with increasing concentration of the neutral phosphate extractant TEHP in the TEHP:HDEHP@PP reservoirs.

Table 6.1. Distribution coefficients of Pu(IV) and U(VI) ions in different compositions of TEHP:HDEHP@PP reservoir from the solution containing 1:100 mol proportion of Pu(IV) to U(VI) ions in 3 M HNO_3.

TEHP:HDEHP	$D(Pu^{IV})$ (mL g^{-1})	$D(U^{VI})$ (mL g^{-1})	$D(Pu^{IV})/D(U^{VI})$
1:0	127 ± 9	16 ± 3	7.9
3:1	217 ± 15	19 ± 3	11.4
1:1	139 ± 10	26 ± 5	5.3
0:1	112 ± 8	29 ± 5	3.9

The kinetics of Pu(IV)/U(VI) sorption is another important aspect for the analytical application of the polymeric reservoirs developed in the present work for TIMS. The rates of Pu(IV) sorption from 3M HNO_3 by the poly(HEMP-co-EHM)-PP and (3:1)TEHP:HDEHP@PP as a function of equilibration time are shown in Figure 6.6. It can be seen from Figure 6.6 that the TEHP:HDEHP@PP reservoir attained optimum sorption equilibrium (92%) within 50 min. In case of the poly(HEMP-co-EHM)-PP, the optimum sorption equilibrium (85%) was achieved at longer period of time of about 100 min. This could be attributed to fact that the functional groups are chained with polymer matrix in the poly(HEMP-co-EHM)-PP leading to diffusion of Pu(IV) by site jumping or direct interactions due to porosity of the grafted matrix. Contrary to this, the carriers are mobile in the liquid fraction of the TEHP:HDEHP@PP reservoir.

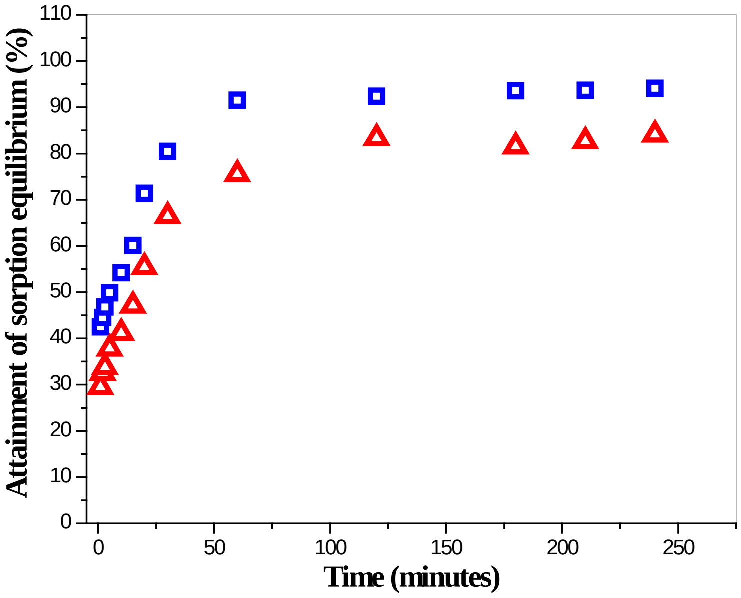

Figure 6.6. Attainment of Pu(IV) sorption equilibrium in the poly(HEMP-co-EHM)-PP and 3:1TEHP:HDEHP@PP from 3 M HNO$_3$.

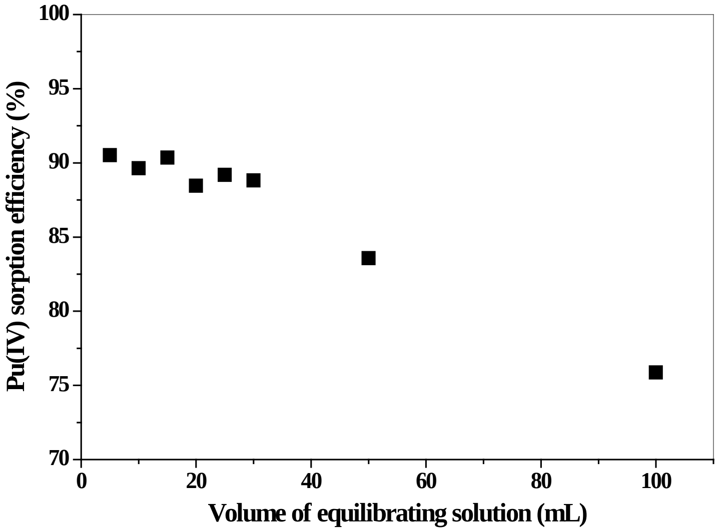

Figure 6.7. Pu(IV) sorption efficiency in (3:1)TEHP:HDEHP@PP as a function of volume of equilibrating solution.

The variation of Pu(IV)-sorption efficiency in the 3:1 TEHP:HDEHP@PP reservoir as a function of volume of equilibrating solution is shown in Figure 6.7. It can be seen from this Figure 6.7 that the Pu(IV)-sorption efficiency remained unaffected (89±2%) up to 30 mL, and decreased to 75±2% thereafter. This may be attributed to the slower diffusion of Pu(IV) ions in the equilibrating solution having volume higher than 30 mL. Therefore, the preconcentration of Pu(IV) ions from a large volume sample, higher than 30 mL, would require the longer equilibration time or better equilibration method like flow cell etc.

6.3.3. Selection of polymeric reservoir for TIMS

One of the important requirements for selecting a reservoir for TIMS is vaporization filament (VF) temperature required for optimum conditions analysis of Pu. Therefore, the variation of $^{239}Pu^{+}$ ion current as a function of vaporization filament temperature was studied by mounting the Pu(IV)-loaded poly(HEMP-co-EHM)-PP/PES and (3:1)TEHP:HDEHP@PP on Re filament in TIMS were measured.

It can be seen from Figure 6.8(a) and (b), the VF temperature was dependent on various factors like the base polymer, method used in forming the reservoir and shape of the reservoir. It is seen from Figure 6.8 that (i) PP is better host matrix than PES, (ii) bead reservoir requires higher VF temperature than flat sheet reservoir and (iii) evaporation profile obtained from the ligand impregnated TEHP:HDEHP@PP reservoirs was comparable to that obtained from solution based loading. The PP matrix was found to decompose completely, but residue was observed in the case of PES. This may be related to their chemical structures shown in Figure 2.1 in Chapter 2. The PP membrane is made up of hydrocarbon which can be completely burned at the analysis temperature of TIMS. Also, the liquid fraction in the TEHP:HDEHP@PP reservoir would be easily vaporized as compared to the polymeric extractants covalently attached to the host matrix. Thus, the polymeric reservoir consisting of the phosphate based ligands physically immobilized in a flat sheet PP membrane are better suited for TIMS analysis of Pu.

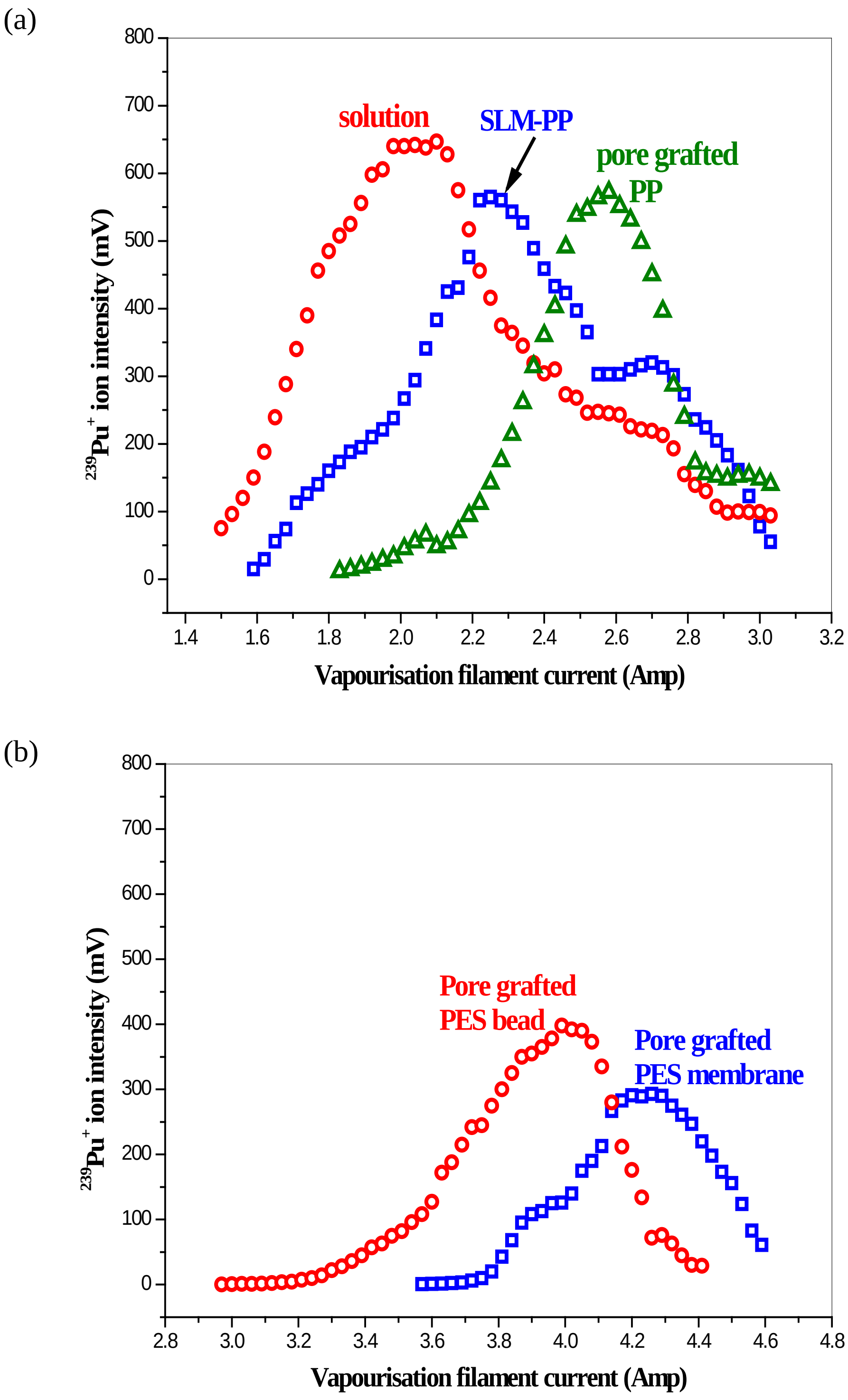

Figure 6.8. Pu evaporation profiles from solution and various polymeric reservoirs loaded on Re filament in TIMS.

To compare reproducibility, the relative standard deviations in the measurement of isotopic analysis of NIST-SRM 947 Pu isotopic standard were studied for TIMS involving solution, poly(HEMP-co-EHM)-PP and TEHP:HDEHP@PP based loadings on Re filament. It can be seen from Figure 6.9 that the precision is slightly less in the reservoir based Pu loading in TIMS as compared to that obtained by solution based loading. Between the poly(HEMP-co-EHM)-PP and TEHP:HDEHP@PP, the precision was better in the TEHP:HDEHP@PP based loading in TIMS. The precision obtained for the ^{240}Pu/^{239}Pu atom ratio is better compared to that of ^{241}Pu/^{239}Pu and ^{242}Pu/^{239}Pu atom ratios, owing to the fact that ^{240}Pu and ^{239}Pu are the major isotopes present in the standard, whereas ^{241}Pu and ^{242}Pu are the minor isotopes. Also isotopic fractionation is lower for ^{240}Pu/^{239}Pu atom ratio due to less relative mass difference between ^{239}Pu and ^{240}Pu isotopes, whereas fractionation is more prominent for ^{241}Pu/^{239}Pu and ^{242}Pu/^{239}Pu atom ratios due to higher relative mass difference between these isotopes. Therefore, TEHP:HDEHP@PP reservoir was found to be best suited for Pu analysis by TIMS in terms of both VF temperature and SD of Pu isotope ratios.

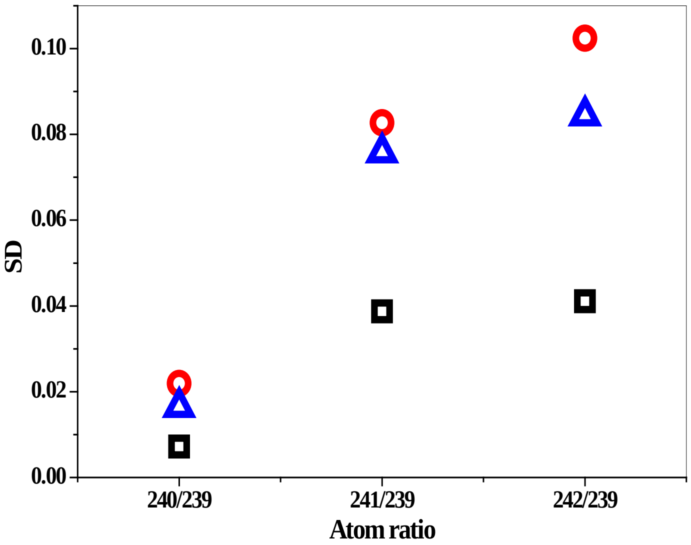

Figure 6.9. Standard deviation of isotopic analysis of NIST-SRM 947 Pu isotopic standard obtained from solution, TEHP:HDEHP@PP, and poly(HEMP-co-EHM)-PP based loading on Re filament in TIMS.

Analysis of uranium isotopic standard ISU-09, having a certified $^{235}U/^{238}U$ ratio of 1.096×10^{-2}, was also analysed by PolymRes-TIMS and the result was compared with solution-TIMS. The $^{235}U/^{238}U$ ratio in ISU-09 standard was found to be 1.0985×10^{-2} and 1.0979×10^{-2}, respectively, by solution-TIMS and PolymRes-TIMS. However, the $^{234}U/^{238}U$ ratio could not be measured since the Faraday cup detectors of the Isoprobe-T instrument are not capable of measuring such low intensity ion beam. The TEHP:HDEHP@PP reservoir was further tested for its analytical performance.

6.3.4. Application of polymeric reservoir based thermal ionization mass spectrometry to natural water and biological samples

The isotope dilution method was used for quantification of the Pu(IV) and U(VI) by PolymRes-TIMS, coupled with isotope dilution because of the fact that it is not affected by experimental conditions, including variation in the sorption efficiency of the reservoir. In isotope dilution method, a known weight W_{sp} of a pre-calibrated spike solution, having known concentration C_{sp}, is added to a known weight W_{sa} of the sample solution. Pu concentration C_{sa} in the sample can be correlated with change of isotope ratio in the spiked mixture (R_m) with respect to those in the sample (R_{sa}) and spike (R_{sp}) [142,143]. It can be seen from Table 6.2, the average concentrations of Pu(IV) in 3-5 measurements of dissolver solution obtained from PolymRes-TIMS was found to be in a good agreement with that obtained from solution-TIMS within uncertainty limit.

Table 6.2. Pu concentrations determined in the dissolver solution by PolymRes-TIMS using TEHP:HDEHP@PP and solution-TIMS employing isotope dilution technique.

Sample	Pu concentration (ppm)			
	PolymRes -TIMS		Solution-TIMS	
	Avg.	RSD(%)	Avg.	RSD(%)
Dissolver solution	12.90 ± 0.07	0.51	13.05 ± 0.04	0.30

The PolymRes-TIMS was also employed for the quantification of Pu(IV) and U(VI) in the seawater, ground water and synthetic urine samples. The natural water samples have pH in the range 6.5–8.5 and did not contain any Pu. Therefore, a weighed amount of Pu was added to each of these samples. Since Pu shows very strong tendency to hydrolyze and polymerize in low acidic medium, acidity of each sample was adjusted to 3 M HNO_3 before addition of Pu. For the determination of Pu(IV), the (3:1)TEHP:HDEHP@PP reservoir was used for preconcentration and subsequent loading in the TIMS as it shows maximum Pu(IV)-sorption efficiency at 3 M HNO_3. The natural concentration of uranium in seawater is about 3.3 ppb; all other natural water samples were added with a known weight of uranium. For the determination of U(VI) the HDEHP@PP reservoir was used, without adjusting the acidity of the sample as U(VI)-sorption efficiency in this reservoir is not affected by the acidity in the equilibrating sample as shown in Figure 6.4. Table 6.3 shows the comparison of U and Pu concentrations, in nanogram per gram, determined in various aqueous samples by PolymRes-TIMS with the respective expected values. The relative standard deviation (RSD %) values given in Table 6.3 were calculated from the triplicate TIMS analyses of each sample.

Table 6.3. Determinations of Pu(IV) and U(VI) in the aqueous samples using isotope dilution based Reservoir-TIMS.

Sample	Volume (mL)	Actinide	Concentration (ppb)	
			Expected	Measured
Synthetic urine (Spiked)	50	Pu(IV)	9.45	9.56 ± 0.21
Seawater (Spiked)	50	Pu(IV)	5.64	5.53 ± 0.11
Seawater (unspiked)	50	U(VI)	3.31	3.62 ± 0.20
Ground water (Spiked)	50	U(VI)	3.12	2.83 ± 0.14

The dissolver solution contained several µg of Pu as shown In Table 6.2, but the aqueous samples listed in Table 6.3 had only a few ng of Pu. Intensities of the ion beams, obtained during TIMS analysis, were much higher for the samples shown in Table 6.2, therefore the uncertainties on the values obtained in Table 6.2 are lower. However, uncertainties on the values obtained in Table 6.3 are higher since the ion beam intensities for these samples were relatively low due to the small amount of Pu available for TIMS analysis. It can be seen from Table 6.3 that for Pu the values are 1.0116, 0.9805 with mean as 0.99±1.6% and for U, 1.0936 and 0.9071 with mean as 1.00±9.3%. Thus, the accuracy of about 2% and 10% were obtained for Pu and U(VI) determinations, respectively, at the ng g^{-1} concentration levels. The lower accuracy related to determination of U, compared to that of Pu determination, can be attributed to the poorer ionization efficiency of U, leading to lower ion currents available for TIMS analysis of U(VI). The measured concentrations of Pu(IV) and U(VI) obtained using the isotope dilution based PolymRes-TIMS were in reasonably good agreement with the expected concentrations, as can be seen from Table 6.3. This clearly demonstrated that the PolymRes-TIMS, developed in the present work, can be applied for the determination of Pu(IV) and U(VI) in a wide variety of aqueous samples.

6.4. Conclusions

The polymeric reservoirs were developed in the present work, for preconcentration and TIMS analysis of actinides, using UV-initiator induced grafting and physical immobilization of the ligands in the poly(propylene) membrane. It was observed that the liquid extractants HDEHP and TEHP immobilized in the poly(propylene) membranes are best suited for dual functions of the reservoir i.e. efficient preconcentration of Pu(IV) and U(VI) from a wide variety of aqueous matrices and isotopic analysis by TIMS with low vaporization temperature. The HDHP and TEHP immobilized in poly(propylene) were applied successfully for the quantification U(VI) and Pu(IV) in the synthetic urine sample, seawater and ground water using isotope dilution method with reasonable good accuracy and precision. U(VI) was preconcentrated in the reservoir without adjusting the acidity of the aqueous samples, but require adjustment to 3 M HNO_3 for Pu(IV) preconcentration. The major advantage of the PolymRes-TIMS developed in the present work is that it provides a single step sample manipulation and loading process that would greatly reduce the analysis time and prolong handling of the radioactivity causing possibility of contamination and exposure to radiations.

Chapter 7

Conclusions & future scope

7.1. Summary

The present dissertation focuses on the development of dual function polymers *i.e.* simultaneous selective preconcentration of actinides from the acidic aqueous matrices and subsequently quantification of the preconcentrated actinides directly from the polymeric substrate. This would reduce number of sample manipulation steps, and enhance the detection limit of conventional methods being routinely used for the quantification of actinides in aqueous matrices such as process sample, waste discharge, environmental and biological samples. A single step sample manipulation process would greatly reduce the analysis time, human errors, and prolong handling of the radioactivity causing possibility of contamination and exposure to radiations. The aim of this thesis was to synthesize bi-functional polymers, containing neutral phosphate groups along with ionic sulphonic acid or quaternary ammonium groups, and application of these polymers for preconcentration of actinides. The choice of phosphate functional group was based on the fact that the P=O moiety is selective towards actinides whereas the presence of ionic sulphonic acid or quaternary ammonium groups improves the sorption kinetics. For the quantification of actinides sorbed on the polymeric substrate, either alpha spectrometry or thermal ionization mass spectrometry (TIMS) was employed. These two techniques are being used widely for the quantification of actinides particularly Pu. The requirements of alpha spectrometry and TIMS are different. Therefore, bi-functional polymer matrix has to be tuned for making it suitable for one of these techniques. Pu(IV) has been selected as analyte due to fact that it is major actinide, highly radiotoxic, and has to be monitored in the samples having high radiation dose, highly acidic solution, and biological fluids and environmental having its ultratrace concentration. Pu consists of multiple isotopes that are important for its uses and nuclear forensic. The overall work carried out in the present work is summarized in figure given below:

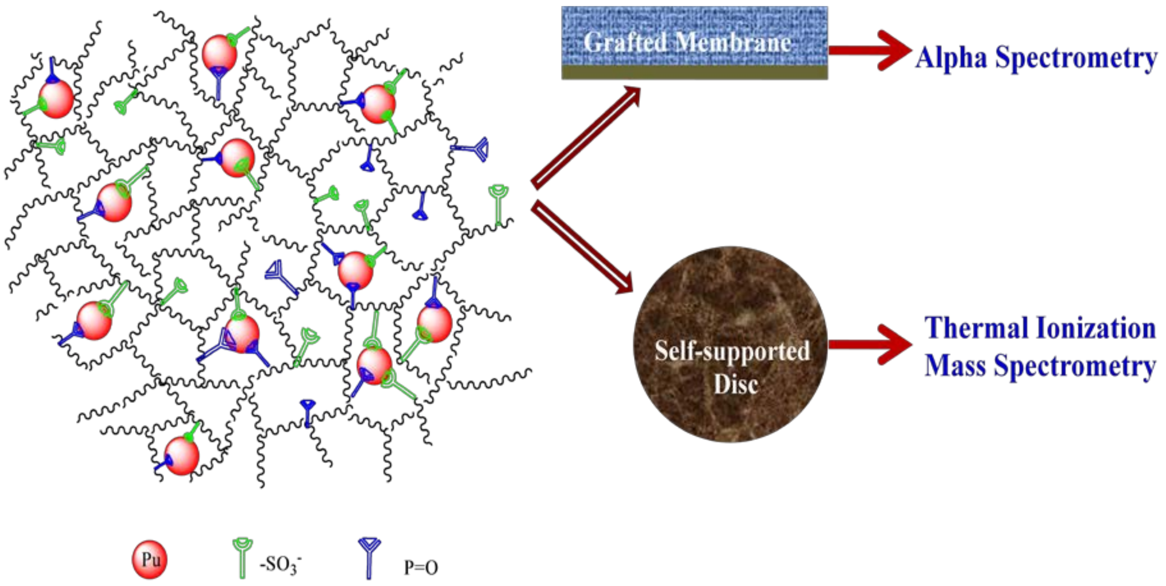

7.2 Conclusions

Self-supported bi-functional polymer discs were synthesized in the present work, by photoinduced free radical polymerization of the HEMP monomer with either AMPS or APATAC monomers, for acidity-dependent selectivity towards actinides. The proportions of phosphate groups and sulfonic acid/quaternary ammonium groups in the bi-functional polymer discs, measured by SEM-EDS, were found to be the same as expected from the mole proportions of monomers in polymerizing solutions used for syntheses. Also alpha track radiography of the bi-functional polymer indicated homogeneous distribution of the functional groups in the substrate. The bi-functional poly(HEMP-co-AMPS) or poly(HEMP-co-APTAC) matrices were found to be better than either poly(HEMP) matrix or poly(AMPS/APTAC) matrix in terms of: (i) higher Pu(IV) sorption efficiency at 3−4 M HNO_3, (ii) selective preconcentration of Pu(IV) in the presence of a trivalent actinide such as Am(III), and (iii) preferential sorption of Pu(IV) in the presence of a large excess of U(VI). The distribution ratio of the bi-functional polymers for Pu(IV), in presence of excess U(VI), were also found to be higher than that of mono-functionalized polymers. This indicated that the bi-functional poly(HEMP-co-AMPS) or poly(HEMP-co-APTAC) matrices could be promising for the selective extraction of Pu(IV) from complex aqueous matrices like various environmental and biological samples, and nuclear fuel dissolver/waste solutions. These bi-functional polymers were suitably tailored for the quantification of the preconcentrated actinides by alpha spectrometry and TIMS.

Quantification of actinides by conventional alpha spectrometry involves multiple steps like matrix elimination, selective preconcentration of the target actinide and solid source preparation by evaporation or electrodeposition. To minimize the sample manipulation steps, membrane based alpha spectrometry method was developed in the present work for the determination of plutonium concentrations in the complex aqueous solutions. The bi-functional poly(HEMP-co-AMPS) polymer was anchored as a 1-2 μm thin layer on the surface of microporous PES membrane by UV induced surface grafting. The thickness of the bi-functional layer was optimized in terms of Pu sorption capacity and good quality alpha spectrum. The optimized membrane was used for preconcentration of Pu(IV) from aqueous solutions having 3–4 M HNO_3, with high chemical recovery efficiency of 86±3%. Am(III) did not sorb significantly by the bi-functional membrane, but U(VI) sorbed with 78±3% efficiency from the solutions having 3 M HNO_3 concentration. However, Pu(IV) chemical recovery in the membrane remained unaffected from the solution containing 1:1000 wt. proportion of Pu(IV) to U(VI). This shows that Pu(IV) is preferentially sorbed in competition with U(VI). For the quantification of Pu(IV) preconcentrated in the membrane by alpha spectrometry, both absolute efficiency calibration and isotope dilution using ^{238}Pu enriched spike were employed. Pu concentrations in the (U, Pu)C samples and irradiated fuel dissolver solutions were determined by the membrane based alpha spectrometry, and the results were found to be in a good agreement with those obtained by conventional alpha spectrometry, biamperometry and thermal ionization mass spectrometry. The advantages of this method are selective sorption of Pu(IV) with high preconcentration factor and highly reproducible quantification, without any separate alpha source preparation step. The figure given below illustrates the concept of membrane based alpha spectrometry,

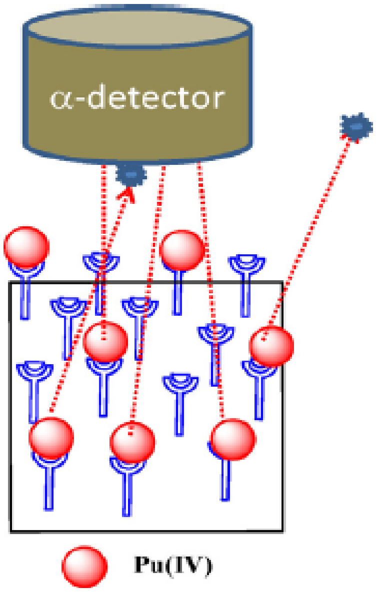

Thermal ionization mass spectrometry (TIMS) is a widely used method for determining Pu isotopic composition as well as concentration with high precision, accuracy and considerably low detection limits. However, TIMS analyses also require an elaborate sample preparation step for matrix elimination and subsequent manual loading of small volume of purified aqueous sample on a filament surface for thermal ionization that is cumbersome, particularly for handling radioactive samples. Therefore, the bi-functional poly(HEMP-co-APTAC) polymer was grafted on the PES beads by UV-induced surface grafting, and used for the single bead based thermal ionization mass spectrometry (SB-TIMS). SB-TIMS offers numerous advantages, including matrix and interfering ions removal in a single step, selective preconcentration of Pu(IV) ions, transportation without heavy shielding, minimizing the possibility of contamination, and the single bead acts as a point source. The PES beads were synthesized in the present work by solvent induced phase inversion method. Silica coated superparamagnetic Fe_3O_4 nanoparticles were embedded in the PES beads so that these beads could be retrieved easily from the large volume aqueous samples. Since these beads were used in highly acidic solution, the Fe_3O_4 nanoparticles were protected with a silica coating formed by hydrolysis and condensation of tetraethoxysilane. The sorption studies indicated that the poly(HEMP-co-APTAC) grafted magnetic PES beads not only have the higher distribution coefficients for Pu(IV) but also higher selectivity towards Pu(IV) compared to U(VI). The analytical performance of the SB-TIMS method for determination of Pu using isotope dilution was compared with the solution based method, validated using Pu isotopic standard reference material NIST-SRM-947, and applied to the real samples such as dissolver solutions and soil leach liquors. The schematic representation of the single bead based thermal ionization mass spectrometry is shown below.

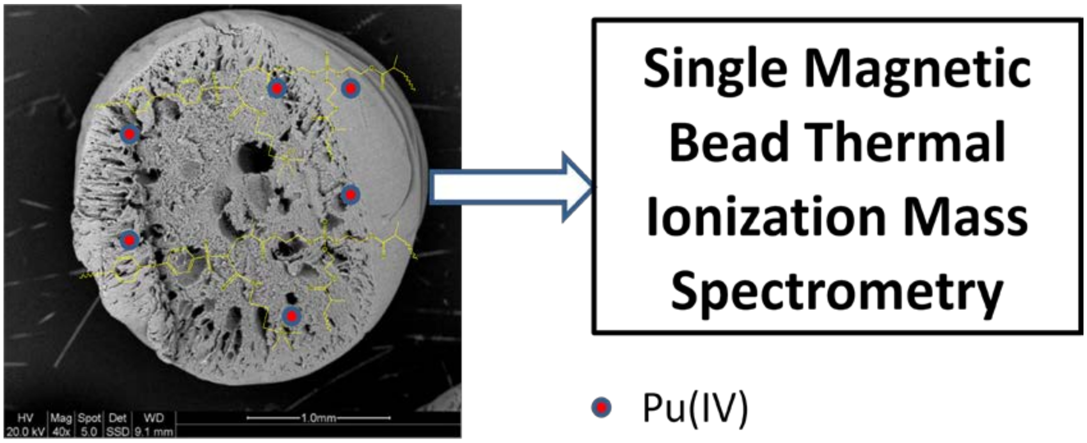

The analysis temperature for SB-TIMS method was significantly higher compared to the conventional solution based TIMS. Therefore, further attempts were made to develop better polymeric material based reservoirs for TIMS analysis of Pu(IV) and U(VI). The polymeric reservoirs were prepared by two different routes using either poly(propylene) (PP) or poly(ethersulfone) (PES) as the base matrices. In one route, a phosphate bearing HEMP monomer along with spacer monomer was polymerized, by UV-induced polymerization, within the pores of PP and PES membranes. In the other route, phosphate functionalized hydrophobic liquid extractants HDEHP and TEHP were physically immobilized by capillary force within the microporous PP membrane and PES beads. The variation of $^{239}Pu^+$ ion current as a function of vaporization filament temperature was studied for the different polymeric reservoirs developed in the present work. It was observed that the flat sheet reservoir required lower analysis temperature than the bead reservoir. Also, PP matrix decomposed at a lower temperature than PES. Thus, the liquid extractant impregnated PP reservoir was pyrolized easily at a filament temperature comparable to that used for solution based sample loading in TIMS and, therefore, was best suited for the TIMS analyses of actinides. The composition of the liquid extractant impregnated PP reservoir was optimized for the U(VI) preconcentration from ground water and seawater, and also for Pu(IV) preconcentration from 3 M HNO_3, which is normally encountered in the nuclear fuel reprocessing facility. The PP reservoir containing 3:1 mole proportion of TEHP:HDEHP was found to have optimum sorption efficiency for Pu(IV) from the acidic medium, whereas pure HEDEHP impregnated PP reservoir was most suitable for preconcentration of U(VI) from ground water and seawater. The parameters affecting the analytical performance of the polymer reservoir based TIMS (PolymRes-TIMS) were evaluated using Pu standard NIST-SRM 947. The PolymRes-TIMS was employed for the quantification in ppb levels of U(VI) in seawater and groundwater samples using ^{233}U spike for isotope dilution. Pu(IV) concentration was determined in the dissolver solution and in 3 M HNO_3 medium using either ^{240}Pu or ^{242}Pu enriched spike for isotope dilution. The accuracy and precision of PolymRes-TIMS was found to be comparable with the conventional solution based TIMS method. The overall PolymRes-TIMS process is shown below.

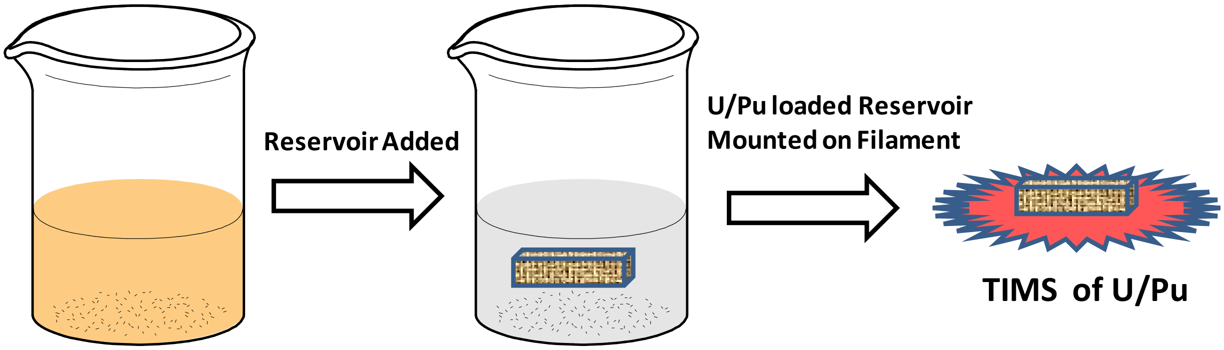

7.3. Future scope

The bi-functional polymers developed in the present work was found to be effective for the selective preconcentration of Pu(VI) from the acidic aqueous samples, and these polymers were suitable tailored for the quantification of the actinides by alpha spectrometry or TIMS. However, there are further scope of improvement by developing polymeric extractants or imprinted polymer more selective toward Pu(IV). Also, mounting the polymeric bead on the filament for TIMS analysis is difficult, which can be replaced by the sugar coated polymeric beads that will easily stick to the filament. The present wok is mainly focused on Pu(IV) ions, but could be extended to other actinides like Np and Am. Np ions in solution have variable oxidation states. Thus, it would be challenging to preconcentrate Np ions selectively and quantitatively in the functionalized polymer matrix.

References:

1. J.W. Grate, O.B. Egorov; Anal. Chem. 70 (1998) 3920–3929.
2. M.H. Lee, J.Y. Kim, W.H. Kim, E.C. Yung, K.Y. Jee; Appl. Radiat. Isot. 66 (2008) 1975–1979.
3. N. Vajda, A. Torvenyi, G. Kis-Benedek, C.K. Kim; Radiochim. Acta 97 (2009) 9–16.
4. G.H. Coleman; The Radiochemistry of Plutonium, NAS-NS 3058 (1965).
5. P.E. Warwick, I.W. Croudace, R. Carpenter; Appl. Radiat. Isot. 47 (1996) 627–642.
6. S. Osvath, N. Vajda, Zs. Molnar; J. Radioanal. Nucl. Chem. 281 (2009) 461–465.
7. B.S. Myasoedov, L.I. Guseva, L.A. Lebedev, M.S. Milyukova, M. K. Chnutova; Analytical Chemistry of Transplutonium Elements, John Wiley & Sons (1974).
8. G.F. Knoll; Radiation Detection and Measurement, John Wiley & Sons (1980).
9. B. Wierczinskia, K. Eberhardta, G. Herrmanna, J.V. Kratza, M. Mendela, A. Nählera, F. Rockera, U. Tharuna, N. Trautmann, K. Weinera, N. Wiehlb, J. Alstadb, G. Skarnemarkc; Nucl. Instrum. Methods Phys. Res. Sect. A 370 (1996) 532–538.
10. J. Moreno, J.J. LaRosa, P.R. Danesi, K. Burns, N. Vajda, M. Sinojmeri; Radiact. Radiochem. 9 (1998) 35–41.
11. X. Hou, P. Roos; Anal. Chim. Acta, 608 (2008) 105–139.
12. M. Ayranov, U. Krähenbühl, S. Röllin, M. Burger; J. Radioanal. Nucl. Chem. 279 (2009) 475–480.
13. G. Bortels, P. Collaers; Appl. Radiat. Isot. 38 (1987) 357–363.
14. M.P.R. Montero, A.M. Sanchez, A.M.C. Lourtau; Nucl. Instrum. Method Phys. Res. B 213 (2004) 429–433.
15. T.A. DeVol, A.H. Ringberg, R.A. Dewberry, J. Radioanal. Nucl. Chem. 254 (2002) 71–79.

16. C. Balpardo, M.E. Capoulat, D. Rodrigues, P. Arenillas; Appl. Radiat. Isotopes 68 (2010) 1358–1367.
17. N. Vajda, C.K. Kim; J. Radioanal. Nucl. Chem. 284 (2010) 341–347 .
18. P.E. Warwick, I.W. Croudace, J.S. Oh; Anal. Chem. 73 (2001) 3410.
19. Z. Varga, G. Surányi, N. Vajda, Z. Stefánka; Radiochim. Acta 95 (2007) 81–87.
20. M.C. Jiménez-Ramos, S. Hurtado, E. Chamizo, R. García-Tenorio, L. León-Vintró, P.I. Mitchell; Environ. Sci. Technol. 44 (2010) 4247.
21. B. Perot, P. Pin; Nucl. Instrum. Methods Phys. Res. A 671 (2012) 76–81.
22. C. Agarwal, S. Poi, A. Goswami, M. Gathibandhe, R.A. Agrawal; Nucl. Instrum. Method Phys. Res. A 597 (2008) 198–202.
23. C. Agarwal, S. Poi, A. Mathre, A. Goswami, M. Gathibandhe; Nucl. Instrum. Method Phys. Res. A 607 (2009) 439–445.
24. S. Paul, A. Sarkar, D. Alamelu, R.V. Shah, S.K. Aggarwal; Radiochim. Acta 100 (2012) 291–296.
25. A. Sarkar, S. Paul, S.K. Aggarwal; BARC Report BARC/2011/E/018, SIRD, BARC, Mumbai, India (2011).
26. J. R. de Laeter; Applications of Inorganic Mass Spectrometry, Chapter 1, John Wiley & Sons (2001).
27. J.S. Crain, L.L. Smith, J.S. Yaeger, J.A. Alvarado; J. Radioanal. Nucl. Chem. 194 (1995) 133–139.
28. H. Ramebaeck, M. Skillberg; J. Radioanal. Nucl Chem. 235 (1998) 229–233.
29. D.E. Vance, V.F. Belt, T.J. Oatts, D.K. Mann; J. Radioanal. Nucl. Chem. 234 (1998) 143–146.
30. Q.J. Chen, I. Christensen, A. Jensen, H. Dahlgaard, S.P. Nielsen, A. Aarkrog; IAEA-SM-354/38P (1999).

31. L. Perna, M. Betti, J.M. Barrero Moreno, R. Fuoco; J. Anal. At. Spectrom. 16 (2001) 26–31.
32. Q.J. Chen, H. Dahlgaard, S.P. Nielsen, A. Aarkrog, I. Christensen, A. Jensen; J. Radioanal. Nucl. Chem. 249 (2001) 527–533.
33. P. Lindahl, P. Roos, M. Eriksson, E. Holm; J. Environ. Radioact. 73 (2004) 73–85.
34. P. Lindahl, P. Roos, E. Holm, H. Dahlgaard; J. Environ. Radioact. 82 (2005) 285–301.
35. N. Guerin, M.A. Langevin, K. Nadeau, C. Labrecque, A. Gagne, D. Laviere; Appl. Radiat. Isot. 68 (2010) 2132–2139.
36. J.J. LaRosa, J.W. Mietelski; J. Radioanal. Nucl. Chem. 283 (2010) 385–387.
37. S.L. Maxwell; J. Radioanal. Nucl. Chem. 275 (2010) 497–502.
38. C.S. Kim, C.K. Kim, P. Martin, U. Sansone; J. Anal. At. Spectrom. 22 (2007) 827–841.
39. L.B. Magnusson, T.J. LaChapelle; J. Am. Chem. Soc. 70 (1948) 3534–3538.
40. S.H. Lee, J. Gastaud, J.J. LaRosa, L.W. Kwong, P.P. Povinec, E. Wyse, L.K. Fifield, P.A. Hausladen, L.M. DiTada, G.M. Santos; J. Radioanal. Nucl. Chem. 248 (2001) 757–764.
41. R.N. dos Santos, L.S. Marquea, F.B. Ribeiro; Appl. Rad. Isot. 56 (2002) 741–750.
42. K. Tagami, S. Uchida; Appl. Rad. Isot. 61 (2004) 255–259.
43. J.S. Becker, M. Zoriy, L. Halicz, N. Teplyakov, C. Muller, I. Segal, C. Pickhardt, I.T. Platzner; J. Anal. At. Spectrom. 19 (2004) 1257–1261.
44. F. Chartier, M. Aubert, M. Pilier; Fresenius J. Anal. Chem. 364 (1999) 320.
45. Y. Muramatsu, T. Hamilton, S. Uchida, K. Tagami, S. Yoshida, W. Robison; Sci. Total Environ. 278 (2001) 151–159.
46. E. Hrnecek, P. Steier, A. Wallner; Appl. Radiat. Isot. 63 (2005) 633–638.

47. R. Jakopic, P. Tavcar, L. Benedik; Appl. Radiat. Isot. 65 (2007) 504–511.
48. M. Yamamoto, S. Igarashi, K. Chatani, K. Komura, K. Ueno; J. Radioanal. Nucl. Chem. 138 (1990) 365–376.
49. J. Qiao, X. Hou, P. Roos, M. Miro; Anal. Chem. 83 (2011) 373–381.
50. T.C. Kenna; J. Anal. At. Spectrom. 17 (2002) 1471–1479.
51. T.C. Kenna; J. Environ. Radioact. 100 (2009) 547–557.
52. J.J. LaRosa, J.W. Mietelski; J. Radioanal. Nucl. Chem. 283 (2010) 385–387.
53. C.W. Sill, D.S. Sill; Radioact. Radiochem. 6 (1995) 8–14.
54. S.L. Maxwell, B.K. Culligan; J. Radioanal. Nucl. Chem. 270 (2006) 699–704.
55. M. Ayranov, U. Kraehenbuehl, H. Sahli, S. Rollin, M. Burger; Radiochim. Acta 93 (2005) 249–257.
56. Y. Ohtsuka, Y. Takaku, K. Nishimura, J. Kimura, S. Hisamatsu, J. Inaba; Anal. Sci. 22 (2006) 309–311.
57. D. Schaumloffel, P. Giusti, M.V. Zoriy, C. Pickhardt, J. Szpunar, R. Lobinski, J.S. Becker; J. Anal. At. Spectrom. 20 (2005) 17–21.
58. P. Tavcar, L. Benedik; Radiochim. Acta 93 (2005) 623–625.
59. O.F.X. Donard, F. Bruneau, M. Moldovan, H. Garraud, V.N. Epov, D. Boust; Anal. Chim. Acta 587 (2007) 170–179.
60. T. Kimura; J. Radioanal. Nucl. Chem. 139 (1990) 297–305.
61. E. Mathew, V.M. Matkar, K.C. Pillai; J. Radioanal. Chem. 62 (1981) 267.
62. I. Giardina, L. Andreocci, S. Bazzarri, S. Mancini, P. Battisti; Czech. J. Phys. 56 (2006) 265–270.
63. J. Zheng, M. Yamada; Anal. Sci. 23 (2007) 611–615.
64. R. Chiarizia, E.P. Horwitz, S.D. Alexandratos, M.J Gula; Sep. Sci. Technol. 32 (1997) 35.

65. J. Qiao, X. Hou, P. Roos, M. Miro; Talanta 84 (2011) 494–500.

66. H. Michel, D. Levent, V. Barci, G. Barci-Funel, C. Hurel; Talanta 74 (2008) 1527–1533.

67. V.A. Ageyev, O.O. Odintsov, A.D. Sajeniouk; J. Radioanal. Nucl. Chem. 264 (2005) 337–342.

68. M.V. Zoriy, C. Pickhardt, P. Ostapczuk, R. Hille, J.S. Becker; Int. J. Mass Spectrom. 232 (2004) 217–224.

69. D. Arginelli, M. Montalto, S. Bortoluzzi, M. Nocente, M. Bonardi, F. Groppi; J. Radioanal. Nucl. Chem. 263 (2005) 275.

70. Z. Varga, G. Suranyi, N. Vajda, Z. Stefanka; J. Radioanal. Nucl. Chem 274 (2007) 87–94.

71. Z. Varga, G. Suranyi, N. Vajda, Z. Stefanka; Microchem. J. 85 (2007) 39–45.

72. J.J. LaRosa, J. Gastaud, L. Lagan, S.H. Lee, I. Levy-Polomo, P.P. Povinec, E. Wyse; J. Radioanal. Nucl. Chem 263 (2005) 427–436.

73. J.V. Cizdziel, M.E. Ketterer, D. Farmer, S.H. Faller, V.F. Hodge; Anal. Bioanal. Chem. 390 (2008) 521–530.

74. C.A. Moody, S.E. Glover, D.B. Stuit, R.H. Filby; J. Radioanal. Nucl. Chem. 234 (1998) 183.

75. H. Qu, D. Stuit, S.E. Glover, S.F. Love, R.H. Filby; J. Radioanal. Nucl. Chem. 234 (1998) 175–181.

76. M. Aguilar, J.L. Cortina; Solvent extraction and liquid membranes: Fundamentals and applications in new materials, Taylor & Francis (2010).

77. M. Pimpl, R.H. Higgy; J. Radioanal. Nucl. Chem. 248 (2000) 537–541.

78. S.N. Kalmykov, R.A. Aliev, D.Y. Sapozhnikov, Y.A. Sapozhnikov, A.M. Afinegonov; Appl. Radiat. Isot. 60 (2004) 595–599.

79. E.P. Horwitz, K.A. Martin, H. Diamond, L. Kaplan; Solvent Extr. Ion Exch. 4 (1986) 449.

80. E.P. Horwitz, H. Diamond, K.A. Martin; Solvent Extr. Ion Exch., 5 (1987) 447–470.

81. C.W. Sill, C.P. Willis; Anal. Chem. 38 (1966) 97–102.

82. J. Guogang, C. Testa, D. Desideri, F. Guerra, C. Roselli; J. Radioanal. Nucl. Chem. 230 (1998) 21.

83. G. Jia, D. Desideri, F. Guerra, M.A. Meli, C. Testa; J. Radioanal. Nucl. Chem. 220 (1997) 15.

84. D.K. Pant, G.A. Chaugule, K.K. Gupta, P.G. Kulkarni, P.B. Gurba, P. Janardan, R.D. Changrani, P.K. Dey, P.N. Pathak, D.R. Prabhu, A.S. Kanekar, V.K. Manchanda; J. Radioanal. Nucl. Chem. 283 (2010) 513–518.

85. S.A. Ansari, P.N. Pathak, P.K. Mohapatra, V.K. Manchanda; Chem. Rev. 112 (2012) 1751-1772.

86. B.A. Moyer, Ion Exchange and Solvent Extraction: A Series of Advances, Volume 19, Taylor & Francis (2010).

87. R.A. Fjeld, T.A. DeVol, J.D. Leyba, A. Paulenova; J. Radioanal. Nucl. Chem. 263 (2005) 635–640.

88. S. Rollin, U.B. Eklund, K. Spahiu; Radiochim. Acta 89 (2001) 757–763.

89. N. Guérin, R. Calmette, T. Johnson and D. Larivière; Anal. Methods, 3 (2011) 1560-1567.

90. F.L. Moore, A. Juriaanse; Anal. Chem. 39 (1967) 733.

91. E.P. Horwitz, M. Dietz, R. Chiarizia, M.L. Dietz, H. Diamond, S.L. Maxwell, M.R. Nelson; Anal. Chim. Acta 310 (1995) 63–78.

92. J. Szpunar, R. Lobinski; Hyphenated Techniques in Speciation Analysis, The Royal Society of Chemistry, (2003).

93. I. Gunther-Leopold, J.K. Waldis, B. Wernli, Z. Kopajtic; Int. J. Mass Spectrom. 242 (2005) 197–202.

94. L. Aldave Heras, M. Sandow, G. Olszewski, D. Serrano-Purroy, S. Winckel, J. Glatz; Revista de la Societat Catalana de Química núm. 12 (2013) 61-67.

95. B. Kuczewski, C.M. Marquardt, A. Seibert, H. Geckeis, J.V. Kratz, N. Trautmann; Anal. Chem. 75 (2003) 6769-6774.

96. C. Ambard, A. Delorme, N. Baglan, J. Aupiais, F. Pointurier, C. Madic; Radiochim. Acta 93 (2005) 665–673.

97. S. Bürger, N.L. Banik, R.A. Buda, J.V. Kratz, B. Kuczewski, N. Trautmann; Radiochim. Acta 95 (2007) 433–438.

98. S. Topin, J. Aupiais. N. Baglan; Radiochim. Acta 98 (2010) 71–75.

99. J.H. Aldstadt, J.M. Kuo, Lesa L. Smith, M.D. Erickson; Anal. Chim. Acta 319 (1996) 135–143.

100. G.E. Fryxell, Y. Lin, S. Fiskum, J.C. Birnbaum, H. Wu, K. Kemner, S. Kelly; Environ. Sci. Technol. 39 (2005) 1324−1331.

101. S.E. Matthews, P. Parzuchowski, A. Garcia-Carrera, C. Grüttner, J. Dozol, V. Böhmer; Chem. Commun. 5 (2001) 417−418.

102. A.Y. Romanchuk, A.S. Slesarev, S.N. Kalmykov, D.V. Kosynkin, J.M. Tour; Phys. Chem. Chem. Phys. 15 (2013) 2321–2327.

103. G.T. Seaborg, J.J. Katz, L.R. Morss; The Chemistry of the Actinide Elements, Volume 2, Chapman & Hall (1986).

104. T.H. Bray, J. Ling, E.S. Choi, J.S. Brooks, J.V. Beitz, R.E. Sykora, R.G. Haire, D.M. Stanbury, T.E. Albrecht-Schmitt; Inorg. Chem. 46 (2007) 3663–3668.

105. P.C. Burns, R.C. Ewing, F.C. Hawthorne; Can. Mineral. 35 (1997) 1551–1570.

106. R.M. Sawant, R.K. Rastogi, N.K. Chaudhuri; J. Radioanal. Nucl. Chem. 229 (1998) 203–206.
107. M. Muthukumar, Shekhar Kumar, P.K. Sinha, U.K. Mudali, R. Natarajan; J. Radioanal. Nucl. Chem. 288 (2011) 819–821.
108. Shekhar Kumar, U.K. Mudali; J. Radioanal. Nucl. Chem. 295 (2013) 1951–1955.
109. L. Newman, P. Klotz; J. Phys. Chem. 67 (1963) 205–209.
110. I. Hagström, L. Spjuth, Ȧ. Enarsson, J.O. Liljenzin, M. Skålberg, M.J. Hudson, P.B. Iveson, C. Madic, P.Y. Cordier, C. Hill, N. Francois; Solvent Extr. Ion Exch. 17 (1999) 221–242.
111. G.C. Pal, A.K. Chakravarti, M. Sengupta. Ion Exch. Membr. 2 (1974) 21.
112. I.M. Abrams; U.S. Patent 2844546 (1958).
113. H. Small; Ind. Eng. Chem. Prod. Res. Dev. 6 (1967) 147.
114. S. Kobayashi, M. Suzuki, T. Saegusa; Macromolecules 16 (1983) 1010.
115. S.D. Alexandratos, D.L. Wilson, P.T. Kaiser; React. Polymers 5 (1987) 23–35.
116. S.D. Alexandratos, D.L. Wilson; Macromolecules 19 (1986) 280–287.
117. K. Brajter, I. Miazek; Talanta 28 (1981) 759.
118. S.D. Alexandratos, D.L. Wilson, M.A. Strand, D.R. Quillen, A.J. Walder, W.J. McDowell; Macromolecules 18 (1985) 835–840.
119. S.D. Alexandratos, D.L. Wilson, W.J. McDowell; Sep. Sci. Tech. 22 (1987) 983–995.
120. S.D. Alexandratos, D.R. Quillen; Solvent Extr. Ion Exch. 7 (1989) 511–525.
121. S.D. Alexandratos, P.T. Kaiser, C.E. Grady; Solvent Extr. Ion Exch. 9 (1991) 309–318.
122. A.W. Trochimczuk, S.D. Alexandratos; J. Appl Poly. Sci. Vol. 52 (1994)1273–1277.
123. S.D. Alexandratos, P.T. Kaiser; Solvent Extr. Ion Exch. 10 (1992) 539–557.

124. S.D. Alexandratos, L.A. Hussain; Ind. Eng. Chem. Res. 34 (1995) 251−254.

125. S. Das, A.K. Pandey, A.A. Athawale, V.K. Manchanda; J. Phys. Chem. B 113 (2009) 6328–6335.

126. Radiochemistry Division, BARC, Mumbai 400 085, India, and Department of Chemistry, University of Pune, Pune 411 007, India

127. G. Kim, W.C. Burnett, E.P. Horwitz; Anal. Chem. 72 (2000) 4882–4887.

128. J. Eikenberg, M. Jäggi, H. Beer, M. Rüthi, I. Zumsteg; Appl. Radiat. Isotopes 67 (2009) 776–780.

129. S.L. Maxwell III, V.D. Jones; Talanta 80 (2009) 143–150.

130. E. Chamizo, M.C. Jiménez-Ramos, L. Wacker, I. Vioque, A. Calleja, M. García-León, R. García-Tenorio; Anal. Chim. Acta 606 (2008) 239–245.

131. C. Labrecque, L. Whitty-Le’veille’, D. Larivière; Anal. Chem. 85 (2013) 10549–10555.

132. B.C. Marroyo, A.M. Sánchez, M.J. Vargas; Appl. Radiat. Isotopes 87 (2014) 328–330.

133. C.W. Sill; Nucl. Chem.Waste Manage. 7 (1987) 201–215.

134. Z.H. Kazi, J.R. Cornett, X. Zhao, L. Kieser; Anal. Chim. Acta 829 (2014) 75–80.

135. J.S. Oh, P.E. Warwick, I.W. Croudace, S.H. Lee; Appl. Radiat. Isotopes 87 (2014) 233–237.

136. A.P. Novikov, V.S. Ryleeva, A.V. Abramova, G.A. Pribylova, I.V. Smirnov; J. Radioanal. Nucl. Chem. (2014) doi:http://dx.doi.org/10.1007/s10967-014-3246-3.

137. K. Joe, S.H. Han, B.C. Song, C.H. Lee, Y.K. Ha, K. Song; Nucl. Eng. Technol. 45 (2013) 415–420.

137. R. Kumar, J.R. Yadav, D.D. Rao, L. Chand; J. Radioanal. Nucl. Chem. 283 (2010) 785–788.

138. J. Parus, W. Raab, H. Swictly, J. Cappis, S. Deron; Nucl. Instrum. Methods Phys. Res. A 312 (1992) 278–283.

139. D. Karamanis, K.G. Ioannides, K.C. Stamoulis, Anal. Chim. Acta 573 (2006) 319–327.

140. R.S. Addleman, M.J.O. Hara, J.W. Grate, O.B. Egorov; J. Radioanal. Nucl. Chem. 263 (2005) 291–294.

141. V. Chavan, S. Paul, A.K. Pandey, P.C. Kalsi, A. Goswami; J. Hazard. Mater. 260 (2013) 53–60.

142. S.K. Aggarwal, G. Chourasiya, R.K. Duggal, C.P. Singh, A.S. Rawat, H.C. Jain; Fresenius Zeitschrift für Anal. Chem. 323 (1986) 148–152.

143. M.V. Ramaniah, H.C. Jain, S.K. Aggarwal, S.A. Chitambar, V.D. Kavimandan, A.I. Almaula, P.M. Shah, A.R. Parab, V.L. Sant; Nucl. Technol. 49 (1980) 121–128.

144. E. Browne, R.B. Firestone, V.S. Shirley; Table of Radioactive Isotopes, John Wiley & Sons, New York (1986).

145. S.K. Aggarwal, S.A. Chitambar, V.D. Kavimandan, A.I. Almaula, P.M. Shah, A.R. Parab, V.L. Sant, H.C. Jain, M.V. Ramaniah; Radiochim. Acta 27 (1980) 1–5.

146. J. Qiao, X. Hou, M. Mirob, P. Roos; Anal. Chimi. Acta 652 (2009) 66-84.

147. M.H. Dai, K.O. Buesseler, J.M. Kelley, J.E. Andrews, S. Pike, J.F. Wacker; J. Environ. Radioactivity 53 (2001) 9-25.

148. S.P. LaMont, C.R. Shick, P. Cable-Dunlap, D.J. Fauth, T.R. LaBone; J. Radioanal. Nucl. Chem. 263 (2005) 477-481.

149. C.G. Lee, D. Suzuki, F. Esaka, M. Magara, K. Song; Talanta 141 (2015), 92-96.

150. M.H. Lee, J.H. Park, S.Y. Oh, H.J. Ahn, C.H. Lee, K. Song, M.S. Lee, Talanta 86 (2011) 99-102.

151. J.W. Grate, M.J. O’Hara, A.F. Farawila, M. Douglas, M.M. Haney, S.L. Petersen, T.C. Maiti, C.L. Aardahl; Anal. Chem. 83 (2011) 9086-9091.

152. N Guerin, R. Calmette, T. Johnson, D. Lariviere; Anal.Methods 3 (2011) 1560-1567.

153. K.L. Ramakumar, S.K. Aggarwal, S.A. Chitambar, H.C. Jain; BARC Report No. 1289 (1985) SIRD, BARC, Mumbai, India.

154. J.D. Fassett, W.R. Kelly; Anal. Chem. 56 (1984) 550-556.

155. R.L. Walker, R.E. Eby, C.A. Pritchard, J.A. Carter; Anal. Letters 7 (1974) 563-574.

156. W.F. Paxton, M.J. O’Hara, S.M. Peper, S.L. Petersen, J.W. Grate; Anal. Chem. 80 (2008) 4070-4077.

157. H. Yamagishi, J.V. Crivello, G. Belfort; J. Membr. Sci. 105 (1995) 237-247.

158. J. Deng, L. Wang, L. Liu, W. Yang; Prog Polym Sci. 34 (2009) 156-193.

159. A. Rios, M. Zougagh, M. Bouri; Anal. Methods 5 (2013) 4558-4573.

160. N. Thakur, S.A. Kumar, H. Parab, A.K. Pandey, P. Bhatt, S.D. Kumar, A.V.R. Reddy; RSC Adv. 4 (2014) 10350-10357.

161. X. Guan, J. Chang, Y. Chen, H. Fan; RSC Adv. 5 (2015) 50126-50136.

162. F. Gao, H. Gu, H. Wang, X. Wang, B. Xiang, Z. Guob; RSC Adv. 5 (2015) 60208-60219.

163. L. Li, M. Xu, M. Chubik, M. Chubik, A. Gromov, G. Wei, W.Han; RSC Adv. 5 (2015) 41611-41616.

164. A.R. King, D. Knight, A. Fairhead; J. Radioanal. Nucl. Chem. 304 (2015) 163-169.

165. A. Milliard, M. Durand-Jézéquel, D. Larivière; Anal. Chimi. Acta 684 (2011) 40-46.

166. D. Larivière, K. Benkhedda, S. Kiser, S. Johnson, R.J. Cornett; Anal. Methods 2 (2010) 259-267.

167. O. B. Mokhodoeva, G. V. Myasoedova, E. A. Zakharchenko; Radiochemistry 53 (2011) 35-43.

168. A.K. Pandey, M.M. Gautam, J.P. Shukla, R.H. Iyer; J. Membr. Sci. 190 (2001) 9-20.

169. J. Lee, H. K. Lee, K.E. Rasmussen, S. Pedersen-Bjergaard; Anal. Chimi. Acta 624 (2008) 253-268.